FINAL REPORT

For the Florida Department of Transportation

Application of Non-contacting Proximity Sensors for Measuring Soil Resilient Characteristics

Research Report No. FL/DOT/RMC/0510815

State Job No.: 99700-3575-119

WPI No.: 0510815

FSU Project No.: 6120-539-39

By

W. Virgil. Ping, P.E.
Chiang Shih, P.E.
Enhong Wu
Zenghai Yang

Department of Civil Engineering
Florida A&M University-Florida State University
College of Engineering
Tallahassee, FL 32310

October 2000

Technical Report Documentation Page

1. Report No.	2. Government Accession No.	3. Recipient's Catalog No.
FL/DOT/RMC/0510815		

4. Title and Subtitle	5. Report Date
Application of Non-contacting Proximity Sensors for Measuring Soil Resilient Characteristics	October 2000
	6. Performing Organization Code

7. Author(s)	8. Performing Organization Report No.
W. V. Ping, C. Shih, Enhong Wu, and Zenghai Yang	FL/DOT/RMC/0510815

9. Performing Organization Name and Address	10. Work Unit No. (TRAIS)
FAMU-FSU College of Engineering Department of Civil Engineering 2525 Pottsdamer Street Tallahassee, Florida 32310-6046	
	11. Contract or Grant No. WPI 0510815, BB-303
	13. Type of Report and Period Covered Final Report September 1997 - September 2000
12. Sponsoring Agency Name and Address Florida Department of Transportation Research Center, MS30 605 Suwannee Street Tallahassee, Florida 32399-0450	14. Sponsoring Agency Code

15. Supplementary Notes

Prepared in cooperation with the Federal Highway Administration, U.S. Department of Transportation

16. Abstract

As recommended by AASHTO, resilient moduli are becoming important fundamental parameters in the mechanistic analysis and design of pavement. Several test methodologies have been proposed by many highway agencies to estimate this parameter. The objective of this research is to practically evaluate the alternation of the LVDTs with non-contacting proximity transducers for resilient modulus measurements. A single apparatus capable of measuring dynamic properties of soils by both non-contacting proximity probe measurement and LVDT measurement is proposed. Discussions on the instrumental design and data acquisition are provided. Experimental results indicated non-contacting proximity probe measurement gave the resilient modulus lower than that from middle-positioned LVDTs but higher than that from full-length positioned LVDTs.

17. Key Words	18. Distribution Statement
Resilient Modulus, Non-contacting probe, LVDT	This document is available to the public through the National Technical Information Service, Springfield, Virginia, 22161

19. Security Classif. (of this report)	20. Security Classif. (of this page)	21. No. of Pages	22. Price
Unclassified	Unclassified	153	

FINAL REPORT

For the Florida Department of Transportation

Application of Non-contacting Proximity Sensors for Measuring Soil Resilient Characteristics

Research Report No. FL/DOT/RMC/0510815

State Job No.: 99700-3575-119

WPI No.: 0510815

FSU Project No.: 6120-539-39

By

W. Virgil. Ping, P.E.
Chiang Shih, P.E.
Enhong Wu
Zenghai Yang

Department of Civil Engineering
Florida A&M University-Florida State University
College of Engineering
Tallahassee, FL 32310

October 2000

METRIC CONVERSIONS

inches = 25.4 millimeters

feet = 0.305 meters

square inches = 645.1 millimeters squared

square feet = 0.093 meters squared

cubic feet = 0.028 meters cubed

pounds = 0.454 kilograms

poundforce = 4.45 newtons

poundforce per square inch = 6.89 kilopascals

pound per cubic inch = 16.02 kilograms per meters cubed

DISCLAIMER

"The opinions, findings and conclusions expressed in this publication are those of the authors and not necessarily those of the Department of Transportation or the U.S. Department of Transportation. This publication is prepared in cooperation with the State of Florida Department of Transportation and the U.S. Department of Transportation."

ACKNOWLEDGEMENTS

Funding for this research was provided by the Florida Department of Transportation (FDOT) and Federal Highway Administration (FHWA) through the Research Center of the FDOT. Bruce Dietrich, State Pavement Design Engineer, provided excellent support and guidance. Emmanuel Uwaibi was the project manager.

The FDOT Research Center staff (Richard Long - Director, John Nicholson, Chris Smith, and Sandra Bell) provided financial and contractual support to the project.

TABLE OF CONTENTS

LIST OF TABLES

LIST OF FIGURES

CHAPTER 1

INTRODUCTION

1.1 Background

The resilient modulus is an index that describes the nonlinear stress-strain behavior of soils under repeated loads. Recently, the measurement of resilient modulus has become more common because of its importance in determining properties of roadbed soils and pavement components. In 1986, the *AASHTO Guide for Design of Pavement Structures* (AASHTO, 1986) replaced the "soil support value" of roadbed soil with resilient modulus. *The Design Guide* recommends that the laboratory resilient modulus test procedure, AASHTO *T 274-82* (AASHTO 1986), be used for determining the basic engineering properties of roadbed soils and pavement components.

Since its introduction, the original AASHTO *T 274-82* has been widely criticized. A number of nationwide studies have been undertaken to search for solutions and alternate test methods, such as the National Cooperative Highway Research Program (NCHRP) 1-28 project. Researchers and agencies have

also proposed several variations of the resilient modulus test procedure. The Strategic Highway Research Program (SHRP) Protocol P46 (AASHTO *T 294-92*) and AASHTO *T 292-91I* (AASHTO 1991 & 1992) are the most commonly used in recent years.

Most often, resilient modulus measurements are conducted using the linear variable differential transducers (LVDT) measurements, as specified by the AASHTO T 292-91I and T 294-92 test procedures. However, there are some notorious problems incurred by the current LVDT measurements. Thus, whether it is possible to find an alternative method has become a major concern of many researchers. This study was conducted on alternating the LVDTs by proximity sensors for resilient modulus measurements.

1.2 Scope of Study

The primary objective of this study was to evaluate the possibility of alternating LVDTs with non-contact proximity sensors for measurement of axial deformation in resilient modulus testing. The goals of this study are to: 1) develop an apparatus by applying the non-contact proximity probes as well as LVDT in a single chamber; 2) critically assess the strengths and weaknesses of utilizing non-contact proximity probes in triaxial tests.

1.3 Report Organization

This report summarizes the design and the implementation of the laboratory experimental program by comparing the non-contacting probes and LVDTs in the resilient modulus test with exactly the same soil specimen in a single chamber. Meanwhile, this research evaluates the feasibility of alternating the LVDTs by non-contact proximity probes to obtain the engineering properties of pavement soils.

The background and objectives of this laboratory study are presented in this chapter. A literature review of the LVDT and non-contacting probes is summarized in Chapter 2. The design of the laboratory experimental program is described in Chapter 3. Chapter 4 analyzes the procedures followed in the data acquisition process. Chapter 5 presents and analyzes the results of the resilient modulus tests. Finally, conclusions and recommendations of this research study are presented in Chapter 6. The bibliography is presented in Appendices.

CHAPTER 2

RESEARCH BACKGROUND

2.1 Introduction

As an index that describes the nonlinear stress-stain behavior of soils under repeated loads, the resilient modulus is defined as the deviator dynamic stress (simulating the moving vehicular traffic) divided by the resilient axial (recoverable) strain. This concept is derived from the fact that the major component of deformation induced into a pavement structure under the traffic loading is not associated with plastic deformation or permanent deformation, but with elastic or resilient deformation.

In recent years, the resilient modulus test has become more common because of its importance in determining properties of roadbed soils and pavement components. It is considered to be a required input for determining the stress-strain characteristics of pavement structures subjected to traffic loading. The Strategic Highway Research

Program's (SHRP) Protocol P46 (AASHTO T294-92) and AASHTO T 292-91I have been most commonly used recently.

2.2 Resilient Modulus Tests

Several methods and test procedures have been used to obtain resilient modulus, varying from laboratory tests and field tests. In general, the laboratory procedures for determination of resilient modulus are essentially based on the exiting cyclic triaxial methods used for determination of soil properties under repeated loads (**Figures 2.1** and **2.2**).

In 1986, a workshop at the University of Oregon reviewed the state of practice in resilient modulus testing. Since then a number of important improvements have been made on the loading cycles per step, which have been reduced from 33 and 200 in AASHTO T 274 to 15 and 100, thus reducing the testing period from approximately 5 hr. to 2.5 hr. The revisions are included in the new AASHTO procedure T 294-92.

The newest AASHTO T 294-92, which basically reflects the procedure suggested by the SHRP, is significantly more convenient to perform when compared to the earlier AASHTO procedure (e.g. AASHTO T 274). However, some aspects of the

testing methodology are still being investigated and modified. A number of researchers have focused on how to better obtain the small strain properties of soils and how to reduce errors in small magnitude measurements of both load and displacement. Ping et al. (1995) and Pezo et al. (1997) have addressed several issues that require further research.

Many factors influence the resilient modulus of soils, including: soil type, soil properties, dry unit weight, water content, stain level, test procedure, and size effect.

A literature review reveals that, in addition to soil properties, testing parameters such as sample preparation, sample preconditioning, loading amplitude and sequence, and confining pressure are the primary factors affecting the magnitude of resilient modulus. Ping et al. (1998) indicated that the resilient modulus measured from the middle LVDTs is significantly different from that determined from the full length LVDTs because of the end effects and system compliance. For the T 292-92I test procedure, the average ratios of the resilient modulus values between the full-length (20.3cm) and middle (10.2cm) LVDT measurements ranged from about 0.75 at lower confining pressures to about 0.85 at higher confining pressures. Based on their study, the effect of stress history results in only about 15 to 20%

difference in resilient modulus, while the difference in resilient modulus values due to LVDT positions may vary from 25 to 30%.

Nazarian (1996) and Pezo (1996) proposed a sophisticated method for accurate measurement of strains using non-contacting proximity sensors. The sensors are able to measure stains directly on the specimen, inside the confining chamber, in the 10^{-4} to 10^{-3} percent range typically observed in resilient modulus testing. Gookin et al. (1996) also developed a cyclic triaxial testing system capable of measuring very small to large strain properties on a single specimen, by combining a wide variety of existing instrumentation.

2.3 Shortcomings of LVDT Measurement

As mentioned above, many factors affect the results of the resilient modulus test. Aside from the soil properties and operational factors, instrumental problems influence the test results significantly.

2.3.1 Frictions inside the LVDTs

LVDT measures the movement of the metallic stick inside the transducer to reflect the deformations of the specimens. Normally these movements are within 0.1 mil, which is very easy to be stalled by the friction between the probe and transducers.

The friction occurs easily due to the narrow space between the metal probe and the hole on a LVDT transducer. The diameter of the hole is at a level that is slightly larger than that of the metal probe, so that the probe can go through the hole and the transducer can detect the relevant position of the probe. Frictions definitely exist as long as there is a contact between them.

An even worse case is the misalignment of the LVDT clamps. Both the metallic stick and the transducer of the LVDT are fixed on the clamps placed around the specimen with two LVDTs in between. To achieve an alignment, both the two clamps must parallel and align to each other, so that the metallic stick can be set perpendicularly to the LVDT and stay right in the middle of the LVDTs. This step must be achieved by repeated visual observations and adjustments, which are less-reliable and time consuming.

One fact is that the alignment is not easy to obtain during a test setup (**Figure 2.2**). Any type of failure in the alignment will lead to contact between the metallic stick and the LVDT transducer, resulting in friction. The worse the alignment, the stronger the friction force that occurs.

2.3.2 Difficulties in Specimen Alignment

As mentioned, good alignment of the LVDT clamps is critical to obtaining accurate resilient moduli. In addition to the clamp alignment, load alignment takes the same roll in the test results. Misalignment errors occur easily due to the axis of the applied load not coinciding with the axis of the specimen (**Figure 2.3a**). Moreover, the ends of a cylindrical specimen must be perpendicular to its long axis. Misalignment errors often cause bending, resulting in non-uniform distribution of strain in the specimen and an erroneous estimate of the resilient modulus.

Normally, the following methods are used to minimize misalignment errors:

(a) the triaxial cell must be carefully machined to be in perfect alignment

(b) the cell must be aligned relative to the external loading ram

(c) the specimen must be a right circular cylinder

(d) the specimen must be aligned with the triaxial cell.

To satisfy the above requirements, the external load ram, triaxial cell, and specimen should all be vertical when the cell is placed on a horizontal surface. The entire alignment of the system should be checked to obtain reliable results.

The alignment is critical and skillful work during a triaxial test, which requires the operator's patience and special skills. In an conventional triaxial apparatus, the top of the cell is supported by the cylindrical plexiglas chamber. Either an O-ring or a flat gasket is placed on the ends of the chamber to form a seal. When a flat gasket is used, load alignment is influenced by the uniformity of tightness of the nuts holding the tie bars down and by the condition and type of gasket used. A thin, low compressibility gasket should be used and the nuts uniformly tightened with a torque wrench. For a properly designed O-ring seal, which results in metal bearing on plexiglas, alignment in not influenced since the top plate of the cell bottoms out on the chamber. It is necessary to check all O-ring sealed interfaces by loading the two parts and measuring deformation to be sure the seal is made correctly.

Even after careful system calibration, alignment errors should also be evaluated during the conditioning phase of each repeated load test. For the two LVDTs used to measure axial displacement, illustrated in **Figure 2.2**, the ratio of maximum axial LVDT displacement (Y_{max}) to the minimum reading (Y_{min}) should be no greater than 1.10 in accordance with the SHRP P-46 procedure. Excessive eccentricity can often be reduced by stopping the test and very lightly laterally tapping the base of the triaxial cell to obtain better specimen alignment. If flat gaskets are used to seal the cell chamber, an alternative approach is to adjust the tension in the rod bolts on one side of the triaxial cell that also changes the alignment of the loading ram.

The eccentricity ratio varies throughout the test. This ratio is directly proportional to the distance of the transducer from the loading piston. Hence, distance is not considered in the eccentricity ratio in which the LVDTs are located away from the load axis. Therefore, the LVDTs should be placed as close as possible to the load piston because of the indeed strict criteria of ratio 1.10.

Based on the tests (R. D. Barksdale et al., 1996) on 29 different specimens at 15 stress levels, which included four different base materials, an average eccentricity ratio Y_{max}/Y_{min} gave 1.14 throughout the test for both external and

clamp mounted transducers. Each external LVDT, however, was located only 2.2 in. from the load axis while each clamp was 4.0 in. away. The standard deviation of the eccentricity ratio for the external transducers was 4% compared to 8% for the clamps. Experience indicates that in setting up a specimen, with careful calibration of the triaxial cell and testing system, an eccentricity ratio of about 1.10 can be initially achieved. Great care must be always taken to minimize the eccentricity.

2.3.3 Less reliability of External Measurement

External deformation measurement is very easy to perform, however, the results are general less reliable and depend upon minimizing system compliance and careful equipment calibration. Remaining compliance effects can then be minimized by calibration using a dummy sample of known stiffness made of steel, aluminum or plexiglas. Displacement can also be measured within the cell between the end platens. This approach eliminates several compliance errors but does not handle non-uniform strain distribution, compliance in the porous stones, and bedding errors. Some studies show satisfactory resilient moduli can be obtained when they are less than 60,000 psi using externally mounted

transducers. However, great care must be taken to minimize system compliance and calibrate the system. Many laboratories will not be able to achieve good results using external measurement.

2.3.4 Special Techniques Required in Calibration

When conducting the resilient modulus test using LVDT, compliance errors may occur if axial deformation is not correctly measured outside the cell. To calibrate compliance in the triaxial cell, a dummy aluminum or steel specimen is placed in the cell and subjected to a full sequence of stress level. The theoretical deformation in the dummy specimen, which has a known modulus, is calculated for a given stress level. The extraneous deformation in the testing system equals the difference between externally measured deflection of the specimen and the deflection occurring in the specimen. So, in order to obtain reliable resilient moduli, a very careful and proficient operation is required for a laboratory technician after the system compliance has been minimized.

Unfortunately, many labs do not have the required capability to perform a reliable calibration. Even with good calibration, the accuracy becomes highly suspect when the

magnitude of the system compliance correction becomes an important portion of the total observed deformation (Filho, et al., 1985). System compliance becomes quite important when resilient moduli becomes greater than about 10,000 psi to 15,000 psi (Barksdale, et al., 1975). With system compliance calibration, resilient moduli greater than about 60,000 psi measured with external LVDTs were found to be unreliable. Moreover, the reliability of compliance at deviator stresses less than about 5 psi is also subject to important errors.

2.3.5 Frequent damage of LVDT and its metal stick

An LVDT transducer, together with its metal stick, must be fixed on the clamps. They must be put on and off for each specimen. Meanwhile, during the setup of a specimen, the LVDT transducers and the metal stick need to be adjusted to different positions to achieve an alignment. Thus, the rubber connection in the middle of the metallic stick is vulnerable in this repeated adjustment. This rubber connection is the weakest part of the stick and suffers damage frequently. Once it is bent or broken, it can no longer provide good alignment. Thus the results obtained are greatly influenced by the damage of rubber connection.

2.3.6 Potential slip between the clamps and the membrane

Clamp slippage is a potential problem in measuring resilient modulus.

The use of clamps placed around the specimen with two LVDTs between the clamps to measure axial deformation has been quite popular for many years. To provide alignment between clamps, the rod holding the LVDT core usually has a hinged connection or is cut in half with a flexible wire between the two segments. The thin, circular aluminum or plexiglas clamps consist of two pieces that are hinged on one side and have a spring loaded connection on the other. Clamps are usually placed at either the one-quarter point in from each end of the specimen or at the one-third point. The gage length used over the center portion of the specimen is a compromise between measuring the axial deformation as close as possible to the center of the specimen, where strain is reasonably uniform, and using a longer gage length which gives larger deformation that can be more accurately measured.

Both clamps must be in a horizontal plane (i.e. perpendicular to the axis of the specimen) to obtain accurate readings from the clamp supported LVDTs. Chisolm et al. (1976) indicated that a jig or gage rod, temporarily

placed beneath each side of the clamp, together with a spirit level can be used to achieve accurate alignment. Both barreling distortion of the specimen and clamp misalignment can cause unwanted tilting of the LVDTs, which results in error in the axial deformation measurement (**Figure 2.3b**).

Clamp slippage is always a potential problem. The force tending to cause slip between a clamp and the membrane is equal to the acceleration acting on the clamp times its mass which includes the mass of the supported LVDTs. Thus, the use of a short pulse duration time or soft specimen, which results in large deformations, is more critical with respect to clamp slippage than for a long pulse time or soft specimen that gives smaller accelerations.

The force resisting slip is equal to the clamping force times the coefficient of friction between the clamp and the membrane/specimen. Using a reasonable clamping force while minimizing clamp weight reduces the tendency of the clamp to slip.

Some proposals have been presented to avoid the slip between the clamps and the membrane, varied from stud to pin supports for axial deformation measurement devices. Chisolm and Townsend (1976) placed a small quantity of epoxy glue on top of each of the clamp contact points with the rubber membrane. Sweere (1990) used individual LVDT support blocks

glued directly to the membrane. For static tests, the relative slip between the specimen and the enclosing membrane does not occur until near or after failure (Burland, 1982).

Metal studs have been placed through the rubber membrane into granular specimens to eliminate possible slip (Boyce, 1976). Use of studs offers an excellent positive method for supporting LVDTs or proximity gages. To prepare a granular specimen with studs, Boyce and Brown used a vibratory table to densify the material. The care required to properly place the studs and prepare the specimen, however, makes this method unsuitable for routine laboratory use. Boyce concluded that measurement of at least three axial strains is necessary to provide a reliable average value. The results of recent studies, however, indicate that two LVDTs are sufficient to give a reliable resilient modulus, provided good alignment is achieved, and two are more practical to use for production type testing.

Dupas (1988) used pins by pushing them into sand plugs placed in the specimen to support proximity transducers. Small cross-shaped vanes have been pushed into a soft cohesive soil. Holes have also been drilled in asphalt concrete specimens and reference plugs glued in.

For aggregate bases, Crockford, et al.(1990), fastened three small, individual aluminum blocks onto the top one-third point of the specimen and three blocks onto the bottom one-third point. A pair of aluminum blocks, one located above the other, supported each LVDT measurement assembly. Clamping action was provided by placing a large O-ring around each level of three blocks. Three axial LVDTs were used to measure deformations which define the plane of the axial specimen deflection.

2.4 Review of Non-contacting Approaches

A number of different non-contacting sensors are available including inducive, optical, ultrasonic and pneumatic types. Ultrasonic non-contacting type sensors have a low sensitivity while pneumatic non-contacting type sensors are large and hence are not suitable for resilient modulus measurement (Linton, 1988). Both inductive proximity sensors and optical extensometers offer excellent methods for measuring both axial and radial deformations. However, an optical measurement system has the disadvantage of a high cost of $30,000 to $50,000 or more depending on the accuracy desired and options selected, comparing to the moderately expense of $500 to $3,000 for each proximity sensor.

An additional important disadvantage of the optical extensometer when used in triaxial testing is that the optical line of sight must pass through a flat, clear plate of preferably optical glass. To overcome this limitation, the chamber of the triaxial cell has to be redesigned to be either square or else round with a small flat window. The flat window, three inches to six inches in size, must extend above a height slightly greater than the gage length over which relative deformation is to be measured.

This study has focused on the inductive non-contacting system using proximity transducer probes. An overview of the literature reveals that a number of researchers have studied and applied non-contacting proximity sensors in soil resilient property tests with different schemes and purposes.

M. H. Maher, et al. (1996) evaluated the utility of non-contacting proximity sensors for the measurement of small strains in resilient modulus tests. The proximity sensor measurements of resilient modulus were compared with those obtained from LVDTs. The important issue of granular soil sample preparation and its effect on the magnitude of resilient modulus was evaluated. The authors proposed two methods to facilitate sample preparation and to provide good contact between the soil and the loading platen. The effect

of conditioning sequence on sample integrity was also investigated for the two proposed methods of compaction. In addition to the experimental program, a number of constitutive models used for prediction of resilient modulus of granular soils were examined.

S. Nazarian, et al. (1996) proposed a procedure for base materials and utilized non-contacting probes to avoid the well-known problems with mounting LVDTs on the specimen in measuring deformations. To maximize the amount of information gained, the researcher measured the lateral deformations with non-contact probes to determine the Poisson's ratio. On the basis of tests on nine synthetic specimens with known properties and nine different base materials from different parts of Texas, the study concluded that the proposed methodology yields accurate and repeatable results.

W. B. Gookin, et al. (1996) developed a cyclic triaxial testing system capable of measuring very small to large strain properties on a single specimen by combining a wide variety of existing instrumentation, including piezoceramic bender elements, internal displacement measurement devices (both contact and non-contact), local displacement measurement devices, a sensitive internal load cell and an external load cell. The bender elements provided information

on soil properties in the nearly linear elastic (very small strain) range. Local and non-contact internal displacement measurements provided information about small strain range properties, whereas more traditional internal displacement measurements provided information in the small to large strain range. In addition, this apparatus can be used over a wide range of loading frequencies to investigate the effect of frequency on dynamic soil properties. By combining this equipment in a single testing system, a number of tests were run on one specimen, eliminating the effects of variability. The broad variety of displacement measuring instruments also allows direct comparisons of these techniques on a single specimen.

Ayushman Gupta, et al. (1996) used non-contacting proximity probes in the resonant column and torsional shear tests to measure radial strain. During the conventional resonant column and torsional shear tests using a Stokoe device, only the change in height of the specimen was measured. The researcher modified the Stokoe device to enable the measurement of change in diameter of the specimen along with the change in its height during resonant column and torsional shear tests. The diameter change measurement system was composed of three proximity probes, coaxial cables, proximitor conditioners, and DC power supply. The

probes (7.9 mm diameter) were capable of making non-contact displacement measurements with a resolution of 0.025 mm using a metallic target. These probes were fixed along the circumference of the outer chamber at equal 120 degree spacing. The vertical location of these probes was such that they corresponded to the midheight of the specimen. Each probe was mounted on a micrometer to enable accurate adjustment of the probe. This system gave a linear output for a distance range of 0.38 to 2 mm between the probe tip and the metallic target. During the tests, the targets (circular copper foils 26 mm in diameter) were fixed on the soil specimen, and output voltage from each of the three proximity probes was recorded directly by a computer. The average readings of the three probes were used to calculate the change in the diameter of the specimen.

R. Pezo , et al. (1998) reported a new triaxial test set-up to examine large specimens (150 mm in diameter and 300 mm in length). The system was designed to use eight proximitors; two placed on opposite ends of a diameter at mid height of the specimen to measure lateral deformation and six placed in pairs along the specimen and distributed at 120 around the specimen, to measure axial deformations. To calibrate this set-up, nine elastomer specimens were manufactured with three different stiffnesses, to cover the

typical range for highway base materials. A quasi-static test program was implemented using these specimens to evaluate the capabilities and shortcomings of the system, the repeatability and accuracy of the test results, and the optimization of the gage length to be used for measuring axial strains in the production test system. An axisymmetric computer model was assembled to predict axial and lateral deformations at the measuring points used in the experimental program. The experimental and numerical results were in fairly good agreement except in the vicinity of the loading end platens. The numerical results indicated overprediction of the moduli by about 15% when the gage length used was the whole length of the specimen rather than the central one-fifth. The experimental data showed somewhat higher discrepancies (about 20%) for the same range of gage lengths.

The studies presented above show that non-contacting proximity probe, in light of precision, is sufficient to measure the deformation of soils and appear to be a potential alternative of LVDT in triaxial tests. However, the details of the advantages and disadvantages need further investigation into the triaxial tests and whether there is any unseen aspect in practice that is incapable of alternating LVDT.

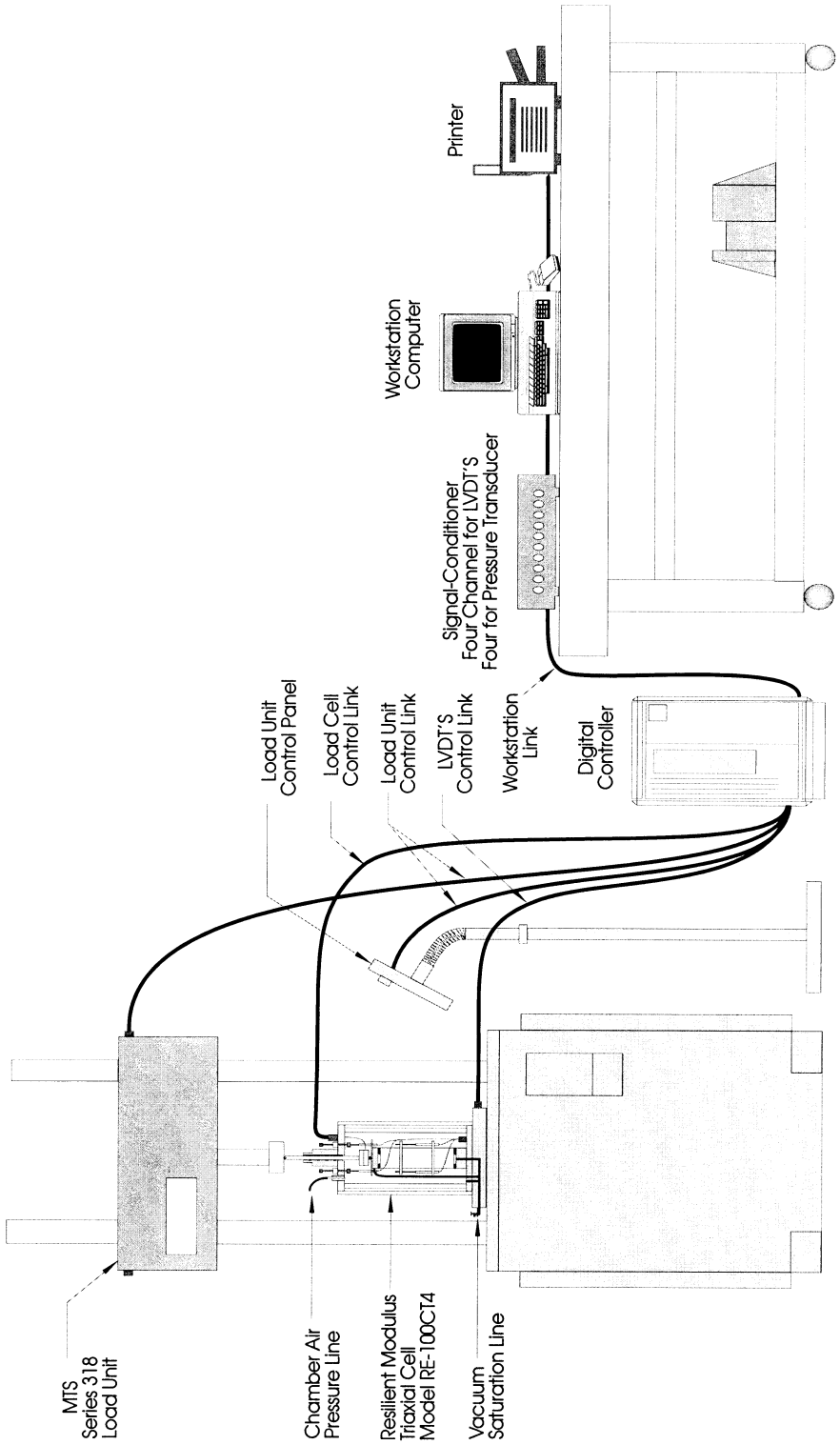

Figure 2.1 Sketch of the resilient modulus testing equipment

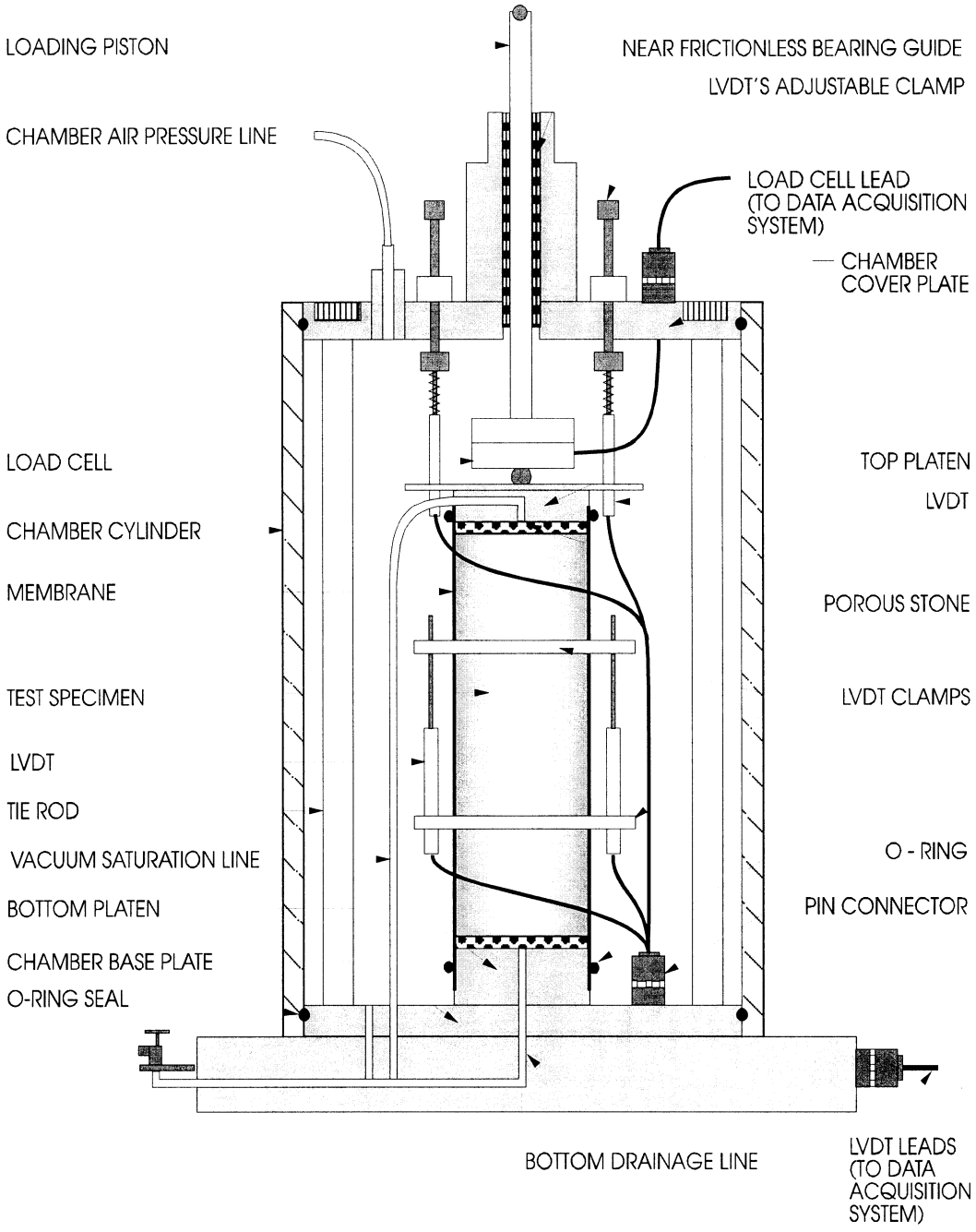

Figure 2.2 Triaxial chamber with internal LVDTs and load cell

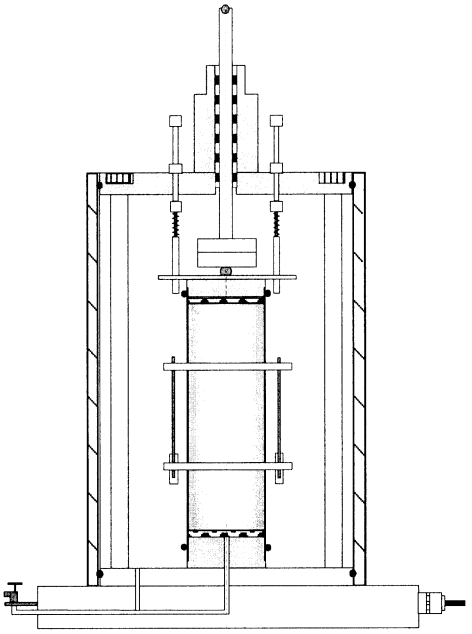

Figure 2.3a Correct Alignment

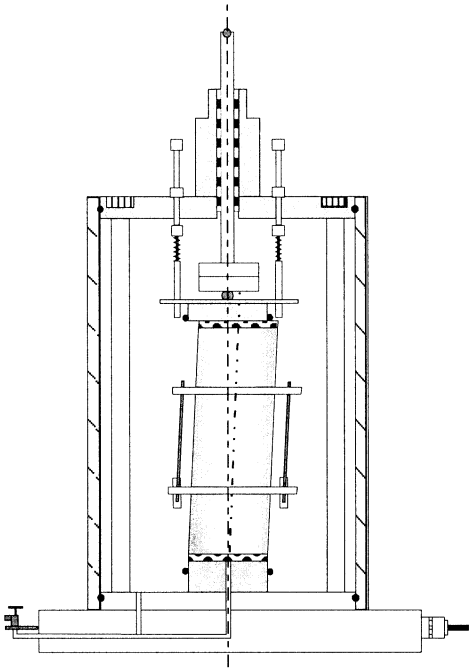

Figure 2.3b Misalignment due to specimen barelling

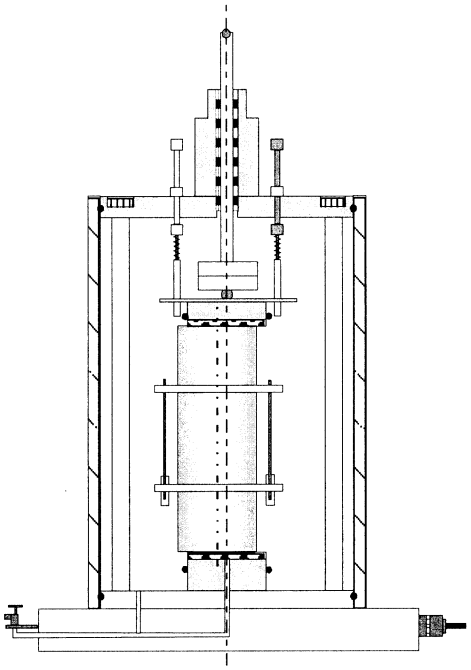

Figure 2.3c Misalignment between the specimen and load cell

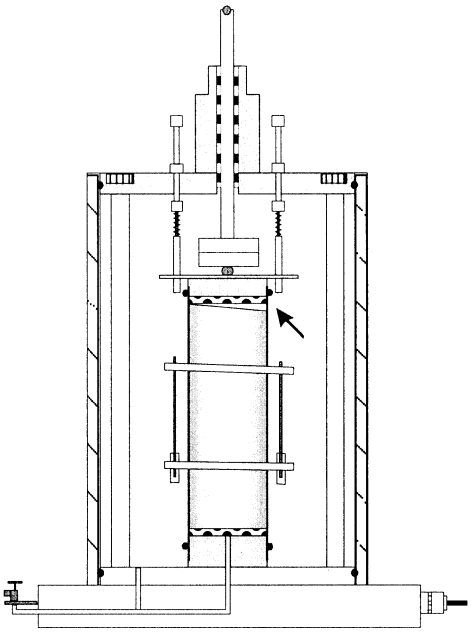

Figure 2.3d Misalignment due to bad compaction

CHAPTER 3

INSTRUMENTATION AND EXPERIMENTAL DESIGN

3.1 General

The purpose of the triaxial test is to simulate and monitor specimen behavior when it subjected to the normal field working conditions, ranging from the small stress pulses of lighter vehicles to moderate stress pulses imposed by the heavier trucks. This monitoring procedure requires the apparatus to measure any small deformation, for which a highly sensitive measurement probe is needed, and the larger range of the precision, corresponding to the behavior of hard soils as well as soft soils. Thus, the proximity probes should be able to cover as many soil types as possible. The selection type of probes is critical. If the initial measurement is not accurate and reliable, all the other efforts will be compromised in the final results, while a well-selected proximity probe can save a lot of effort in the system tune-up and data acquisition stratagem.

Since a main goal of this research is to evaluate the plausibility of alternating the LVDTs with non-contacting

proximity probes in the resilient modulus tests, the MTS triaxial testing system has to be modified to ensure both LVDT measurement and non-contacting proximity measurement to be performed simultaneously on a single specimen.

3.2 Probe Selection

Basically, proximity probes are non-contacting, gap-to-voltage transducer systems that measure static as well as dynamic distances between the probe tip and the observed target. Their general application requires an accurate, reliable, non-contacting displacement measurement. However, their most common use is as shaft position and vibration measurements on rotating and reciprocating machinery. They are designed to measure radial vibration and axial thrust motion on large machine rotors. Due to the similarity of the measuring circumstances of the triaxial test, the proximity probes have been studied and implemented in soil resilient modulus tests in recent years.

Principally, the non-contact inductive displacement transducers perform two functions: 1) generate a high-frequency signal that is transmitted to the probe tip; and 2) receive and process a signal from the probe tip, so as to provide a direct current proportional to the distance

between the target material and the probe tip. The high frequency signal is passed through an active coil located in the probe, which creates a magnetic field around the probe tip. When a conductive material (the target) interferes with the magnetic field at the probe tip, eddy currents are generated in the target. The impedance of the active coil changes depending on the strength of the eddy currents, thus the output voltage of the balance bridge is modulated by the target material moving in front of the magnetic flux around the probe tip. The travel distance over which this "voltage-to-gap" proportion is linear, may be from several mils to as much as one inch. An important advantage of the eddy-current probe is its immunity to oil and dirt, making it particularly suitable for use in machinery.

From a mechanical viewpoint, vibration transducer systems are naturally divided into two groups, based on the type of measurement made by each:

- proximity transducer systems measure shaft or target relative vibration
- seismic sensors (velocity and acceleration) measure target absolute vibration

Consequently, applications for such probes fall into two categories:

1. Distance Measurement: Typical applications are for measuring thermal expansion of machine casings and rotors, thrust bearing wear, etc. The probe is chosen to match the range of distance to be measured. Output sensitivities vary from 20mv/mil to 200mv/mil, depending on the distance range. In general, the greater the linear range required, the greater the probe tip size, in order to have its magnetic field extend over a greater distance.
2. Vibration Measurement: The non-contacting operation of the eddy-current probe permits vibration of rotating shafts to be readily measured. The probe is positioned at some nominal gap (usually near the center of the linear range) and peak-to-peak vibration amplitude is measured. Frequency response to 10 kHz is possible, giving an electrical replica of the vibration waveform. Two or more probes may be installed to obtain vibration at various points and in orthogonal axes.

An eddy-current probe system consists of a probe connected to an associated probe driver, together with a power supply. Such a system is used with a variety of indicator, controller, or monitoring devices.

A typical probe system has a linear measuring range of 80 mils and an output of 200mv/mil with a 4340 steel target.

There are several brands and models of the proximity probes available in the market, with different prices and diverse capacities. Many companies have been designing and manufacturing eddy-current proximity probes for more than 30 years, namely, Bently Nevada Incorporation, Metrix Instrument Co., Indikon Company, Inc., etc.

The selection of the proximity probes is influenced by several factors. The most important factor should be mechanical movement or vibration characteristics of the specimen (target) under both normal and malfunction operating conditions. Since the majority of strain measurements in soil property tests are cylindrical or radial, the optimum transducer is the type that can best indicate a change in shaft or position vibration.

The optimum transducer probe should also be the type that produces a maximum change in output signal as a result of a minimum change in target vibration condition. Also, the ideal transducer probe would be best suited for both dynamic monitoring of movement and malfunction diagnosis.

Aside from the above considerations, the following factors entered in the selection process:

- dimension of the probes
- sensitivity
- linear range

- output signal compatibility

The selected probes for this study were model 590(5M) Oscillator/Demodulators manufactured by Indikon Company, Inc. with a nominal linear scale factor of 100 millivolts/mil. The laboratory calibration showed the same scale factor with a power supply of 24 volts using a target plate of AISI 4340 steel.

3.3 Probe Specifications

The Model 590 non-contacting proximity probes have the following specifications:

- a range from 0 to 200 mils
- sensitivity of 100 mV/mil for vibration measurement and gap measurement with output range -2 to -20 volts
- linearity of ±1 percent between 20 and 90 percent of full scale (for probe cables up to 10 ft)
- frequency response of DC to 10,000 Hz (-10%)
- temperature range up to 300°F (149°C)
- power at -24V DC, 7mA (supplied to models 590 and 591 oscillator/demodulators) and intrinsic safety requirements readily met when suitable measuring instruments are used

- target materials included a variety of magnetic and nonmagnetic steels which work well; chrome and aluminum are measurable, but specifications are more limited
- temperature stability
  - probe: -0.04% per degree C over operating range
  - oscillator/demodulator: +0.03% per degree C over operating range
- a probe cable length that is up to 50 feet (15 meters)

All probes are interchangeable to within ±5% and most within ±3%.

Meanwhile, the following three advantages claimed by the manufacturer were some of the reasons involved in the final decision:

1. Less sensitive to surface conditions

The operating frequency of the selected probes (Indikon Company) is approximately 200 kHz. This means that the probes produce eddy currents that penetrate farther into the metallic surface opposite the probe, rather than being confined to a layer of only a few thousandths of an inch, and are less susceptible to so-called "electrical runout". (Electrical runout is due to circumferential inhomogeneities on the surface of a shaft. It produces what appears to be a

vibration signal on a perfectly round shaft that is rotated.) Because of their deeper penetration, the selected probes generally avoid electrical runout effects when used with turned surfaces. Special shaft preparation, such as grinding, polishing, burnishing, peening and knurling, can generally be avoided.

2.Linearization

Indikon Company has developed proprietary linearizing techniques that enable a probe of a given tip diameter to have a larger operating range. In applications where space is limited, linearization allows a smaller probe to be used.

3.Operation to zero gap

The selected probes operate down to the point of contact between the probe tip and the metal target, as contrasted with other makes where the probe dies as the surface is approached.

3.4 Probe Placement

3.4.1 Probe Position

Proper design and installation of the transducer components are as important as proper transducer selection. Although various kinds of mounting hardware, specifically

designed for complete electrical and mechanical protection, were available in the market, the particular and limited space in the existed triaxial cell prohibited the use of those accessories. The mounting position and hardware had to be specifically designed. The four LVDTs, four proximity probes as well as the four targets had to be accommodated in the eight-inch-diameter cell properly, meanwhile enough space needed to be left for the operator to install the parts and make alignment during the test setup.

A key point noticed in the design is that the LVDT and non-contacting proximity probes measured the deformations of the specimen in different ways. These differences existed in both the relative movements between the probes and the computations of the deformations. Comparing to a non-contacting proximity probes, the LVDT and its target were small and light, thus were easy to be attached to the specimen. When the specimen experienced a deformation, both the LVDT and its target moved closer or further. One set of a LVDT and its target was sufficient to reflect the deformation of the specimen. While the size and the weight of a proximitor tip disallowed it to be mounted in the same way. The proximity probe, with its long shield cable, was mounted to a rigid place and the deformation of the specimen measured by monitoring the movement of the target, attached

on the specimen. Thus, it required two sets of proximitors and targets to obtain a deformation and a rigid support system to ensure there was no movement on the probes during testing.

This was accomplished by mounting each probe tip on a racket mounted on the rods inside the cell (**Figure 3.1**). The mounting had to be accomplished in such a manner that the probes can be conveniently adjusted at the beginning of a test to place the probe tip at about 10 to 20 mils from the target.

The mounting rackets were locked in place with screws on two of the three rods connecting the top and bottom plates of the triaxial cell (**Figure 3.2**). The design of the mounting ring and the assembly of the probe in the triaxial cell are shown in detail in **Figure 3.3** through **Figure 3.7**.

To compare the behavior of the non-contacting probes and LVDTs, altogether four proximitors were placed in the cell with two on each side (Figure 3.1).

3.4.2 Probe Orientation

The proximity probes measured the displacement of the target as the metal target approached or moved away from the probe tip. However, during a triaxial test, the specimen experienced a significant deformation after the 1,000 cycles

of conditioning. It is important to let the target go as far as possible in the tests, otherwise, the probes may suffer damage when the specimen experiences a larger deformation (**Figure 3.8(a)** and **Figure 3.8 (b)**).

The axial deformations were measured along the middle one-half of the specimen with four proximitors. Two were installed about 51 mm high from the bottom of the specimen and two were installed about 51 mm high from the top. At each height, the two proximitors were located at 180-degree intervals. The axial deformation was calculated as the average of the deformations measured at the two sides. The variations between the deformations measured at each side were carefully monitored to ensure that the specimens deform uniformly under the applied axial load.

Meanwhile, the internal LVDTs measured the exactly same deformations using a clamping device. Deformation along the full length of the specimen was measured by the two LVDTS mounted above the specimen.

3.4.3 Probe Calibrations

In order to obtain high accuracy, it was necessary to calibrate the proximitors using the same target that was used in the test set-up and the calibrations had to be performed at the test temperature and with an identical

constant power supply. Several stages of systematic calibration were conducted before and after the installation of probes.

First, each individual proximitor was calibrated with a modified calibrator, which can move the target at a precision of 0.0001 inch. During this stage of calibration, a 24v DC power supply was used and the output signals were measured with a multimeter. The results of the calibration of each probe are shown in **Figure 3.9** through **Figure 3.12**. All the four probes were able to provide a perfect linear range from 10 mils to 150 mils, with regression rate over 0.999.

Secondly, each probe was calibrated by connecting to the MTS machine. Data were collected with both multimeter and computer. The regression lines were the same to those obtained in the first stage of calibration. The data readings from the computer were fluctuated, however, the average readings were very close to the data from the multimeter.

Next, in addition to calibrating each probe individually, overall calibrations of the testing apparatus were conducted by adding an element to the system each time. Typical calibration graphs are shown in **Figures 3.13** and

3.14. All the four probes performed in a linear range of 10 mils to 140 mils.

To best calibrate the system, a micro-positioner was installed between the probe and the mounting ring for in-place calibration. This single stage positioner measured only 0.20 x 0.44 x 1.03 inches with 0.125 inch travel. It provided precise and smooth motion with no backlash, by a positive spring loaded carriage, straight within 1 micron and less than 1 micron maximum wobble. It featured a fine 80 TPI screw adjustment. On the 0.4 inch square mounting surface there was a 0.155 inch tapped center hole for transmission and mounting. These features were specifically designed for linear positioning and calibration.

The results of these in-place calibrations are shown in **Figures 3.15** and **3.16**. Note that the slopes of the regression lines were very close to the previous results.

Generally, the output signals of the proximity probes are proportional to the target position with respect to the probe tip. This voltage increases when the gap increases from 0 to 200 mils at an average rate of 100 millivolts per mil. Best linearity (<=0.5% of F.S.) was attained in the range of 10-140 mils.

3.5 Target Placement

3.5.1 Target requirement

The target material and size have a significant effect upon probe performance. The probe response depended upon both the magnetic properties and the bulk conductivity of the target material. The performance of probes with the materials most used in machinery (alloy and stainless steels) is well-known and was conducted by the manufacturer.

Since the penetration of eddy-currents into the target material is small, target thickness is determined mostly by the need for mechanical rigidity, 50 mils being more than adequate. Probe connectors, when mated, must not touch any machine metal parts to avoid faulty grounding.

3.5.2 Target Design

The calibration made by the manufacturer of the proximity probe and oscillator/demodulator was based on a target material of type 4340, 4140 or equivalent carbon steel. Following this, the target material for this research was type 4340. Two sets of targets were designed and used during the study, one set with a diameter of 1.2 inches, the other set with a diameter of 1.7 inches.

Knowledge obtained from this study was that a smaller target results in non-linearity as the probe gap increases. The target area for the probe must have a diameter of at least 1.75 inches concentric with the probe tip, as required by the manufacturer. However, due to the very limited space in the triaxial chamber and the special supporting techinique of the target, the size of the target was designed as 1.2 inches, on the basis that it would perform well in both static and dynamic calibrations. A smaller sized target with a lighter weight would avoid the initial displacement after mounting it to the clamp.

Figure 3.17 shows the primary design of the target with a diameter of 1.2 inches.

Repeated tests show that the 1.2 inch targets are sufficient with the stiff soils having higher resilient modulus. The effect of the size is not detectable when the gap is at the lower side of the range. The influence becomes significant only when the distance comes closer to the upper side of the range. The minimum target size should be determined by the size when the target is at the end of the linear range (**Figure 3.18**). A larger range needs a larger target diameter.

For a softer soil with a lower resilient modulus, the deformation after the 1000 cycles of conditioning can exceed

100 mils or even higher. With the testing loads, the total deformation will be higher than 120 mils or more. When the distance between the target and the probe reaches the upper side of the measuring range, the system gave irrational data. To solve this problem, the operator needs to move the probes closer to the targets.

The surrounding environment of the probe also needs to be considered. Of extreme importance is to provide the probe tip circular clearance. The magnetic field of the probe extends beyond the immediate area between the probe tip and the target, so any metal at the side of the probe also affects the performance. Since this metal appears to the probe as an additional target, it is important that the metal to the side of the probe be sufficiently distant so as not to affect its linearity.

As recommended by the manufacturer, any metal other than the one being sensed should be at least 1.0 inch away from the probe tip's centerline over a distance of 1.5 inches from the target towards the probe body. A metallic surface in a plane x inches away from the probe tip's centerline has much less effect than placing the probe tip in a hole whose radius is x inches. Adjacent metal should preferably be one or two probe diameters distant. Where this

is not possible, special linearization techniques are needed to achieve the desired result.

During the first phase of the instrumentation, many days elapsed before noises were introduced to the circuit. The noises were cut down significantly after the metallic micro-positioner was moved away from the probe tip. (**Figure 3.19a** and **Figure 3.19b**)

3.5.3 Clamp Design

As discussed in Chapter Two, a clamping device is essential to the specimen and LVDT alignment. Clamps in bad condition will result in a failure of the test. Meanwhile, slippage between the membrane and the specimen is always a potential problem.

Although the non-contacting proximity probes may ultimately eliminate the clamps by mounting the targets with O-ring, glue, or make it L-shape, in this study, the clamps were used to better compare the non-contacting proximity probes with LVDTs. The positions of the LVDTs were required to horizontally rotate to an angle to make room for the target. The clamp slippage was minimized by raising the clamp forces. This stronger clamp force was also required by the extra weight of the targets.

3.6 Power Supply

The proximity probes required -24v DC power to produce an eddy current.

A Preteck DC (model 3003B) power supply was first used. This was a regulated digital DC power supply, with the output DC voltage of 0~30v, current 0~3A. Both load regulation and line regulation <= 0.02 + 2 mv. ripple & noise voltage <= 0.2 mv(rms), 4 mv(p-p); ripple & noise current <= 2mA(rms), 10 mA(p-p).

This power supply works well in static calibration. However, after the dynamic calibrations and tests were conducted, this power supply proved to be unsuitable to the system, because it brings noise to the system. The noise was detected and illustrated by connecting an oscilloscope to the system. This power supply produced noises with the frequency around 200 kHz, coincided with the frequency of the oscillator/demodulator of the proximity probes, and was one of the sources of the unstable data.

The final decision on power supply was made to use two 12v acid batteries in a series connection. The batteries were model UN2796. The total voltage was around 24.6~25.4v after recharging, which was higher than the requirement, but did not apparently adversely affect the measurement.

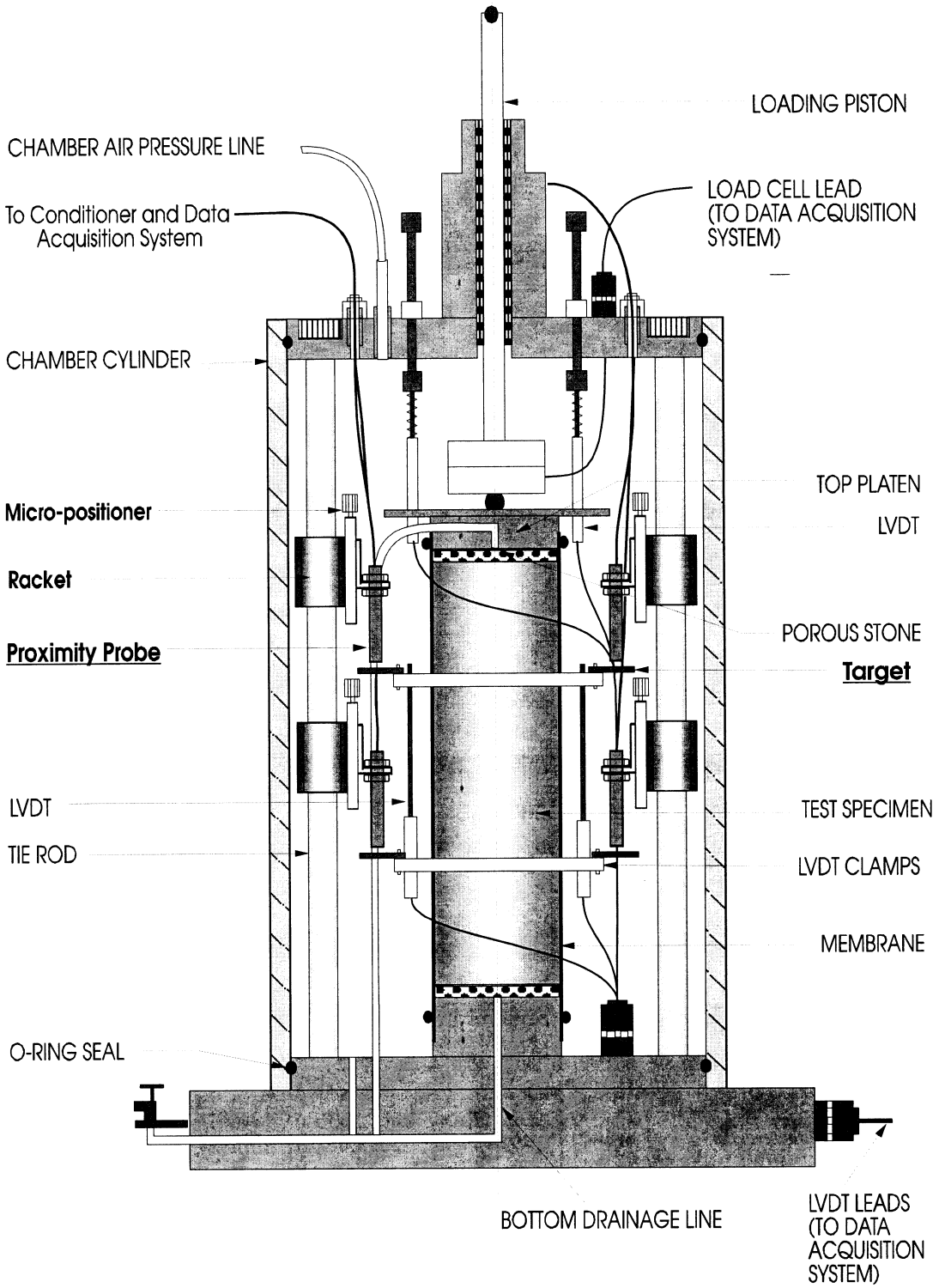

Figure 3.1 Triaxial chamber with proximity probes and LVDTs

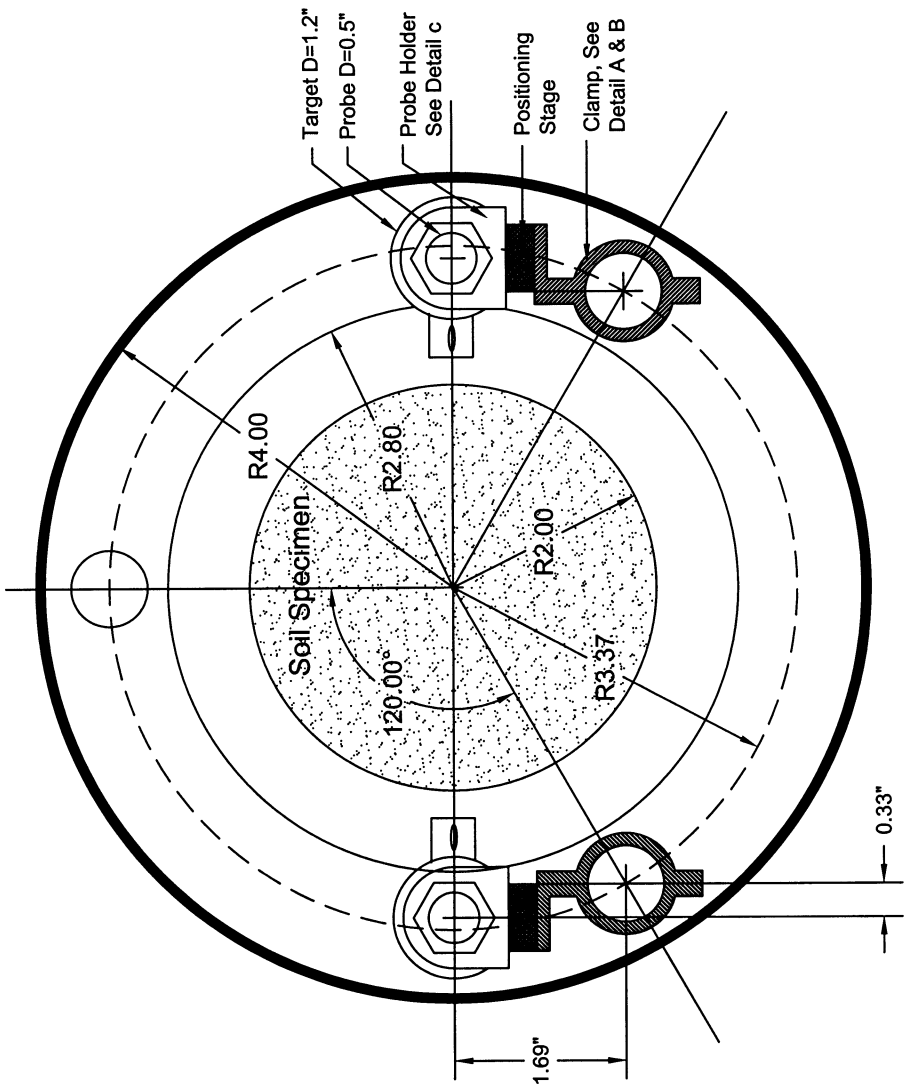

Figure 3. 2 Plan view of the mounting for the proximity probe in the chamber

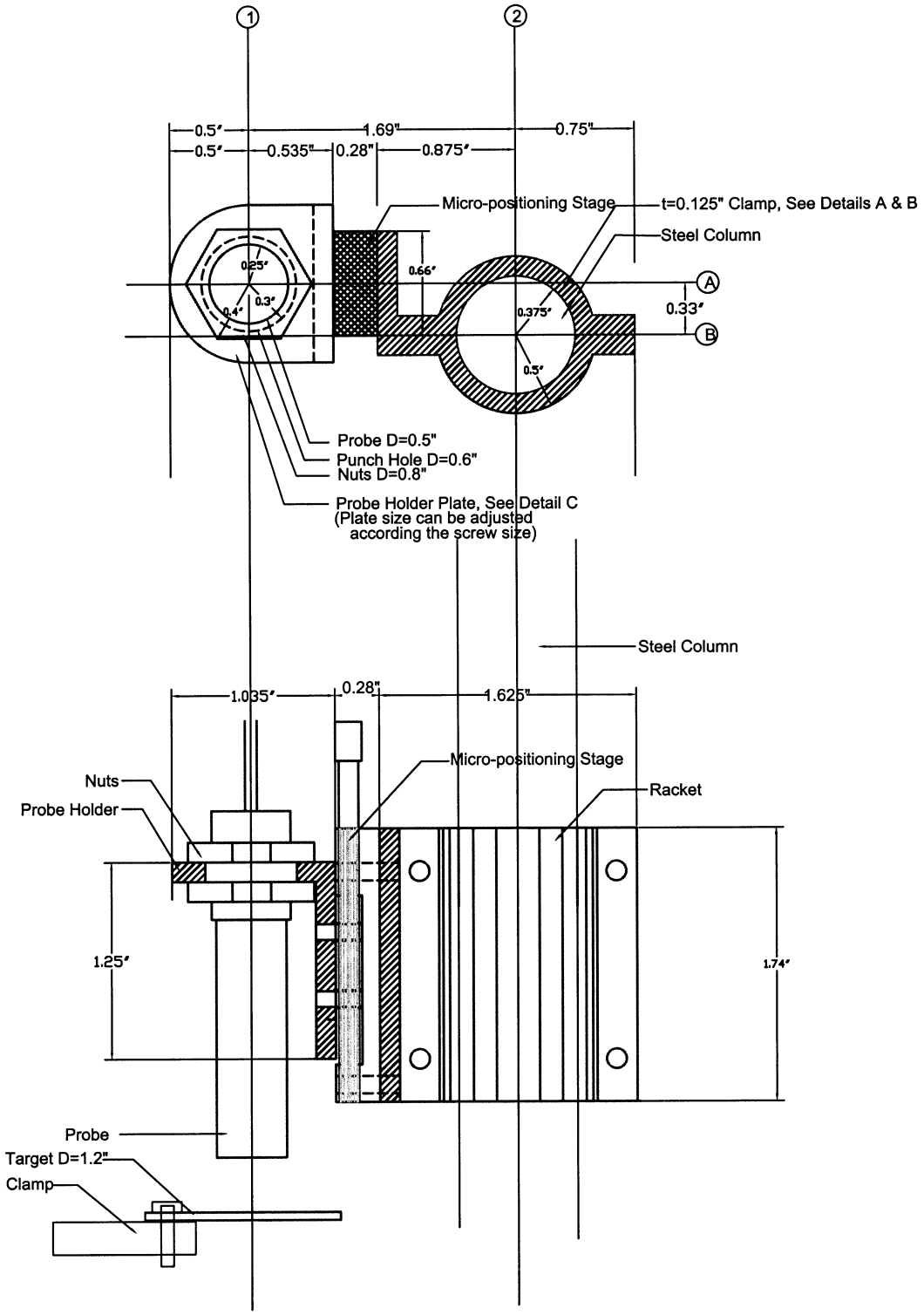

Figure 3.3 Assembly view of the probe

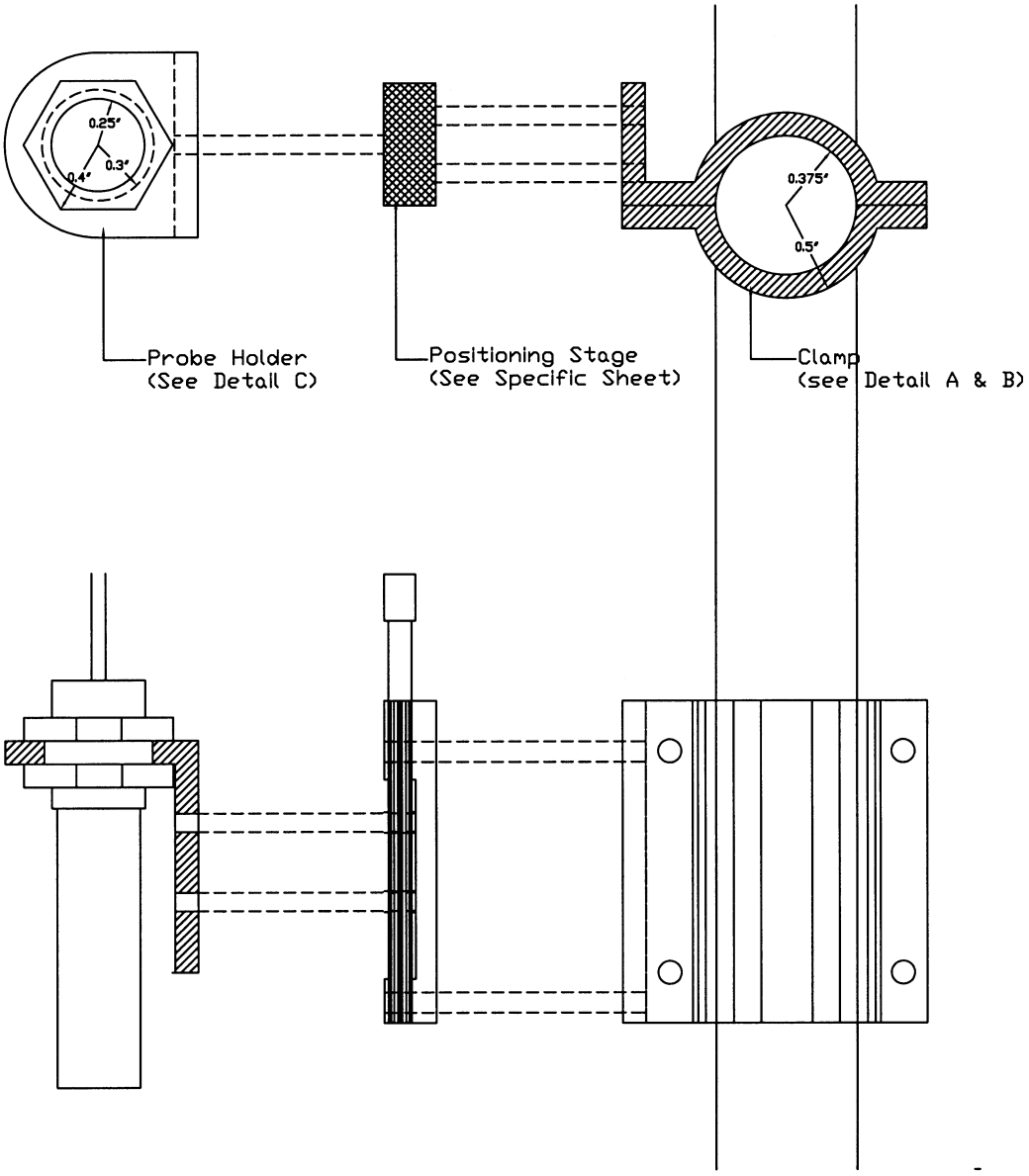

Figure 3.4 Mounting of the proximity probe

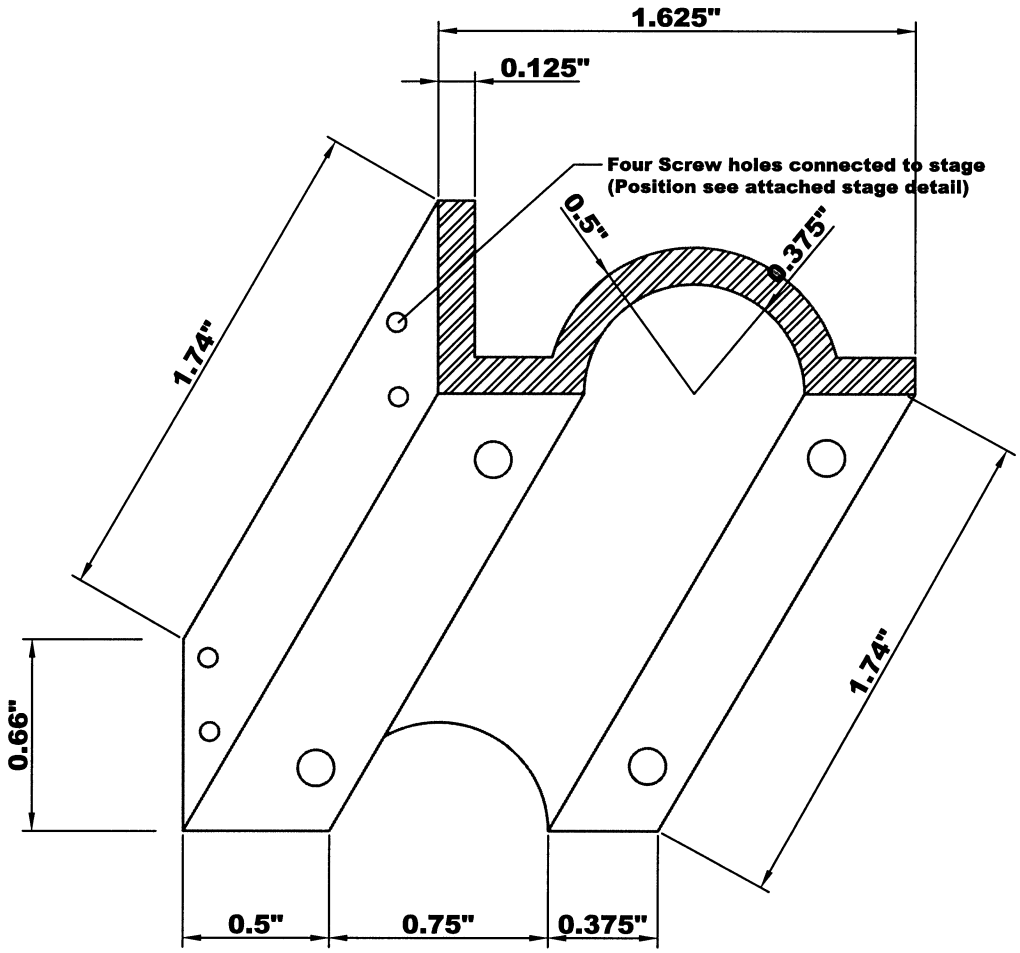

Figure 3.5 Detail of the racket (Part A)

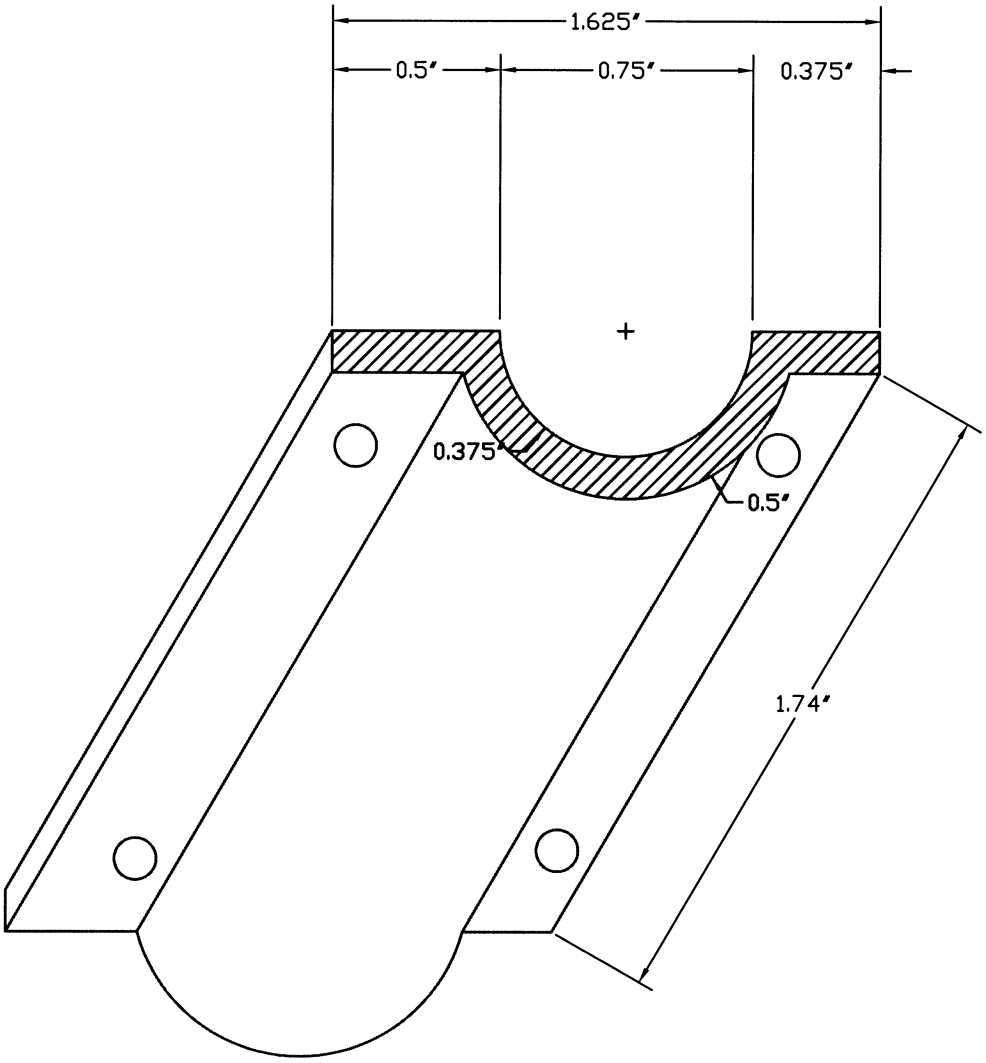

Figure 3.6 Detail of the racket (Part B)

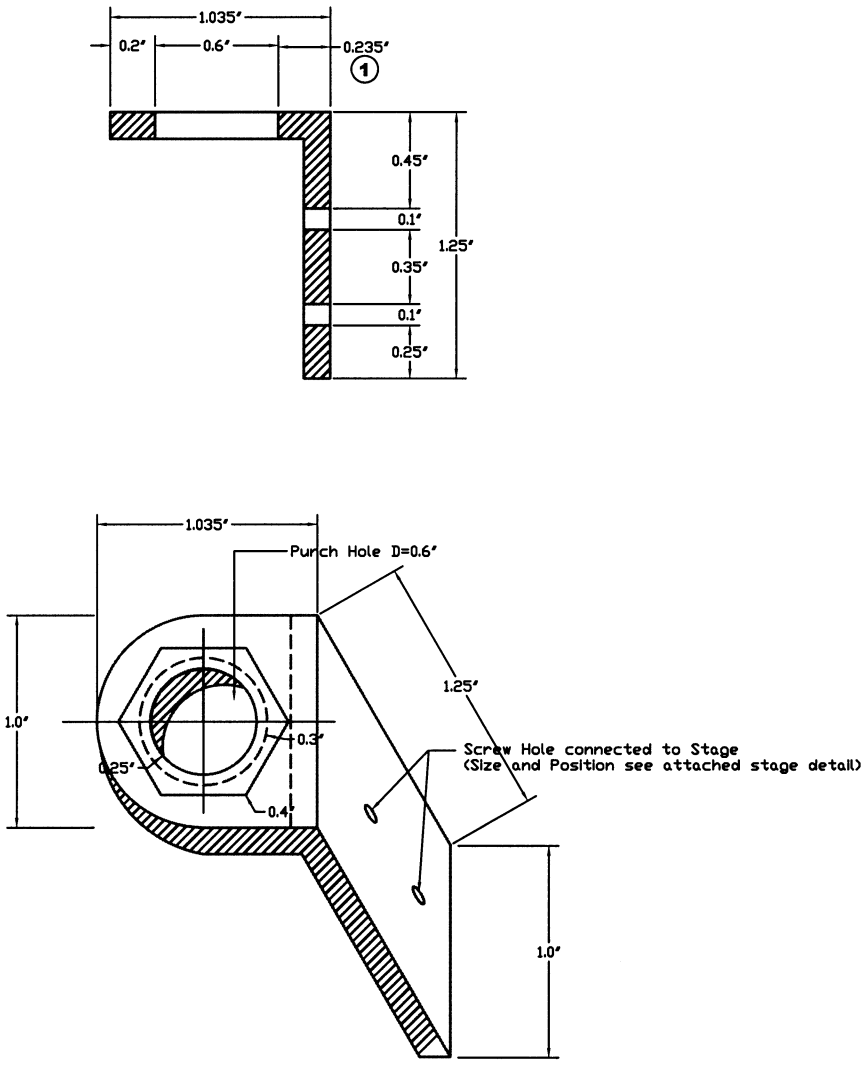

Figure 3.7 Detail of the racket (Part C)

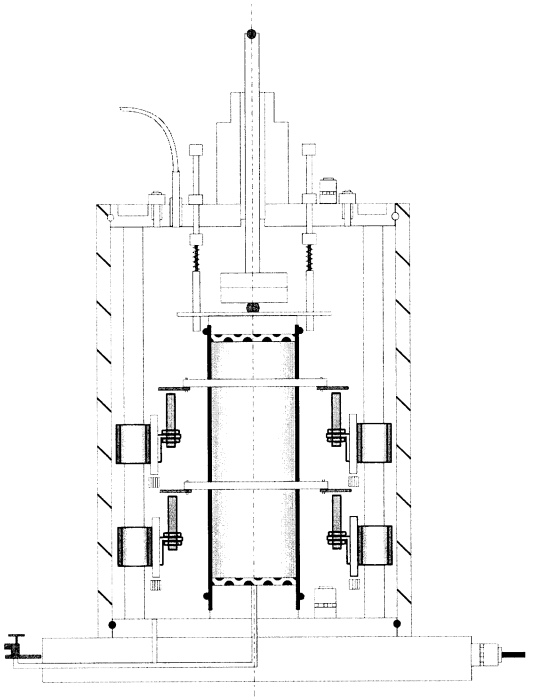

Figure 3.8 (a) Targets go closer to the probes during a test

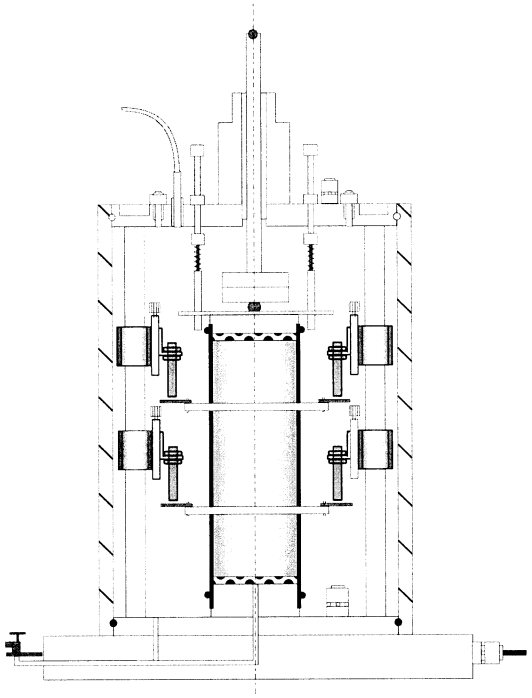

Figure 3.8 (b) Targets go further from the probes during a test

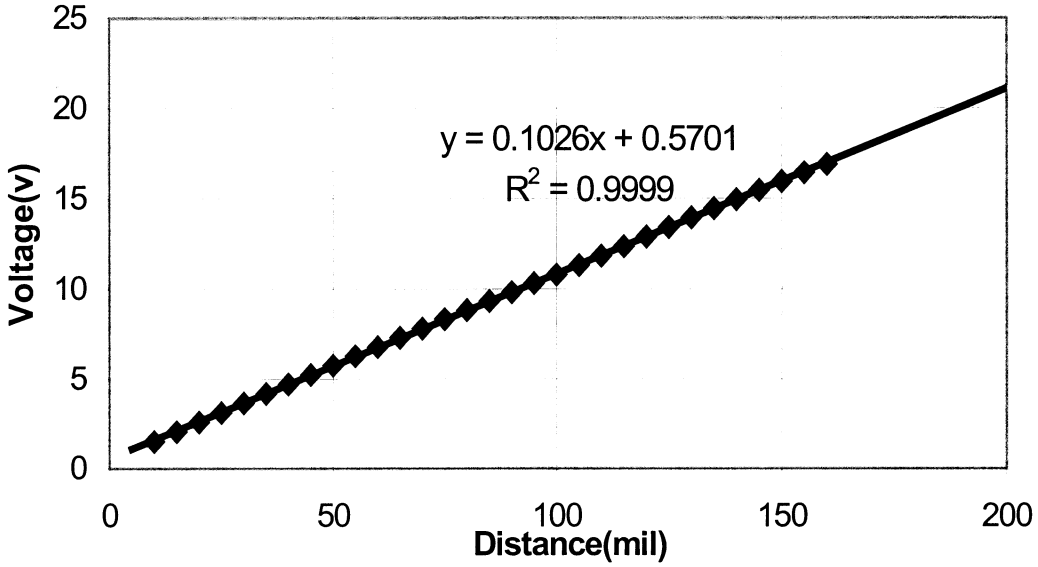

Figure 3.9 Calibration line of probe No.1

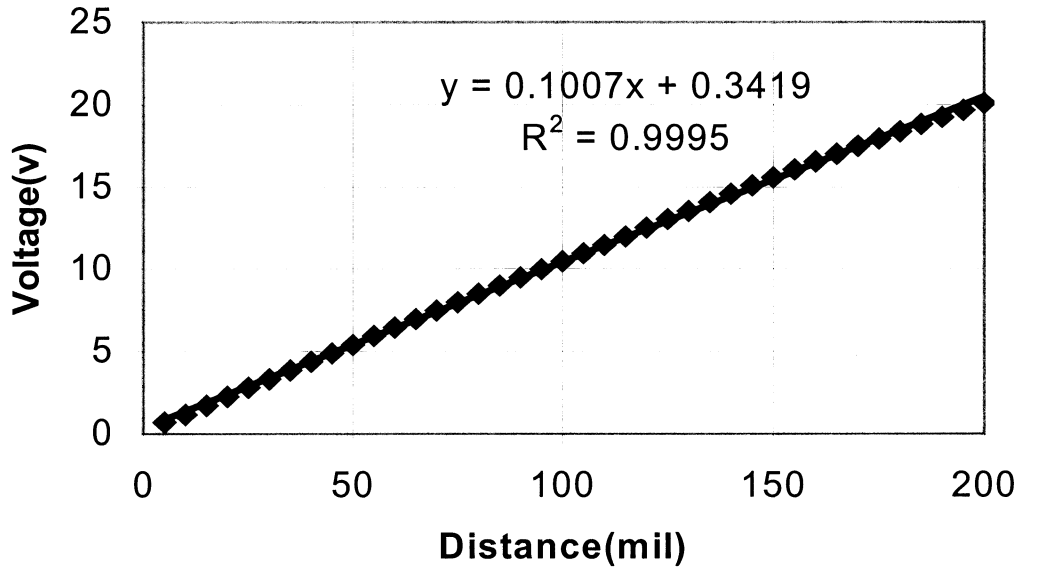

Figure 3.10 Calibration line of probe No.2

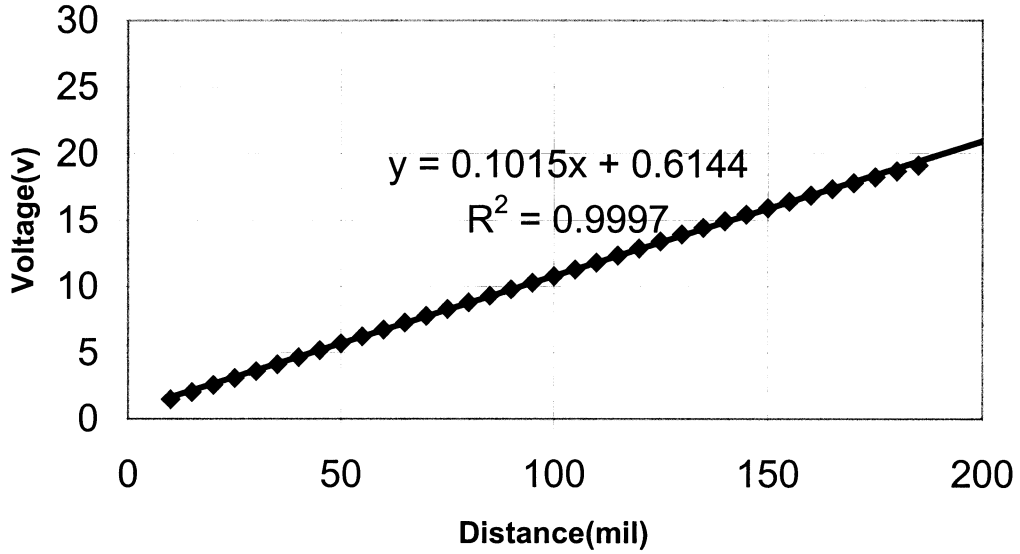

Figure 3.11 Calibration lLine of probe No.3

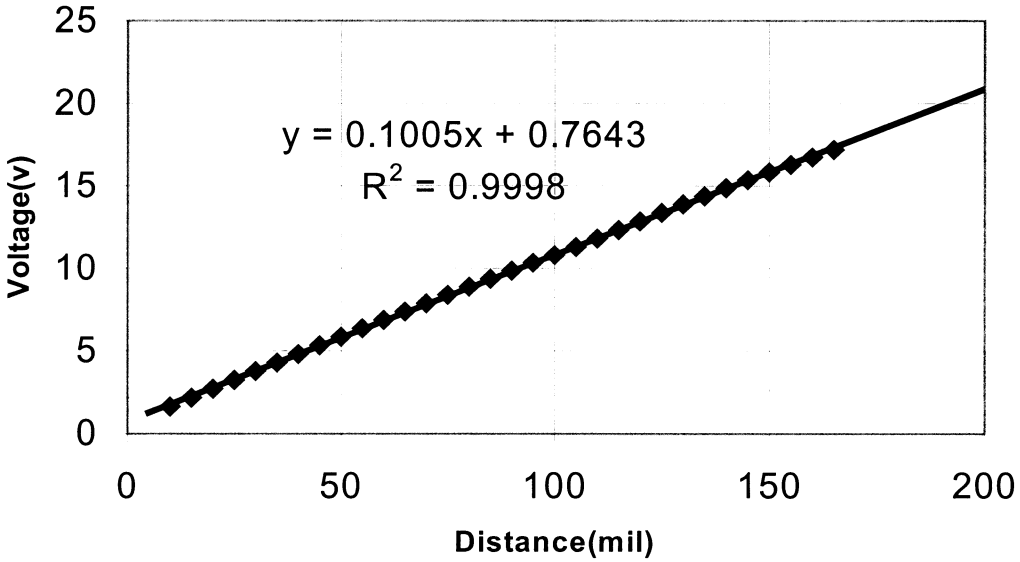

Figure 3.12 Calibration line of probe No.4

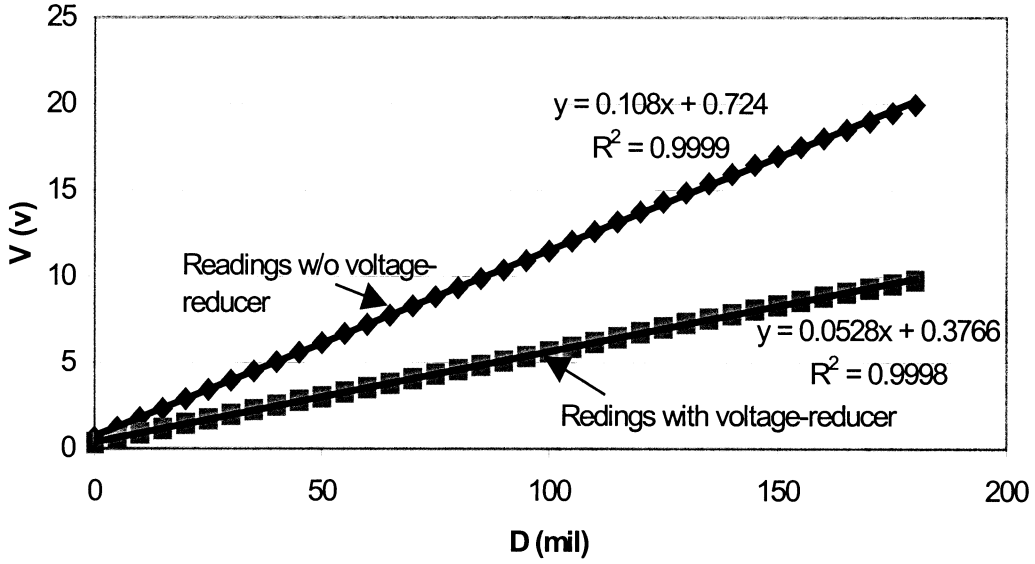

Figure 3.13 Calibration of Probe2 with 100k Resistor

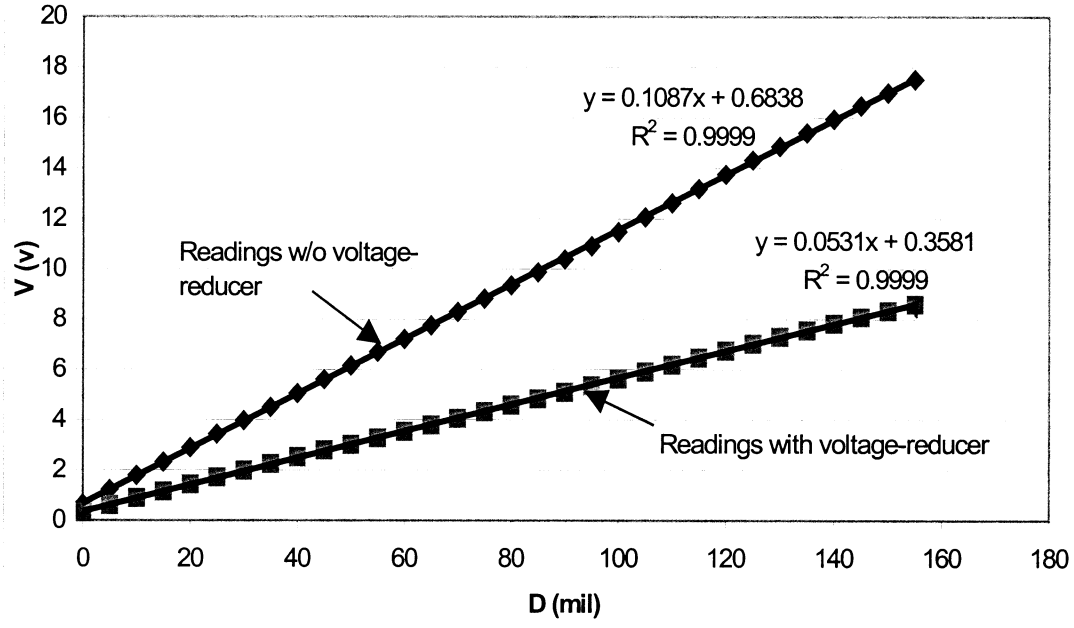

Figure 3.14 Calibration of probe2 with 10k resistor

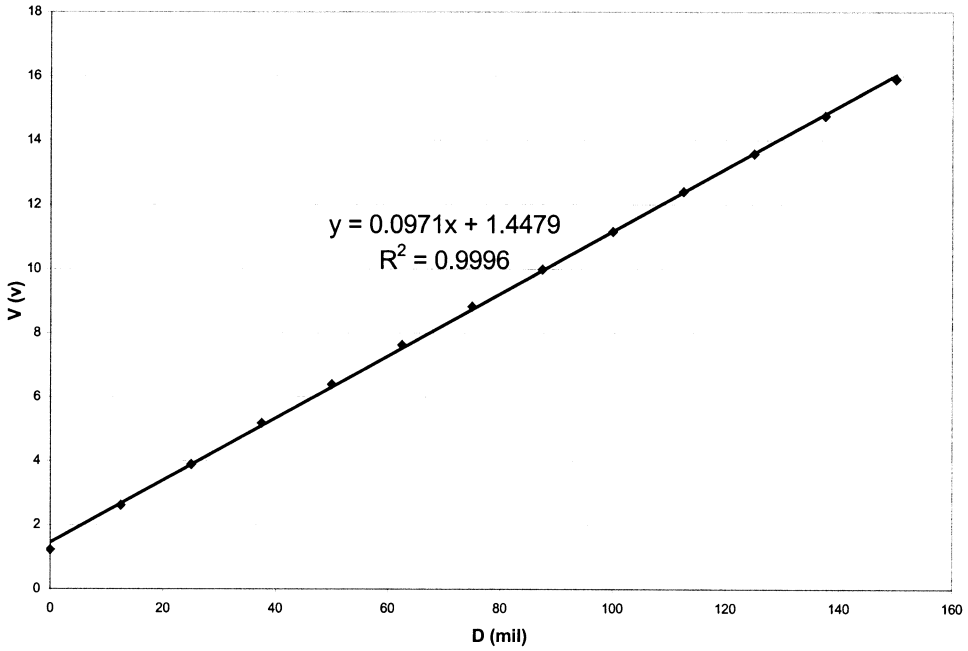

Figure 3.15 In-place calibration of probe 1

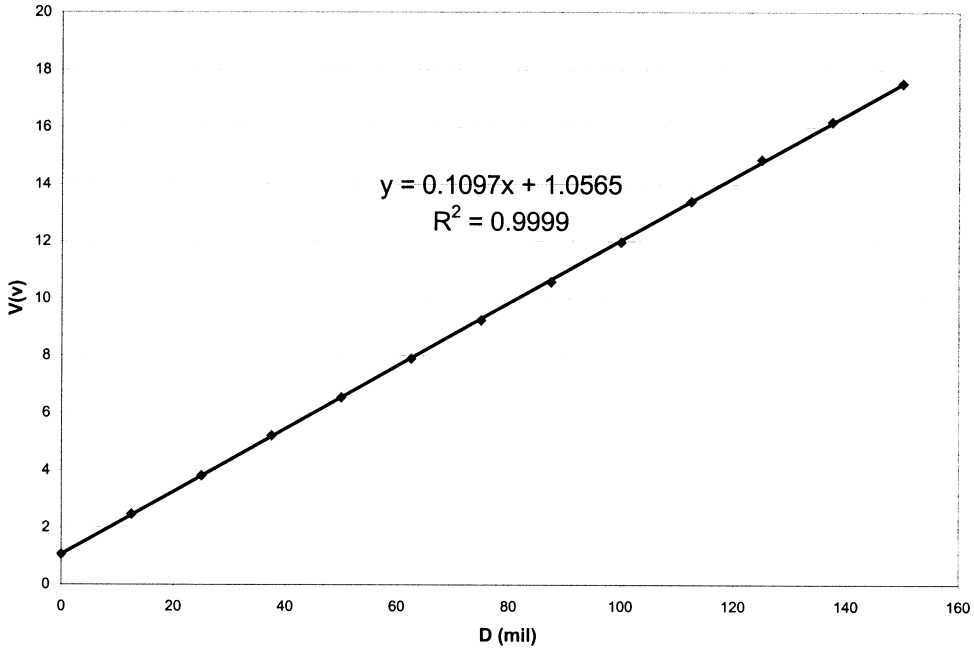

Figure 3.16 In-place calibration of probe 2

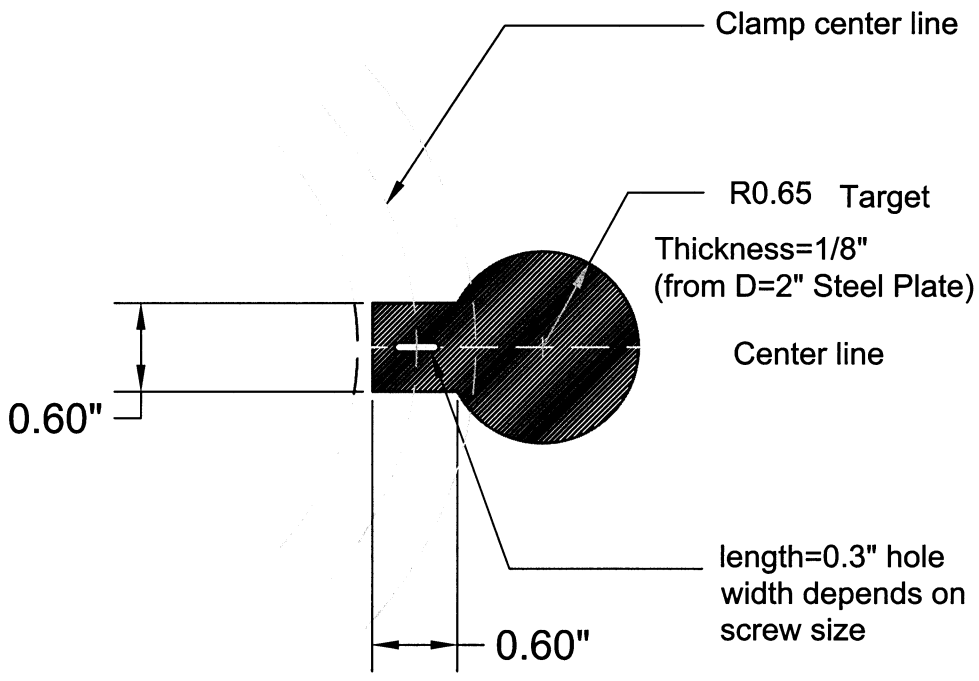

Figure 3.17 Target assembly

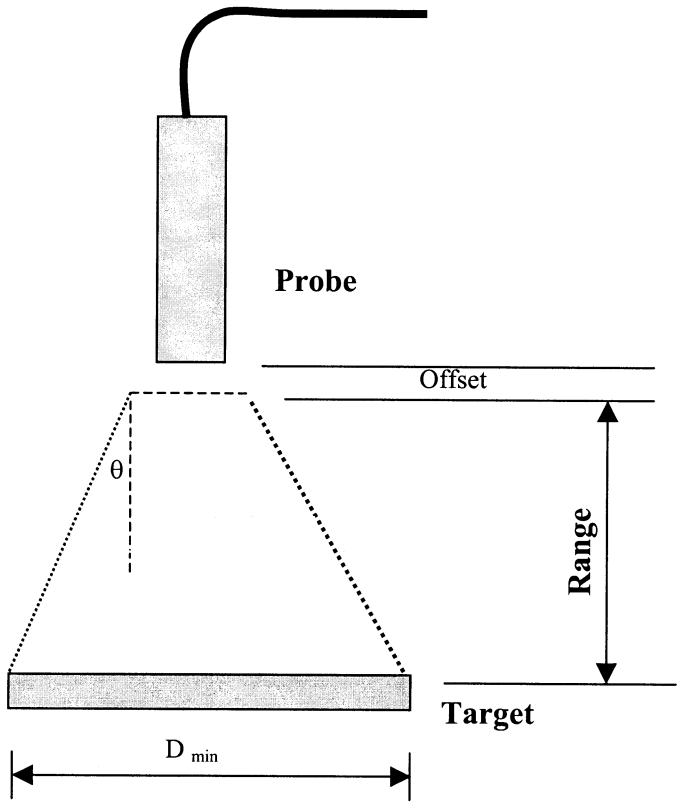

Figure 3.18 Determination of the minimum size of the target

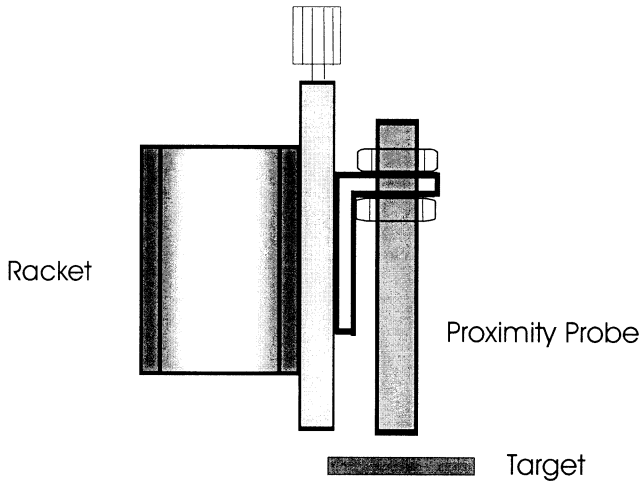

Figure 3.19(a) Probe position in bad clearance

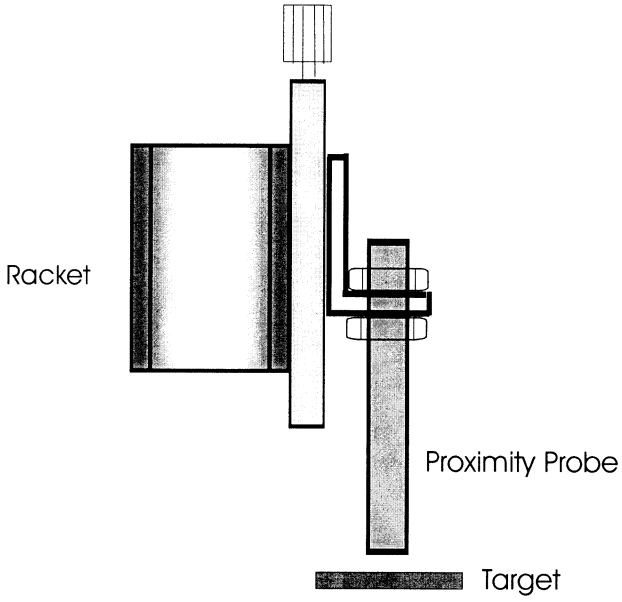

Figure 3.19 (b) Probe position in good clearance

CHAPTER 4

DATA ACQUISITION AND PROCESSING

4.1 General

A data acquisition system was set up to conduct the measurements. Since the output signals of the proximity probes were analog, a data-converting device (A-to-D converter) was needed to transform the analog output signals of the probes into recordable digital signals. However, the maximal input voltage of the A-to-D converter was 12.5 v, while the maximum output of the proximity probes was 22 v. A voltage reducer was needed to bridge the difference. In addition, noises existed in the non-contacting proximity probe system. The magnitude of the noise came in the same level of the measuring signal and made the collected data unstable.

In this chapter, selections of the A-to-D converter and voltage reducer are discussed and the solution to the noise problem is presented. The procedure for processing the data is also described in this chapter.

4.2 A-to-D Converter

Since the signals from the probe conditioner were analog, while the computer can take only digital signals, a data collection device was needed to convert the analog signals of the probes into digital files. This was achieved by adding an A-to-D converter.

To best compare the non-contacting probes with LVDTs, it was important to compare them based on the same data acquisition system. For this concern, the same MTS analog-to-digital converter used for the LVDTs was used to collect the probe output signals. Thus, the output signals from both LVDTs and proximity probes were collected simultaneously by the same A-to-D board.

This A-to-D converter of the ATM controller had eight input channels in the external input connector (connector J42). These channels were set up as shown in **Table 4.1**.

4.3 Voltage Reducer

A problem occurred after using the MTS A-to-D converter concerning the range of the output signal of the proximity probes (0~22v not matching the range of the A-to-D converter

(0~12.5v). Thus, a voltage reducer was needed to minimize the difference between the two parts by linearly reducing the upcoming signals to a lower voltage range. This was achieved by a voltage divider consisting of resistors (**Figure 4.1**). The resistance of the resistors was sufficiently higher than the down stream resistance so as to provide the linearity. The existing resistance in the A-to-D converter board was around 200Ω; therefore, two 100kΩ resistors in a series connection were used for the voltage reducer. As shown in Figure 3.13 and Figure 3.14, resistors of 100kΩ and 10kΩ all gave good linearity in the calibrations.

4.4 Data Stabilization

4.4.1 Noise Features

Noises existed in the test system, ranging from the frequency of 10 Hz to 1000 kHz. The results of LVDT measurements were quite stable. However, the collected data from the non-contacting proximity system contained noises as shown in **Figure 4.2**. The deformations of the specimen computed with noises varied significantly as shown in **Figure 4.3**. These deformations, if correctly measured and recorded, would have been distributed closely around its average line, as the deformations from the LVDTs shown in Figure 4.3. Under

the influence of the noises, the data collected by the non-contacting system were very unstable.

The noises were picked up by the unshielded wires between each proximity probe and the A-to-D converter. The noises came at a level of 0.3v, which is about the same level of the output voltage produced by the deformations of the soil sample under the tests.

To better recognize the feature of the noises, a Channel Signal Analyzer (Type 2032, made by Bruel & Kjar, Denmark in 1987) was used to analyze the properties of the noises that existed in the system. The Analyzer is a self-contained peripheral device that allows users to collect spectral information.

The typical shape of the noise detected by the analyzer and collected by the system is illustrated in **Figure 4.4**. Several domain noises of around 60 Hz and 200 kHz existed in the system, coincident with the frequency of the electric power supply and proximity probes oscillator/demodulator.

4.4.2 Build-in Frequency of the Proximity Probes

As previously stated in Chapter 3, an eddy-current probe used in this system has a tip containing an inductance element which was excited by a high-frequency current from

its associated oscillator/demodulator. The resulting AC magnetic field at the probe tip induced eddy currents in the metal target or shaft opposite it. These eddy currents in turn changed the impedance of the probe, thereby changing the voltage across it. Since the magnitude of the eddy current interaction is dependant upon the gap between the probe and the metal opposite, the voltage across the probe was proportional to the distance or gap between the probe tip and the target. The distance over which this voltage-to-gap proportion is linear, may be from several mils to as much as one inch.

Particularly, the Indikon proximity probes used in this study consisted of a support rod having a coil at its sensitive end. The coil was energized with a current of approximately 200 kHz, then developed a magnetic field which was disturbed by the presence of metal. This disturbance, or eddy-current loss, was sensed by the probe system as the metal target approached or moved away from the probe tip. The output of a proximity probe is expressed as either a DC position signal or an AC peak-to-peak vibration signal.

These proximity probes operated at a frequency of approximately 200kHz. As a result of this lower operating frequency, the proximity probes were less sensitive to cable changes as well as able to penetrate deeper into the metal

surface, thus minimizing the problems due to electrical runout. Electrical runout was caused by local inhomogeneities on the surface of a shaft or target which even though perfectly round, gaves rise to signals that appeared to be due to vibration. This is an advantage designed by the manufacturer. In most cases, Indikon proximity probes can be utilized on a turned surface, while competitive probes require the surfaces to be polished, ground, burnished, peeled and in some cases even knurled.

This low frequency might be one of the sources of the noises introduced to the triaxial test system, since there were a lot of noises with a frequency of 200kHz as detected by the oscilloscope and signal analyzer. The 200kHz frequency joined the noises causing the collected data unstable and should be filtered before the A-to-D converter.

4.4.3 Filter Circuit and Data Reduction

The simplest way of eliminating the noises was to add a capacitor to each circuit between a proximity probe and the A-to-D converter. The capacitors function as filters to sieve out the alternative signals with the frequencies higher than a given level.

Trial-and-error tests were conducted with the capacitors ranging from 1μF to 4700μF. However, only capacitors between the range of 4.7μF and 100μF were found to function well in the noise filtering to this particular circuit. Further studies on the selection of the capacitors were conducted for this range.

Capacitors need to work together with resistors. A particular capacitor must be selected to best filter the noises with the specific resistance in the circuit. The optimum capacitor should be able to filter out the signals with higher frequencies and have least effects on the working signals. Many tests were conducted with timed data by changing different capacitors in the system, and the results showed that the capacitors affected the signals in three different ways.

1. The magnitude of capacitors affected the proportions of the noises it was able to filter out. Lower capacities can filter only a small portion of the noises while higher capacities will remove many low-frequency signals, including those working signals of the load and deformation cycles. As shown in **Figure 4.5,** there were more noises left in collected data filtered with 1μF capacitor than that filtered with 47μF capacitor.

2. Capacitors make time shifts in the signal curves. The magnitude of the time shift is proportional to the capacity. Larger capacities gave a longer time shift (**Figure 4.6** and **Figure 4.7**). The time shift of capacitors was critical to the Peak/Valley mode of the data acquisition system of the MTS. This mode recorded data when the master channel signal detected a peak or valley. It acquired data every time a peak or valley was detected on a force channel (master channel) and, at the same time, took data on the displacement channels (slaved channel). With time shifts, the peaks of the signals of the slaved channels came later than the peaks of the master channel. Thus, the recorded points of the slaved channels were the points before the exact peaks.

Because the peak/valley mode could not correctly record the peak and valley values of all channels, the MTS data acquisition mode was changed to a timed mode, that recorded the data of all channels at a selected time segment. The segment of this study was set to 0.01 second.

3. The capacity decreased the magnitude of the signal. The higher the capacity was, the more signals were cut out. A number of systematic tests were conducted on the selection of the capacitors. **Figure 4.8** shows the effect of different capacitors to the system regarding the particular resistors. This figure also shows that capacitors greater than 10μF

would reduce the signals sharply while capacitors lower than 10μF would retain too much noise in the system.

Since the 10μF capacitor was around the critical point that could filter the noises with an acceptable level of time shift and reduction on the signals, it was determined as the final noise filter to the specific system.

The procedure of the final data acquisition system is illustrated in **Figure 4.9. Figure 4.10** shows one unit of the filter circuit while **Figure 4.11** illustrates the difference in deformation readings with and without a filter.

Still, small noises remained in the system with 10μF capacitors. This problem was solved by averaging the 35 cycles out of the 50 cycles of recorded data with a Visual Basic Application program that was run in Microsoft Excel.

4.5 Compution of Resilient Modulus

As the data collection mode was changed from Peak/Valley to Timed Data (0.01seconds/cycle), the data processing program was modified accordingly for computation of the resilient modulus.

4.5.1 Computational Procedure for AASHTO T-292

According to AASHTO T 292-91I, in a resilient modulus test, a series of tests with different deviator stresses at different confining pressures can be performed after the specimen conditioning stage. The data were recorded for every cycle of each test, however, only the last five cycles of each test were used for final averaging. The resilient modulus (MR) was calculated from the load and deformation using the equation:

$$M_R = \sigma_d / \varepsilon_R \qquad (4.1)$$

where σ_d is the deviator stress and ε_R is the resilient or recoverable strain.

4.5.2 Modified Program for Data Processing

As the data collection mode changed to Timed Data, the recorded data files appeared different from that of Peak/Valley mode. With a Timed Data mode, loads and displacements of LVDTs and proximity probes were recorded 100 times in one load cycle, comparing to that of two points a cycle with Peak/Valley mode. For each soil specimen, 14 series of tests with different deviator stresses and confining pressures were conducted. 50 cycles of loads were repeated in each test. The recorded file size of the Timed Data mode was about 100 times greater than that of the

Peak/Valley mode, giving more detailed information about the loads and deformations.

The data were processed using an Excel program on a tabular format. The program was written in Visual Basic Application, which can be run in Microsoft Excel by clicking "Run Macro" in the "Tools" menu. The program was executed in the order of the flow chart illustrated in **Figure 4.12** with the following steps:

1. The first 14 cycles and the last one cycle were deleted. Only the data of the remaining 35 cycles between the 15^{th} and 49^{th} cycles were kept for averaging due to the appearance of instability in the loads during the first 15 cycles and the last cycle. As shown in **Figure 4.13**, the loads in the 35 cycles after the 15^{th} cycle were relatively stable with a reliable repeatability.

2. The remaining 35 cycles of data were averaged. Since the data file recorded the test information exactly 100 times in one load cycle (1 second), the averaging was done on the related points at the same position of each cycle. As demonstrated in **Figures 4.14** and **4.15**, no phase shift occurred between the cycles and the curve shapes remained the same after averaging.

3. The peak and valley points of each variable in the averaged data were found, the resilient modulus then

calculated using the difference between the peaks and valleys. Using this method, the time shift effect caused from the filters was eliminated as the peaks and valleys in each curve were found independently.

On the final report sheet, the resilient moduli obtained by full-length-positioned LVDTs, middle-length-positioned LVDTs and proximity probes were presented together. The differences between the resilient modulus from the middle-positioned LVDTs and proximity probes were also computed. All the results of resilient modulus computed by this modified program were in positive agreement with the results obtained by the T292 data collecting method and processing program.

4.6 Test Program

4.6.1 Soil Materials

Three types of soils: A-3, A-2-4, limerock were selected for triaxial tests using the established non-contact proximity instrument. All the soil samples chosen for experimentation in this study were tested for previous LVDT based resilient modulus studies. Thus the consistency of the test results may be checked by comparing the recent results with previously obtained data. The basic properties

of each soil, such as optimum moisture content and dry unit weight, were evaluated in the previous studies. Experiments for each type of soils were targeted for conducting under the same conditions, the same moisture content and the same compaction efforts, using the same test procedure. The basic soil properties and test conditions are summarized in **Table 4.2**.

4.6.2 Resilient Modulus Test Procedures

The procedures used for the laboratory testing were generally in accordance with those suggested by the American Society for Testing and Materials (ASTM) and the Manual of Florida Sampling and Testing Methods (FDOT 1988) and T292-91I. The 292-91I was used as a main reference for all tests. However, due to the changes in the apparatus, the test procedure needed to be adjusted accordingly. This adjustment was mainly reflected in the setup of the specimen and the data acquisition of the test data. As stated previously in chapter 3, the LVDT and non-contacting proximity probes work simultaneously in a single triaxial cell. Thus, a specimen should be set up with both LVDT and non-contacting probes in each alignment. This combined alignment was critical even though it took longer than the alignment in the respective single test measurement. More attention was given to the

alignment of the LVDTs, since bad LVDT alignment often results in test failure, while the non-contacting probes were not very sensitive to the slight misalignment.

During the resilient modulus test, 1000 cycles of specimen conditioning were conducted first. Then, a series of tests at different deviator stresses and confining pressures were performed, the same as T 292-91I. Timed data were recorded for every cycle of the tests and the middle thirty-five cycles were used for computation of resilient modulus. The resilient modulus (M_R) was calculated by dividing the deviator stress by the resilient strain (Equation 4.1).

For each test, the resilient modulus results were reported in a tabular form comparing the results from LVDT measurements and non-contacting proximity probe measurement. A regression model was used to get the regression equation of M_R from the confining pressure and bulk stress. Replicate resilient modulus tests were conducted on each type of soils to check the repeatability of the tests.

Table 4.1 External Input Channels of the MTS A-to-D Converter

Channel No.	1	2	3	4	5	6	7	8
Channel Name	J42-1,2	J42-3,4	J42-5,6	J42-7,8	J42-9,10	J42-11,12	J42-14,15	J42-16,17
Signal	Probe1	Probe2	Probe3	LVDT1	LVDT2	LVDT3	LVDT4	Probe4

Table 4.2 Soil Properties and Test Conditions

Soil Type	A-3	A-2-4	Limerock
Source	State Road 70	State Road 70	Lee Co., Site #1B, S.R. 884
Optimum Moisture Content (%)	11.40	10.60	7.40
Max Dry Density (kN/m^3)	17.6 (112.1pcf)	19.6 (122.1pcf)	20.5 (130.6pcf)
Labratory Moisture Content (%)	11.1~11.46	10.3~10.7	7.32~7.35
Labrotory Dry Density (kN/m^3)	17.97~18.78	20.62~20.84	21.70~21.98
Number of Tests	4	3	2

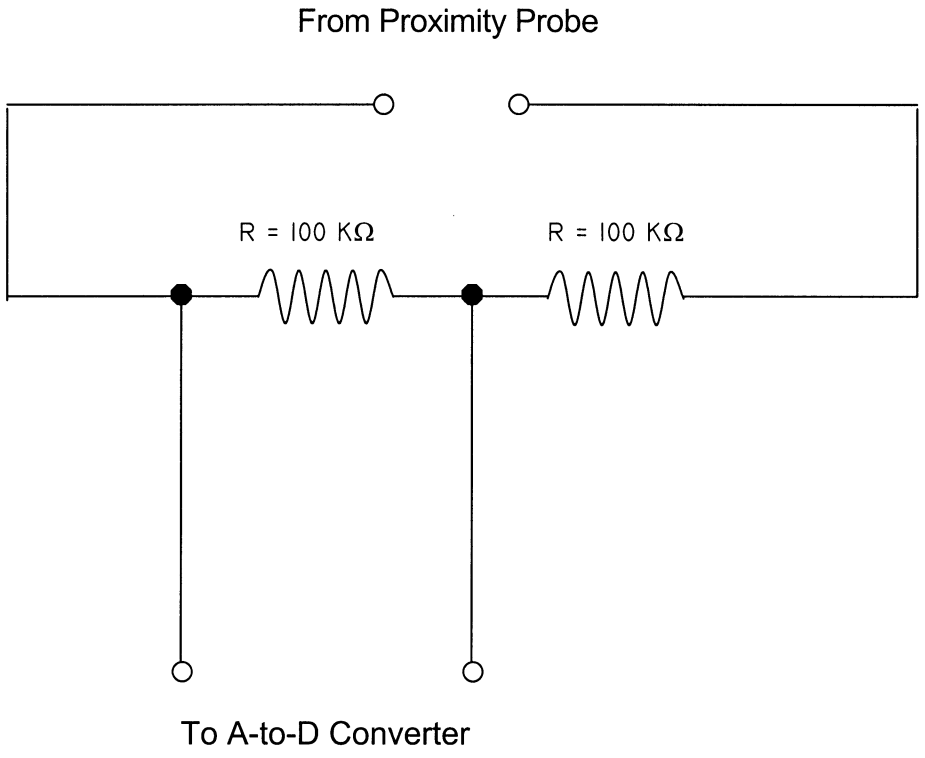

Figure 4.1 Voltage Reducer Circuit for a Probe

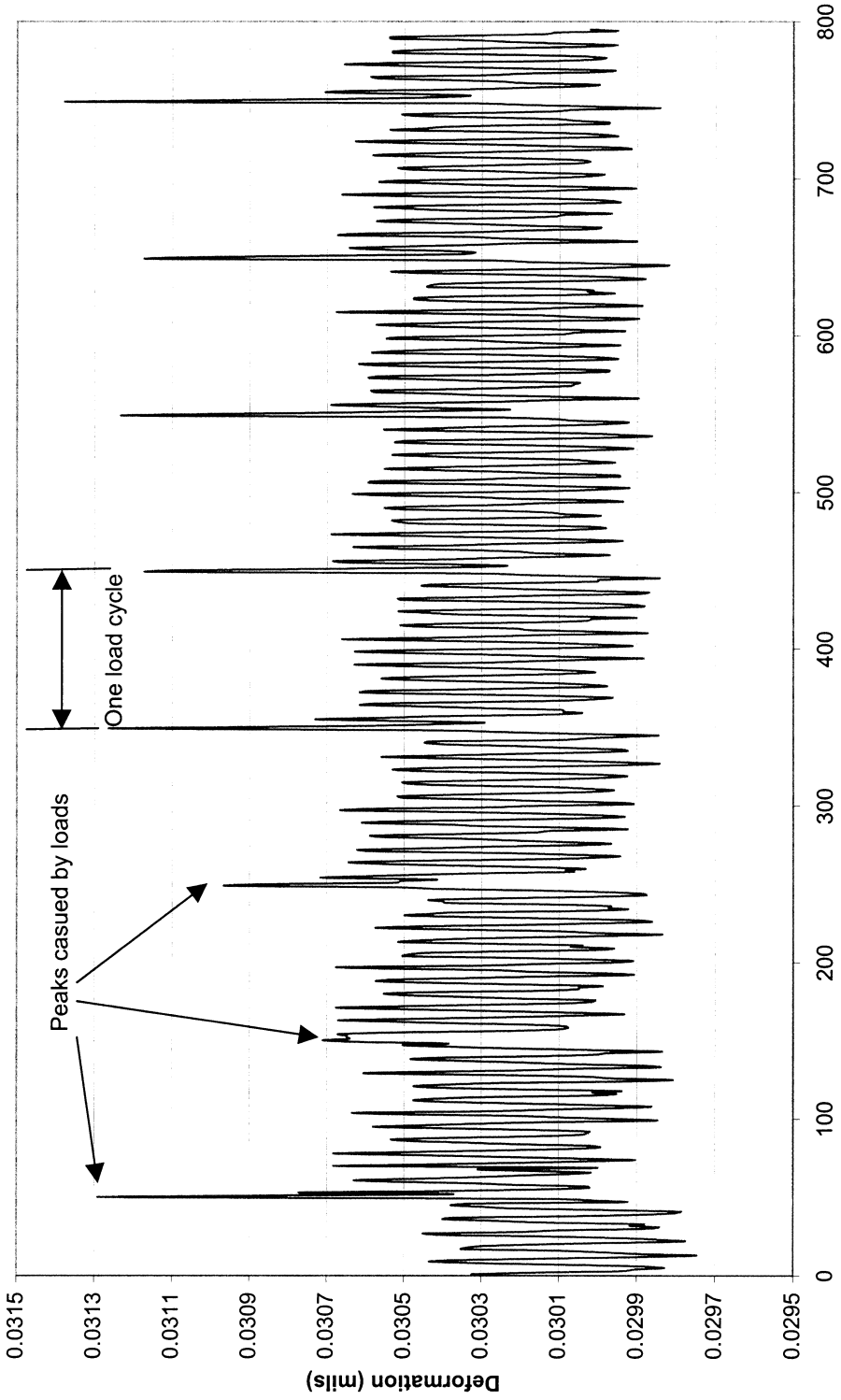

Figure 4.2 Typical Features of Noises in the Data of Probes without Filters

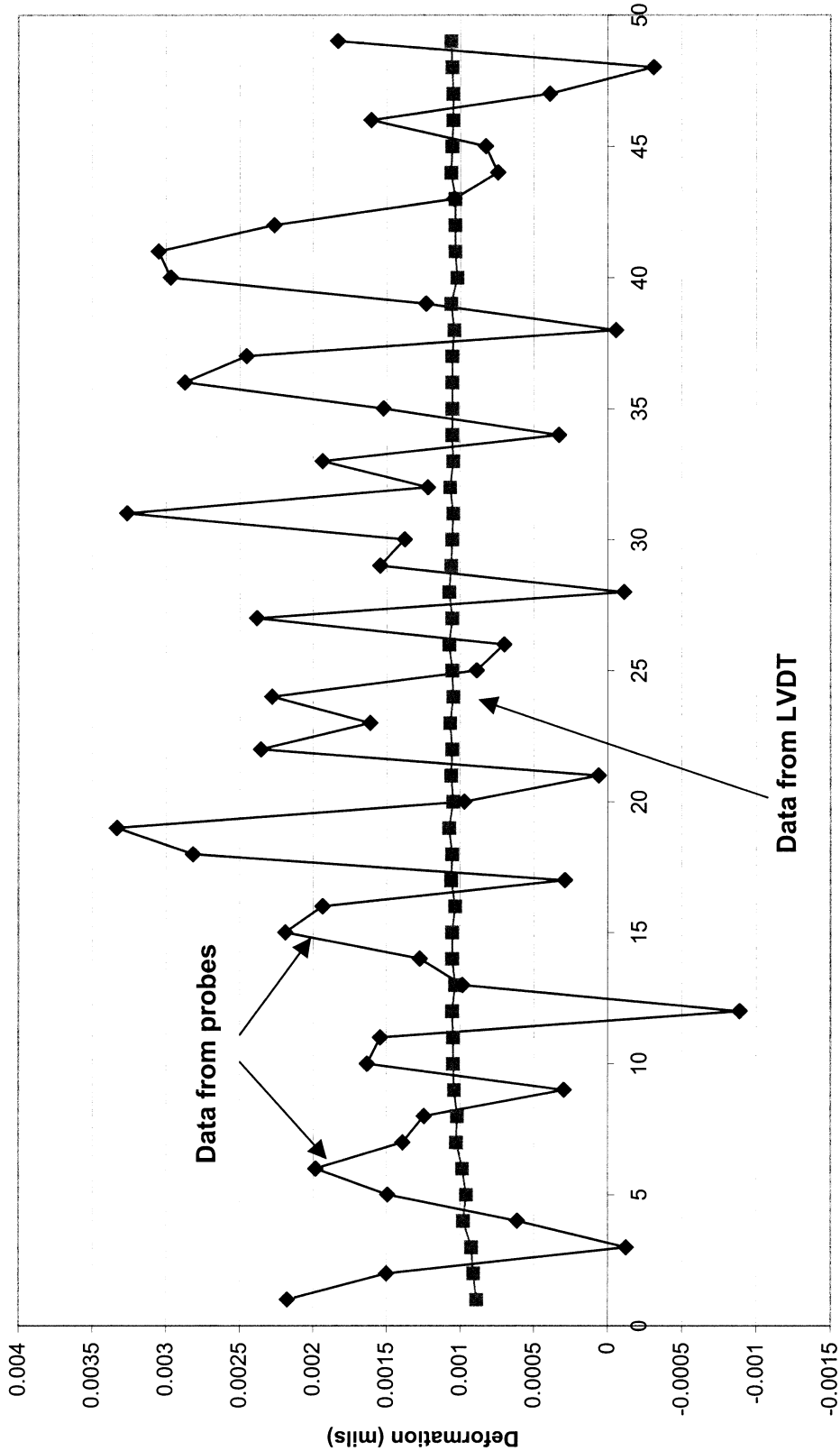

Figure 4.3 Typical noised data of deformations detected by probes

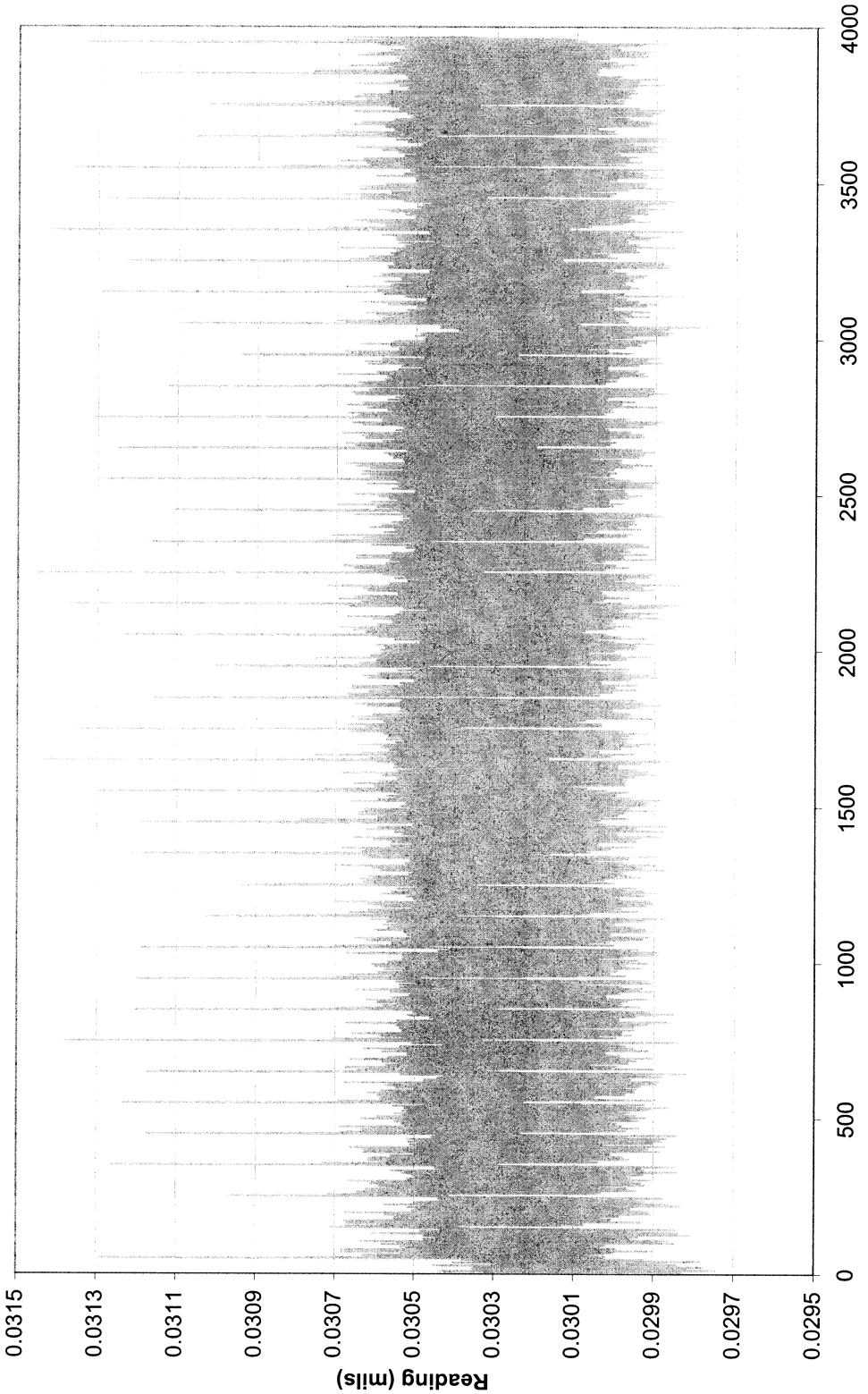

Figure 4.4 Noise feature in the data of the probe without filter

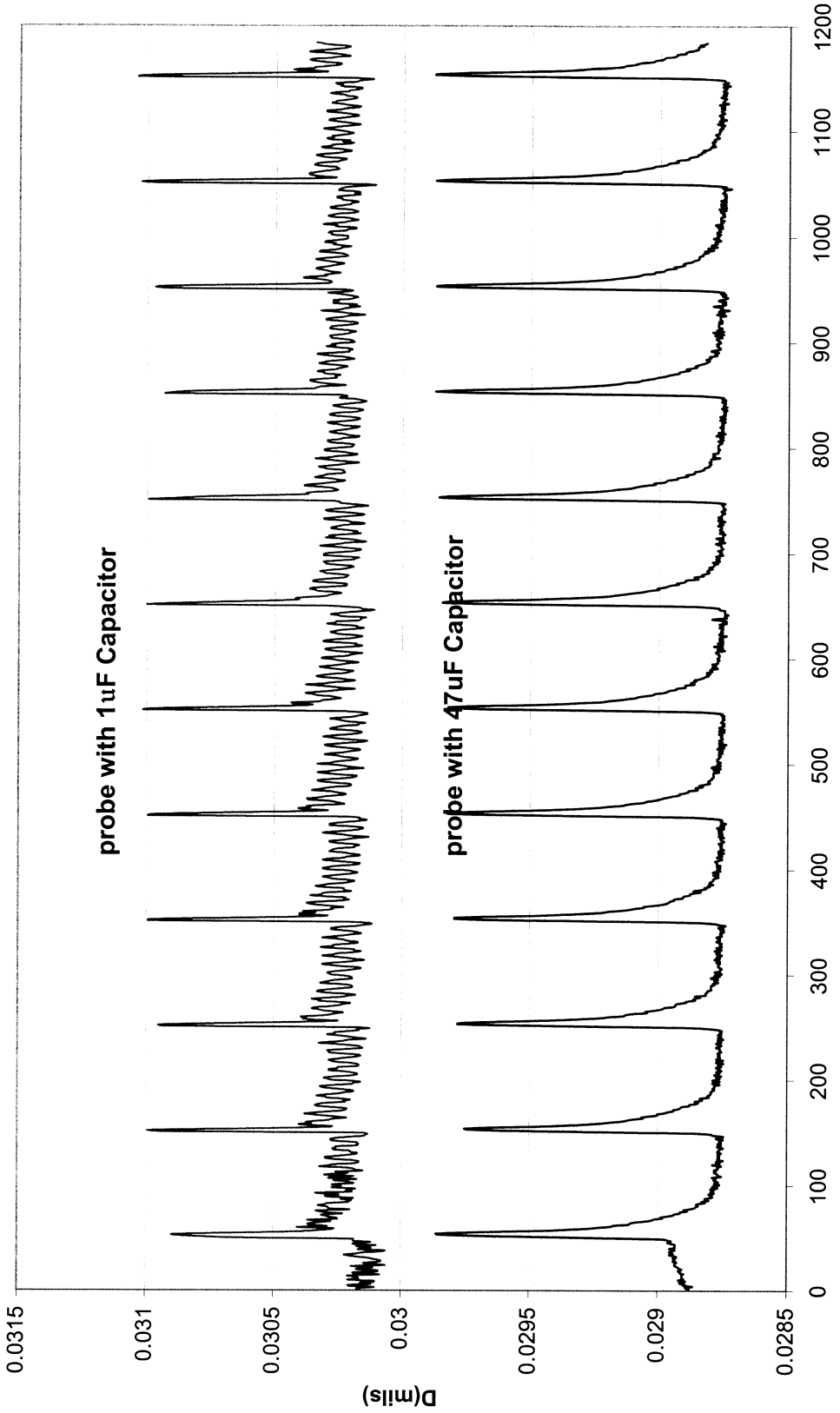

Figure 4.5 Effect of noises reduction by different capacities

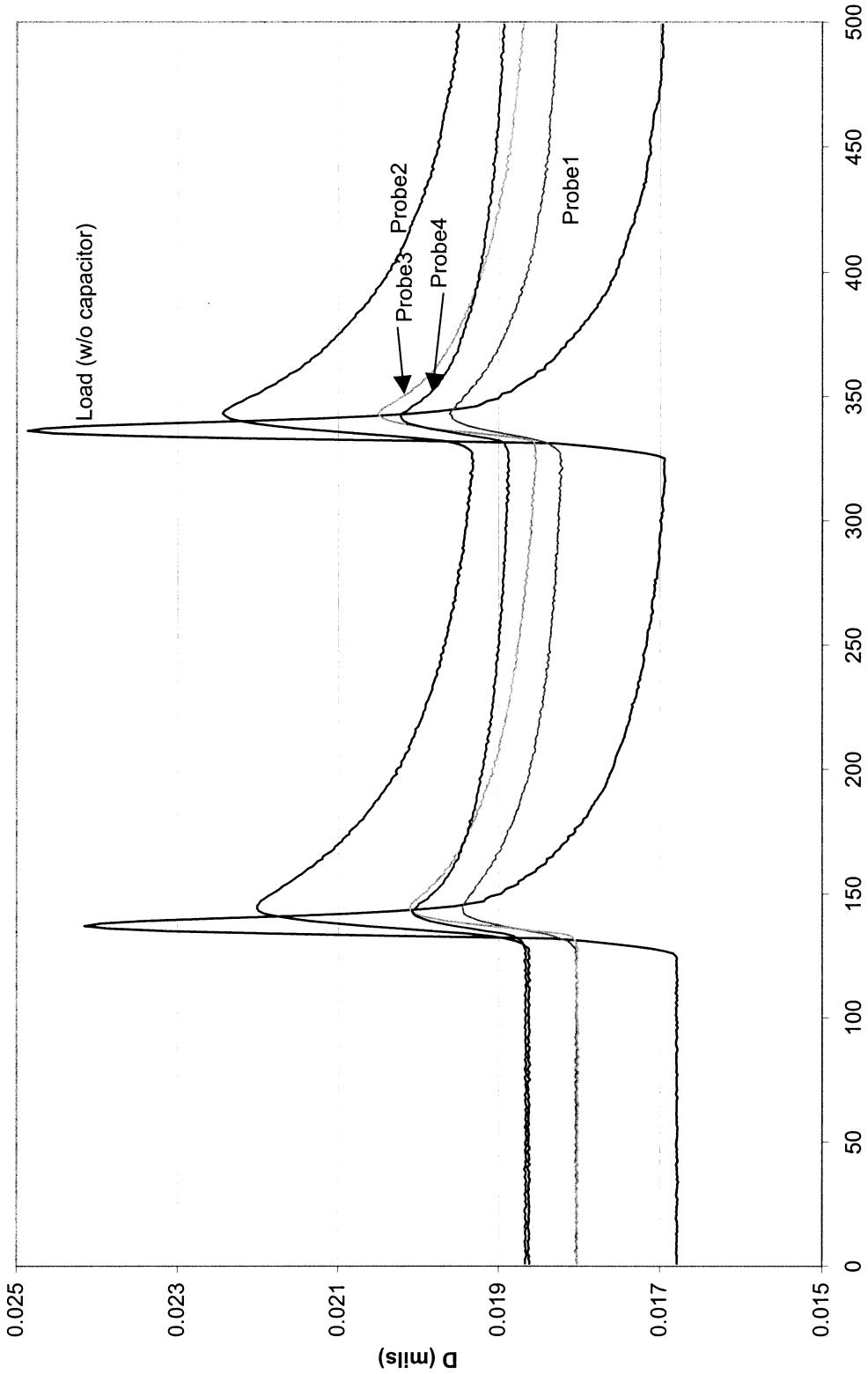

Figure 4.6 Time Shift of probes with 100uF capacitors

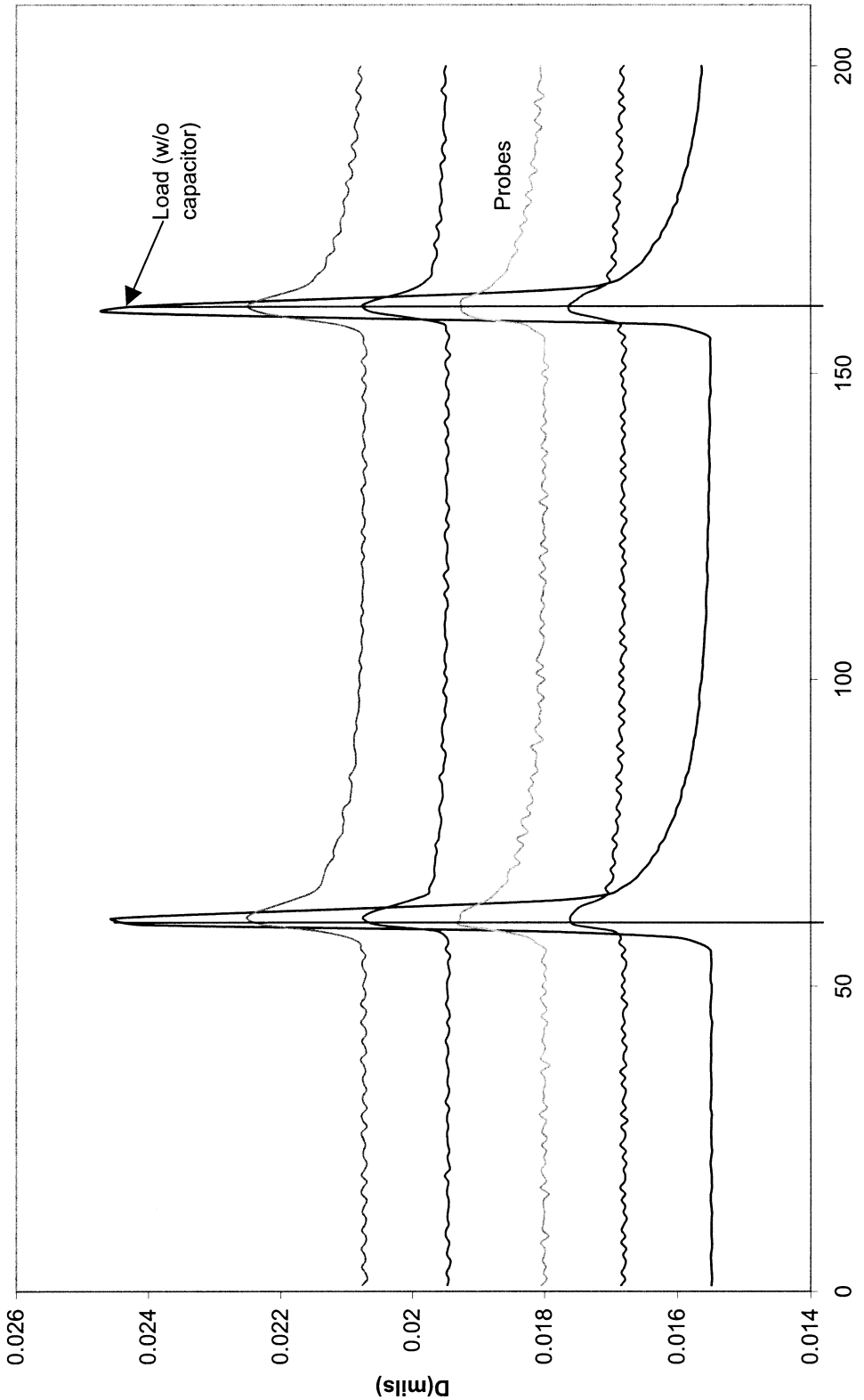

Figure 4.7 Time shift of probes with 4.7uF capacitors

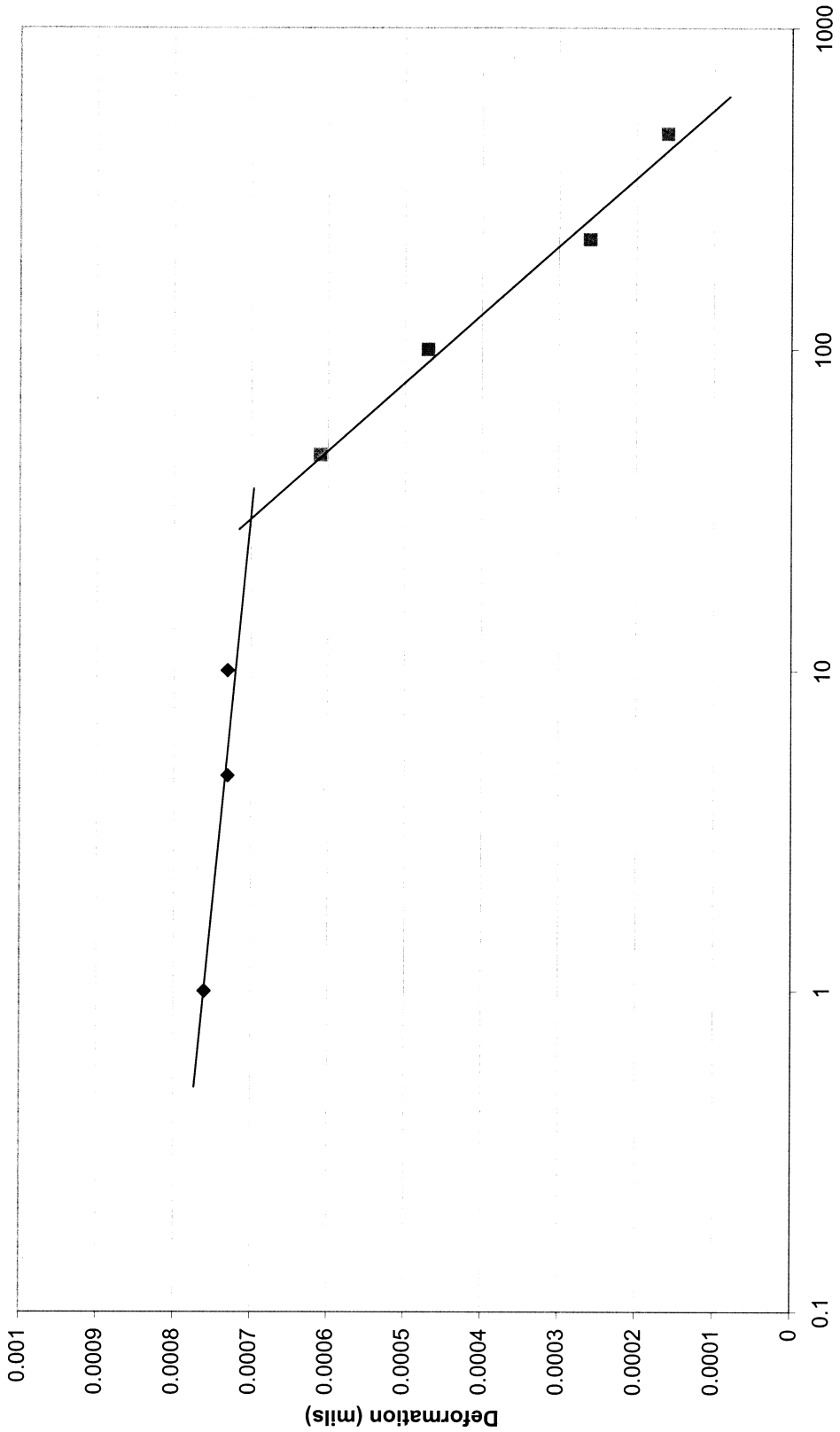

Figure 4.8 Effect of capacity on the signals

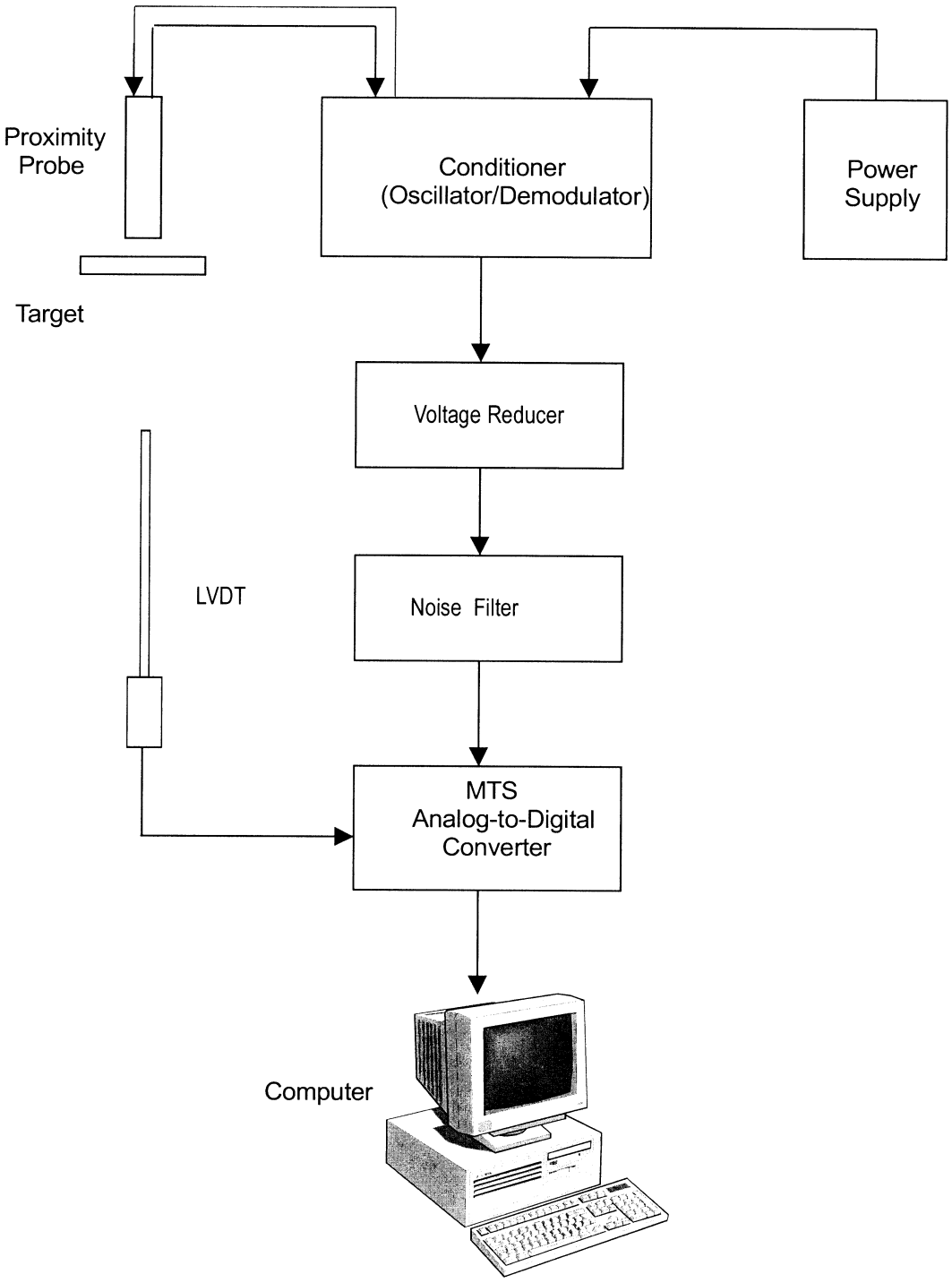

Figure 4.9 Data acquisition system

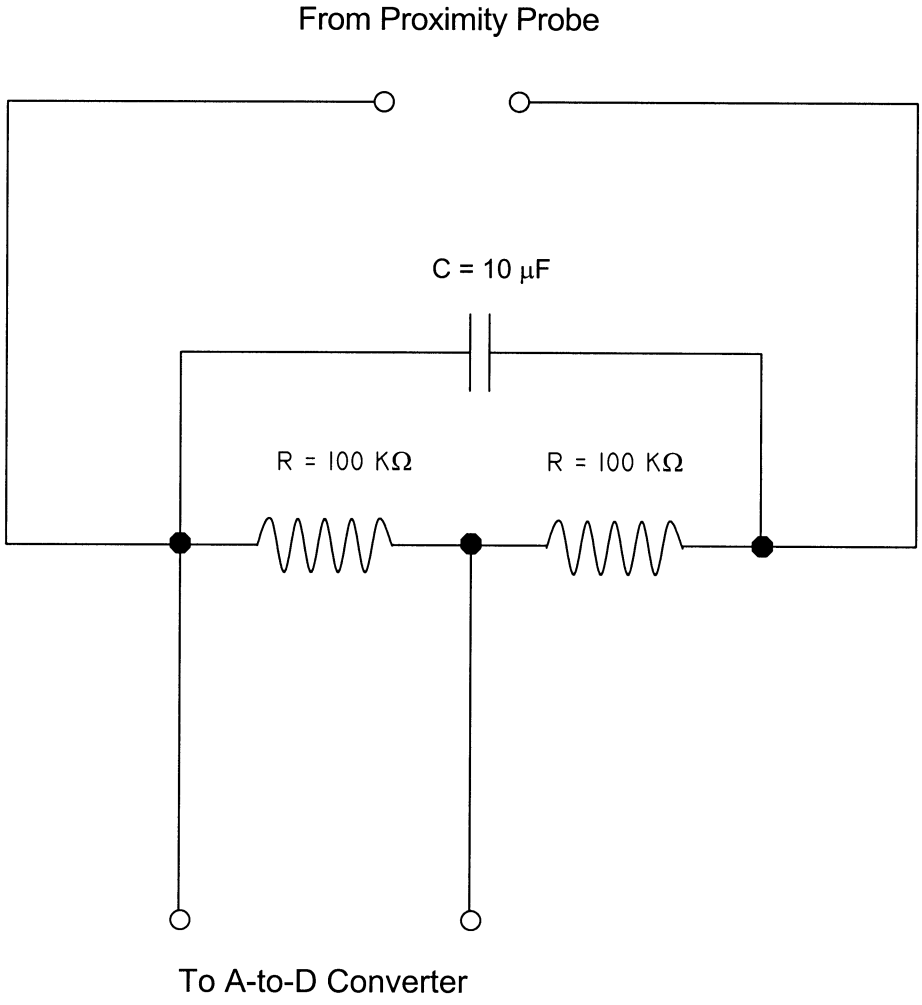

Figure 4.10 Filter and voltage reducer circuit for a probe

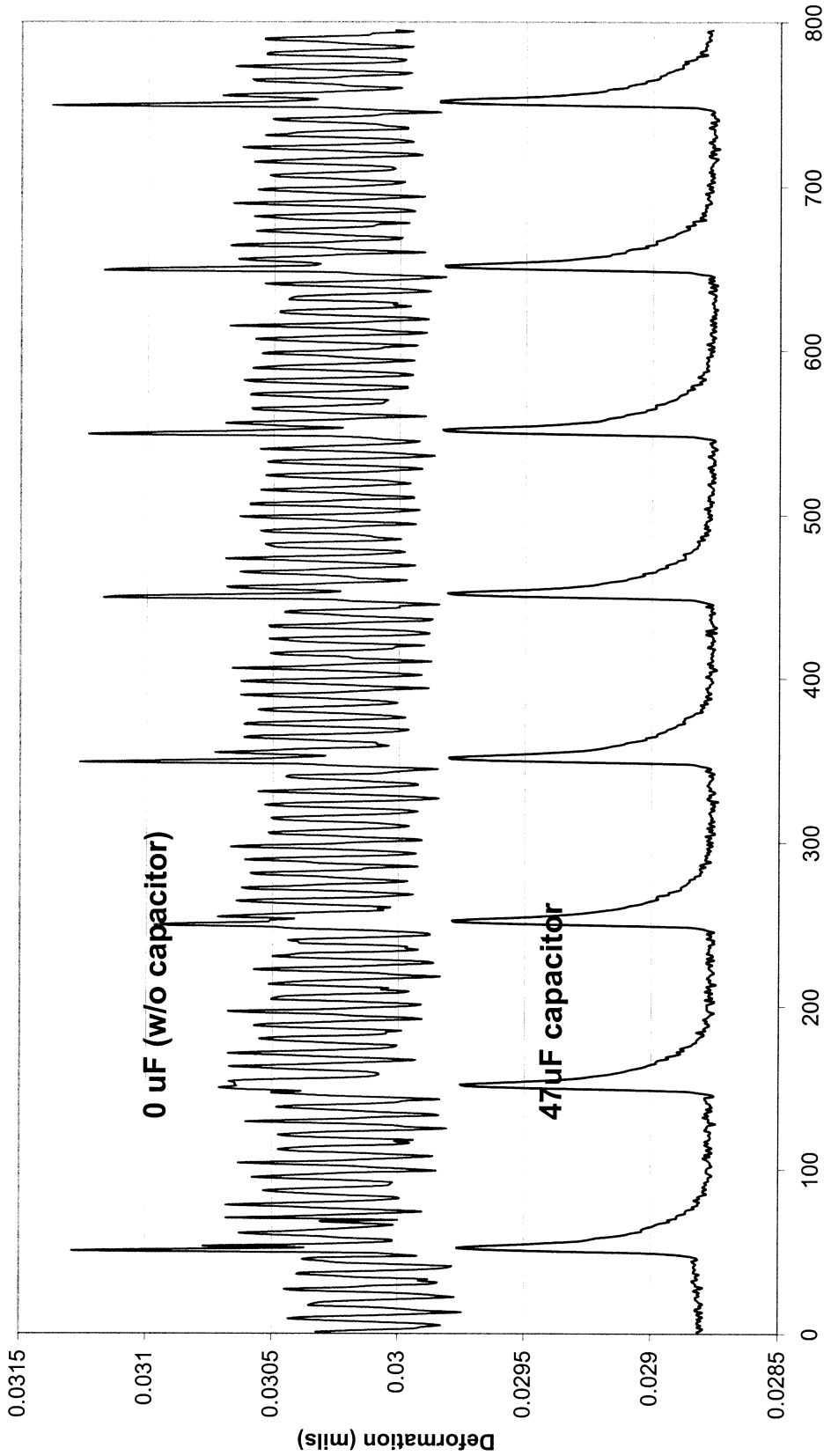

Figure 4.11 Timed data of the probes w/ and w/o filters (Under same loads and on same clamp)

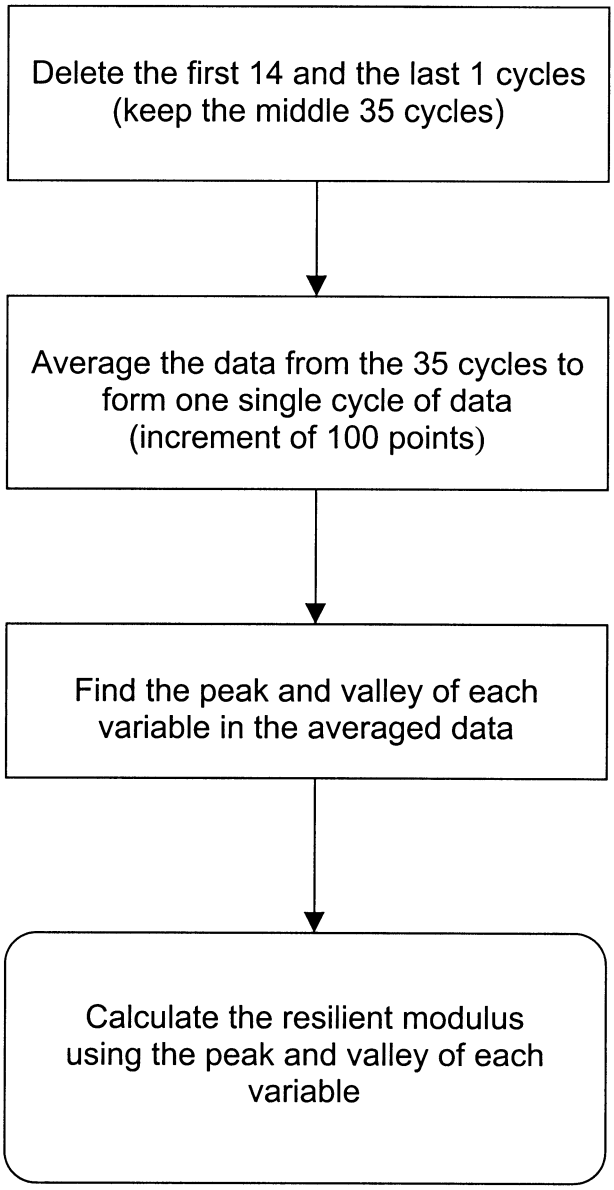

Figure 4.12 Flow chart for computing resilient modulus

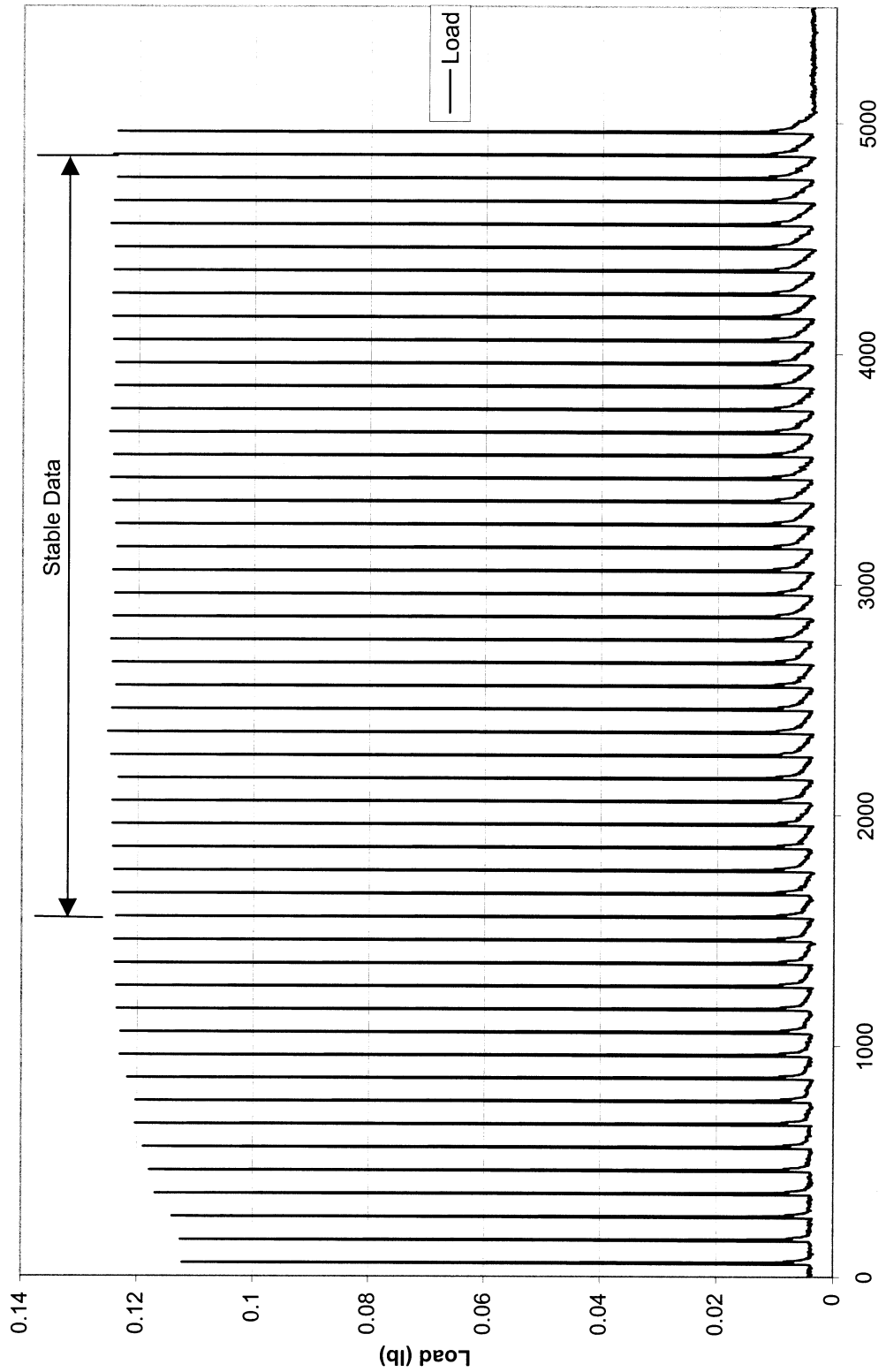

Figure 4.13 Raw data of 50 cycles of loads

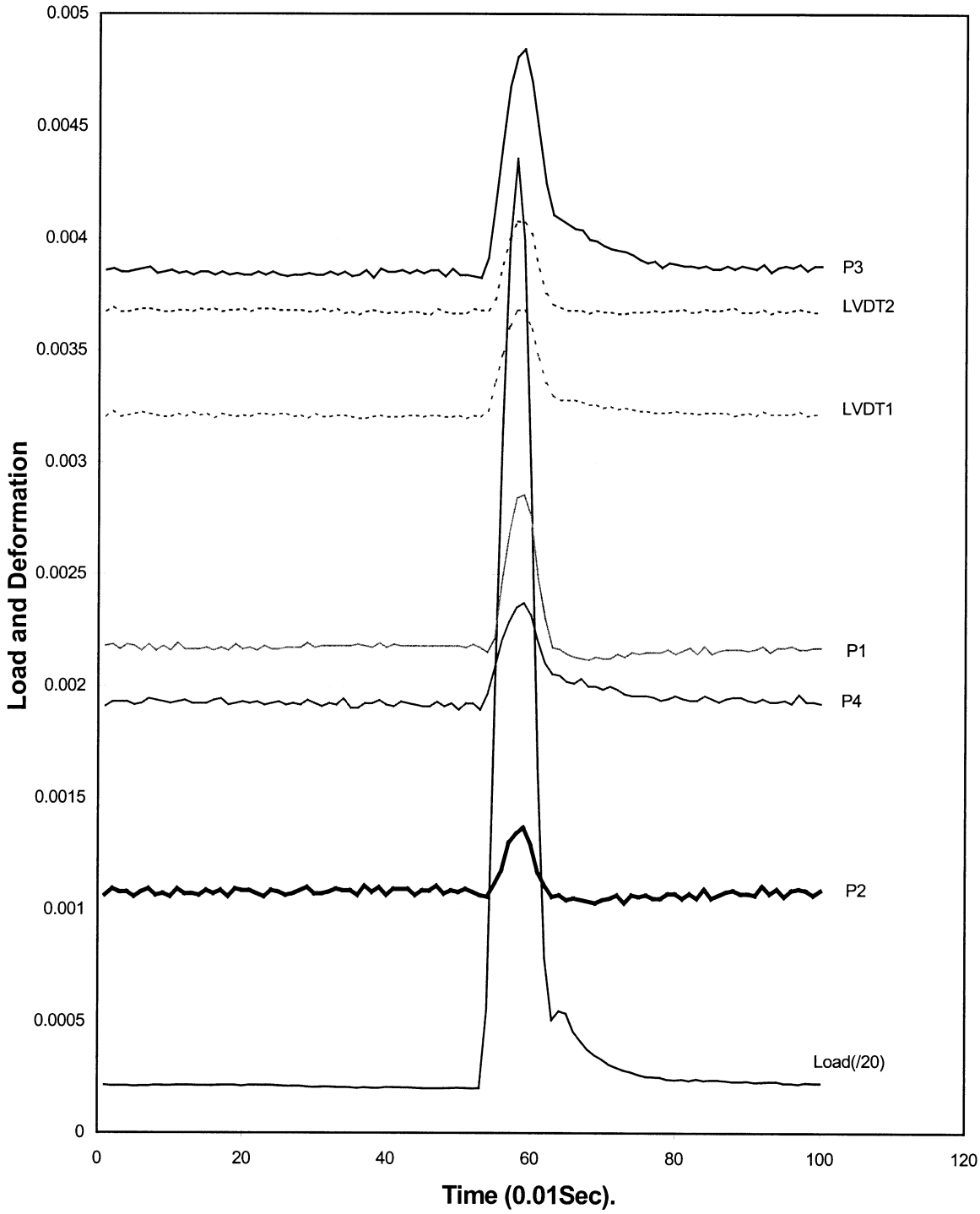

Figure 4.14 Load and deformation of a cycle before averaging

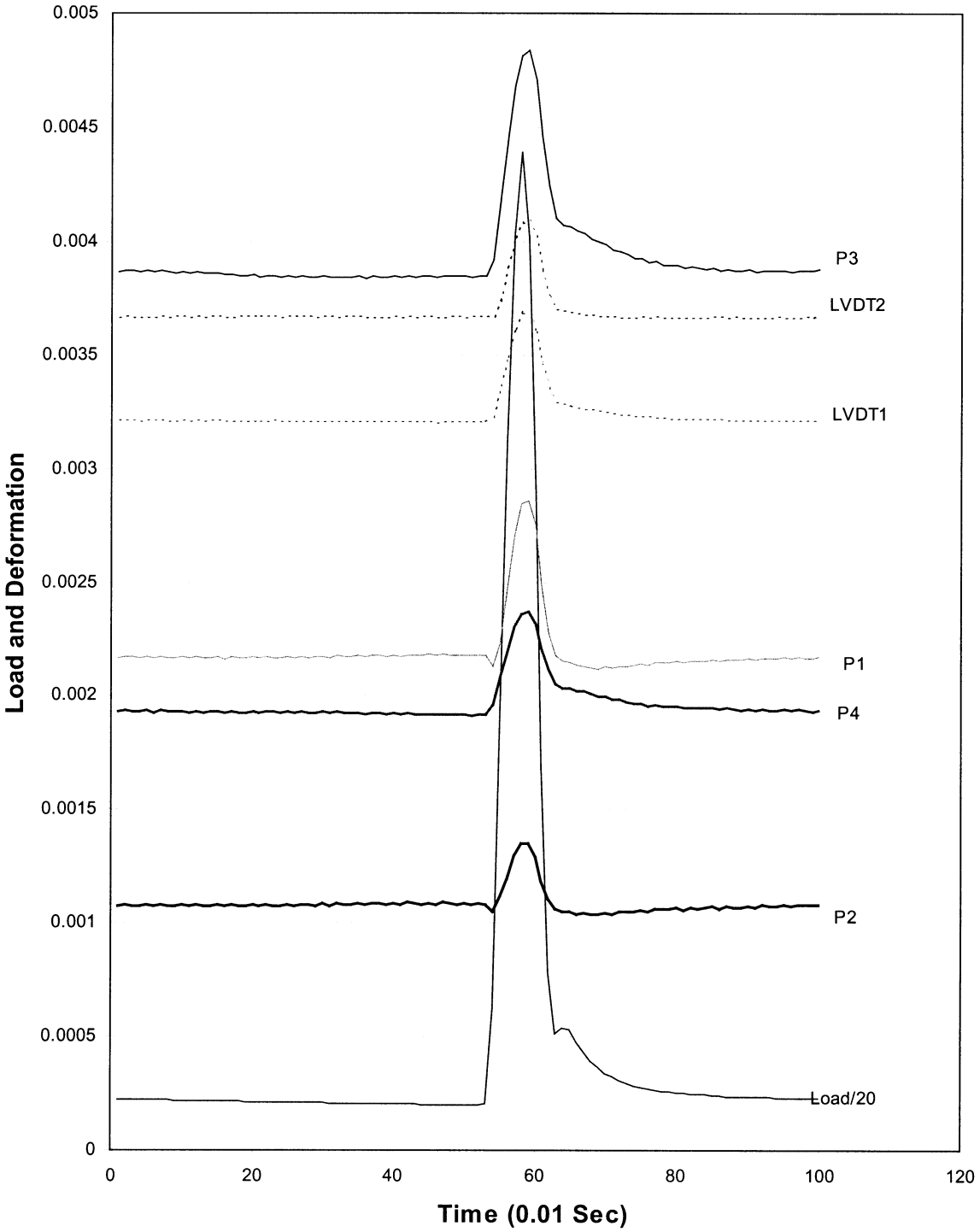

Figer 4.15 Load and deformation after averaging

CHAPTER 5

SUMMARY AND PRESENTATION OF EXPERIMENTAL RESULTS

5.1 Resilient Modulus Test Results

The materials tested in this research consisted of limerock, AASHTO A-3 material and AASHTO A-2-4 material. Typical results of resilient modulus tests are presented in this chapter, including the confining pressure, deviator stress, bulk stress, axial strain, and the corresponding resilient modulus values by each test sequence. Comparisons of the resilient modulus obtained by different measurements, regarding to the test sequence, confining pressure, and bulk stress for each soil type are presented as follows.

5.1.1 Resilient Modulus Values for A-3 Soil

A total of four samples of A-3 soil (sandy subgrade material) were tested in the laboratory under the same test conditions. The results are summarized in **Tables 5.1** through **5.4**. Comparing to A-2-4 soil and limerock, the A-3 specimens were difficult to set up since they are often soft, unstable and usually tilted after extruding from the compaction mold.

The data for the four tests are shown in **Figures 5.1** through **5.12** in terms of the test sequence, confining pressure and bulk stress with the corresponding resilient modulus values. For different types of measurements, the results show that the middle-positioned LVDTs gave the highest resilient modulus values whereas the resilient modulus values obtained from the non-contacting proximity probes were in between the results obtained by the middle and full-length LVDT measurements.

5.1.2 Resilient Modulus Values for A-2-4 Soils

The A-2-4 soil was more stable than the A-3 soil after compaction, thus it was easier to set up. Three tests were conducted and all results fell in a closer range than those of the A-3 soil. Summaries of the test results are given in **Tables 5.5** through **5.7**. **Figures 5.13** through **5.21** demonstrate the results for each test. The figures display the same trend as that for the A-3 soil: the resilient modulus values obtained from the non-contacting proximity probes were in between the two resilient moduli obtained by the middle and full-length LVDT measurements during each test sequence.

5.1.3 Resilient Modulus Values for Limerock Material

The results of two specimens of the Florida limerock materials are summarized in **Tables 5.8** and **5.9**. Comparisons

of resilient moduli and their regression lines are shown in **Figures 5.22** through **5.27**.

The Florida limerock materials displayed a wide range of resilient behavior under different loading and confining conditions, as shown in the tables and figures. This was consistent with the results from previous studies.

Though the results were volatile, the trend for each test of limerock was the same as for the A-3 and A-2-4 soils: the resilient modulus value obtained by the non-contacting proximity probes was higher than that obtained by the full-length-positioned LVDTs but lower than that from the middle LVDTs.

5.2 Analysis and Discussion of the Test Results

The resilient modulus values obtained from the non-contacting proximity probes as measured by the deformation of the half length of specimen were always lower than that of the middle-positioned LVDTs. The middle-positioned ones measured the same deformation of the same length of specimen but were higher than that of the LVDTs at the full length as measured by the deformation of the full length of the specimen. The test results are further discussed in following sections.

5.2.1 Repeatability of Resilient Modulus Tests

At least three replicate samples were conducted for each type of soil to investigate the repeatability of the tests and to ensure the validity of the resilient modulus test results. **Figures 5.28** and **5.29** show the comparisons of the resilient modulus results from the replicate samples of A-3 and A-2-4 soils. The data points were close to the line of equality, though some were a little scattered. The repeatability of the resilient modulus test was satisfactory for each type of soils.

Some data points were away from the line of equality. One possible reason for the variation may have been due to the variation of the soil specimens. The variation might be induced by the offset of moisture content and dynamic compaction during the specimen preparation. Although the duplicate samples were compacted at the same energy level (the soil samples were divided into the same number of layers with the same number of blows for each layer), variations existed in the moisture content and density of the specimens. Another reason could be due to the problem with installation of LVDTs. Since the installation of LVDTs especially the alignment was very difficult and inconvenient, there might be inaccuracy of placement, which led to variations in all of the three measurements.

5.2.2 Deformation Loss in Middle-positioned LVDTs

As discussed in Chapter 2, middle positioned LVDTs required a skillful alignment during the sample set-up. This alignment required three-dimension adjustments, which are achieved by adjusting the two clamps, to which the LVDTs were vertically attached. Specimen tilting or clamping tilting resulted in the friction between the metal stick and the coil sensor of middle-positioned LVDTs. The problem is that a perfect alignment can hardly be achieved in a regular test, therefore, frictions always exist in the middle-positioned LVDT measurement.

Since the middle LVDTs and non-contacting probe targets were both attached on the same clamps, they measured exactly the same deformations as the specimen. As shown in every test result, middle positioned LVDTs always measure a lower deformation (higher resilient modulus) than non-contacting probes and full-length-positioned LVDTs. This difference become more significant when there is a misalignment that caused one of the middle LVDTs stuck (**Table 5.10**).

While the proximity probes, which were easy to install and align, measured the deformation in a more stable and reliable way than the middle-positioned LVDTs, the probes were not sensitive to the misalignment either. In all cases of the tests in this study (over 150 loading sequences on

more than 11 specimens), the proximity probes measured the deformations about 5-10% higher than the middle LVDTs (**Table 5.11**).

5.2.3 End Effect of Full-length-positioned LVDTs

Full-length-positioned LVDTs can induce errors to the deformation measurements because of air gaps (**Figure 5.30**) between the specimen and accessories such as porous stones and platens, and errors due to specimen tilting etc.

In every test of the study, the full-length-positioned LVDTs, though easy to install, provided resilient modulus values that were lower than those obtained by the other two measurements. The differences became more significant when the soil type was coarser and harder, for example, limerock. As shown in **Figures 5.1** through **5.12**, for A-3 soils, the full-length LVDTs gave resilient modulus values approximately 20~25% lower than the other two measurements. However, for Limerock, this difference ranged from 30% to 50% (**Figures 5.22** through **5.24**).

The effect of air gaps was increased in limerock tests as the samples were very hard and the deformations on the air gaps occupied a significant portion in the total deformation of the specimen. In limerock tests, there were more air gaps between the specimen surface and the porous stones due to the

larger diameter of the limerock particles, which made it difficult to surface the specimen as good as A-3 and A-2-4 soils after compaction. Generally, the limerock specimen needs to be prepared with more effort in the surfacing step by flattening pulverized particles to the surface.

Figures 5.25 through **5.27** show a test in which the limerock specimen was prepared by a loose effort in surfacing. Obviously, it increased the difference between the resilient moduli from full-length-positioned LVDT and the other two measurements.

Theoretically, the differences of the sensitivity and accuracy among each measurement should not change because of the change in soil type. The phenomenon appeared in this study, that the differences of the test results increase when the soil specimens were prepared with air gaps, is evidence of the existence of the end effect in the full-length LVDT measurement.

This observation is in agreement with previous studies. Ping et al. (1998) compared the full-length positioned and middle-positioned LVDTs and indicated that the resilient modulus measured from the middle LVDTs was significantly different from that determined from the full length LVDTs. For the T 292-92I test procedure, the average difference of

the resilient modulus values between the full-length and middle LVDT measurements ranged from about 15% to 25%.

Maher et al. (1996) compared the non-contacting proximity probes with full-length-positioned LVDTs by fixing the targets to the specimen using double-sided tape. The study concluded that the use of non-contacting proximity probes with a gauge length of one-third gave more accurate and repeatable results than that of LVDTs with a gauge length of one (AASHTO T294-92). According to this study, the use of full-length-positioned LVDTs underestimated the resilient modulus values by 20% when testing dense granular materials. The study of Pezo et al. (1998) verified this discrepancy of about 20% and suggested using the middle one-third of the specimen length to avoid the end effect.

5.2.4 Reliability and Benefits of the Proximity Probe Measurement

As practiced in the experiments and supported by the results, the proximity probes appeared to be a good alternative of the LVDTs. The major advantage of the proximity probes was the higher sensitivity and accuracy with lower chance of test failure. These transducers did not bear on the specimen, though it needed to mount metallic targets that moved rigidly with the specimen.

The high accuracy came with requirements of thorough calibration of the transducer, with the same target used in the system set-up, and identical constant voltage supply during testing and calibration operations. The high accuracy and sensitivity also required that the target be in close proximity to the probe tip, not exceeding its linear range.

Another advantage of the non-contacting probes was reflected in the alignment of the specimen setting up. Parallelism between the target and the sensor was not critical as long as the angle between the sensor face and the target was within approximately 15 degrees. Thus, the proximity probe output was not influenced by tangential movement of the targets and is sensitive only to displacements in the axial direction. Furthermore, these probes had a transient response of 10 μsec. Thus, hundreds of data points were recorded for each cycle of loading even at high frequency (>100 cycles/sec). Temperature changes and environment conditions, such as surface contamination and humidity between the sensor and the target, had minimal or no effect on the system accuracy.

Of course, errors may be induced to the non-contacting probe measurement as well as the middle positioned LVDTs measurement from the system compliance of triaxial cell accessories or from slippage of the membrane. Claros et al.

(1990) also stated that it was difficult to secure the LVDT clamps to ensure there was no movement. With the current clamp mounting method, poor alignment of the specimen or inaccuracy of installation caused by the difficulty in the set-up of the measurement system may induce errors. In addition, the data from the non-contacting proximity probes may contain noises ranging from 60Hz to 200 kHz, coincident with the frequency of the electrical power supply and proximity probes oscillator/demodulator. The filtering process may have induced errors on the test results.

Table 5.1 Resilient Modulus Test Results for A-3 Soil (Sample A)

Sample : No. 1
Date: Jan.20, 2000
Opt. Moisture Cont : 11.40%
Opt. Density : 112.1 pcf

Soil Identification: A-3 SR70
Test Procedure: **T292-91I**
Lab. Moisture Cont. : 11.10%
Lab. Density : 118 pcf

Test No.	Confining Presure	Axial Load	Dev. Stress	Bulk Stress	Mid LVDT Strain	Probe Strain	Full LVDT Strain	Mid LVDT Modulus	Probe Modulus	Full LVDT Modulus
	kPa	kN	kPa	kPa				MPa	MPa	MPa
1	103.42	0.3362	45.7707	356.0307	0.000145	0.000157	0.000169	316.12	292.21	270.72
2	103.42	0.4865	66.2454	376.5054	0.000211	0.000226	0.000246	314.04	293.51	268.90
3	103.42	0.7425	101.0880	411.3480	0.000316	0.000334	0.000372	319.57	302.40	271.90
4	68.95	0.2342	31.8928	238.7428	0.000123	0.000132	0.000145	259.73	240.89	219.68
5	68.95	0.3334	45.3924	252.2424	0.000176	0.000190	0.000209	257.21	238.82	216.85
6	68.95	0.4944	67.3128	274.1628	0.000261	0.000278	0.000312	257.64	241.95	215.51
7	68.95	0.7344	99.9887	306.8387	0.000378	0.000398	0.000453	264.19	250.94	220.50
8	34.47	0.1358	18.4856	121.8956	0.000096	0.000101	0.000121	193.05	183.83	152.41
9	34.47	0.2341	31.8715	135.2815	0.000169	0.000177	0.000211	188.78	180.23	151.19
10	34.47	0.3373	45.9287	149.3387	0.000237	0.000250	0.000297	193.59	183.62	154.50
11	34.47	0.4916	66.9385	170.3485	0.000332	0.000343	0.000418	201.85	195.16	160.33
12	20.69	0.1344	18.3055	80.3755	0.000136	0.000143	0.000174	134.76	127.72	105.21
13	20.69	0.2353	32.0333	94.1033	0.000223	0.000237	0.000291	143.76	135.44	110.11
14	20.69	0.3392	46.1895	108.2595	0.000331	0.000338	0.000426	139.48	136.57	108.54

Table 5.2 Resilient Modulus Test Results for A-3 Soil (Sample B)

Sample : No. 2
Date: Feb.19, 2000
Opt. Moisture Cont 11.40%
Opt. Density : 112.1 pcf

Soil Identification: A-3 SR70
Test Procedure: **T292-91I**
Lab. Moisture Cont. : 11.60%
Lab. Density : 118 pcf

Test No.	Confining Presure	Axial Load	Dev. Stress	Bulk Stress	Mid LVDT Strain	Probe Strain	Full LVDT Strain	Mid LVDT Mr	Probe Mr	Full LVDT Mr
	kPa	kN	kPa	kPa				MPa	MPa	MPa
1	103.42	0.3669	45.2714	355.5314	0.000120	0.000143	0.000162	377.80	317.14	280.30
2	103.42	0.3720	45.8914	356.1514	0.000127	0.000142	0.000161	361.17	323.44	285.72
3	103.42	0.8184	100.9759	411.2359	0.000287	0.000304	0.000351	351.66	331.81	287.48
4	68.95	0.2572	31.7330	238.5830	0.000104	0.000122	0.000140	306.27	260.78	226.30
5	68.95	0.3723	45.9276	252.7776	0.000160	0.000176	0.000202	286.15	261.23	227.88
6	68.95	0.5404	66.6793	273.5293	0.000238	0.000253	0.000294	280.19	263.97	226.48
7	68.95	0.8190	101.0480	307.8980	0.000365	0.000371	0.000430	277.11	272.43	235.23
8	34.47	0.1472	18.1638	121.5738	0.000084	0.000097	0.000116	215.54	186.90	157.09
9	34.47	0.2594	32.0025	135.4125	0.000159	0.000174	0.000206	201.03	183.69	155.19
10	34.47	0.3684	45.4472	148.8572	0.000234	0.000243	0.000290	194.04	186.83	156.92
11	34.47	0.5394	66.5473	169.9573	0.000322	0.000340	0.000407	206.88	195.52	163.42
12	20.69	0.1491	18.4006	80.4706	0.000126	0.000143	0.000173	145.49	128.97	106.15
13	20.69	0.2589	31.9431	94.0131	0.000217	0.000236	0.000289	147.51	135.64	110.65
14	20.69	0.3728	45.9897	108.0597	0.000320	0.000339	0.000412	143.80	135.80	111.51

Table 5.3 Resilient Modulus Test Results for A-3 Soil (Sample C)

Sample : No. 3
Date: Mar.02, 2000
Opt. Moisture Cont 11.40%
Opt. Density : 112.1 pcf

Soil Identification: A-3 SR70
Test Procedure: **T292-91I**
Lab. Moisture Cont. : 10.40%
Lab. Density : 119 pcf

Test No.	Confining Presure	Axial Load	Dev. Stress	Bulk Stress	Mid LVDT Strain	Probe Strain	Full LVDT Strain	Mid LVDT Modulus	Probe Modulus	Full LVDT Modulus
	kPa	kN	kPa	kPa				MPa	MPa	MPa
1	103.42	0.3730	46.0112	356.2712	0.000135	0.000145	0.000159	340.09	317.05	289.63
2	103.42	0.5401	66.6161	376.8761	0.000200	0.000215	0.000232	333.25	309.77	286.84
3	103.42	0.8177	100.8562	411.1162	0.000305	0.000327	0.000354	330.22	308.61	284.62
4	68.95	0.2591	31.9531	238.8031	0.000118	0.000129	0.000140	269.90	248.54	228.12
5	68.95	0.3677	45.3493	252.1993	0.000171	0.000185	0.000204	265.52	245.74	222.22
6	68.95	0.5341	65.8788	272.7288	0.000248	0.000266	0.000294	265.46	247.57	223.90
7	68.95	0.8060	99.4112	306.2612	0.000368	0.000392	0.000439	269.95	253.77	226.65
8	34.47	0.1482	18.2840	121.6940	0.000095	0.000100	0.000121	191.83	182.40	151.02
9	34.47	0.2558	31.5533	134.9633	0.000167	0.000177	0.000210	189.13	178.06	150.12
10	34.47	0.3674	45.3198	148.7298	0.000236	0.000249	0.000298	191.78	181.73	152.28
11	34.47	0.5310	65.4922	168.9022	0.000330	0.000349	0.000418	198.34	187.88	156.84
12	20.69	0.1457	17.9755	80.0455	0.000138	0.000145	0.000184	130.40	123.82	97.50
13	20.69	0.2600	32.0735	94.1435	0.000229	0.000239	0.000308	139.87	134.22	104.21
14	20.69	0.3719	45.8676	107.9376	0.000323	0.000336	0.000433	142.13	136.32	105.99

Table 5.4 Resilient Modulus Test Results for A-3 Soil (Sample D)

Sample : No. 4
Date: Feb.19, 2000
Opt. Moisture Cont 11.40%
Opt. Density : 112.1 pcf

Soil Identification: A-3 SR70
Test Procedure: **T292-91I**
Lab. Moisture Cont. : 11.40%
Lab. Density : 119 pcf

Test No.	Confining Presure	Axial Load	Dev. Stress	Bulk Stress	Mid LVDT Strain	Probe Strain	Full LVDT Strain	Mid LVDT Modulus	Probe Modulus	Full LVDT Modulus
	kPa	kN	kPa	kPa				MPa	MPa	MPa
1	103.42	0.3656	45.0968	355.3568	0.000101	0.000120	0.000152	448.04	374.34	296.14
2	103.42	0.5339	65.8572	376.1172	0.000161	0.000184	0.000223	408.22	357.44	295.63
3	103.42	0.8186	100.9734	411.2334	0.000257	0.000287	0.000339	392.47	352.40	297.63
4	68.95	0.2557	31.5333	238.3833	0.000085	0.000100	0.000135	369.03	315.03	233.79
5	68.95	0.3700	45.6349	252.4849	0.000136	0.000156	0.000193	335.89	292.49	236.38
6	68.95	0.5419	66.8347	273.6847	0.000209	0.000235	0.000278	319.36	284.96	240.04
7	68.95	0.8152	100.5571	307.4071	0.000320	0.000349	0.000415	313.89	287.98	242.13
8	34.47	0.1497	18.4654	121.8754	0.000063	0.000075	0.000112	294.32	247.02	165.15
9	34.47	0.2587	31.9077	135.3177	0.000131	0.000149	0.000194	244.00	214.09	164.28
10	34.47	0.3749	46.2455	149.6555	0.000197	0.000218	0.000277	234.43	212.20	166.87
11	34.47	0.5375	66.2943	169.7043	0.000287	0.000312	0.000389	231.33	212.47	170.23
12	20.69	0.1495	18.4368	80.5068	0.000107	0.000120	0.000176	172.66	153.29	104.54
13	20.69	0.2583	31.8646	93.9346	0.000194	0.000213	0.000289	164.44	149.54	110.09
14	20.69	0.2014	24.8394	86.9094	0.000859	0.000110	0.000354	128.91	115.57	70.16

Table 5.5 Resilient Modulus Test Results for A-2-4 Soil (Sample A)

Sample : No. 1
Date: Jan.6, 2000
Opt. Moisture Cont 10.60%
Opt. Density : 122pcf

Soil Identification: A-2-4 SR70
Test Procedure: **T292-91I**
Lab. Moisture Cont. : 10.62%
Lab. Density : 132 pcf

Test No.	Confining Pressure	Axial Load	Dev. Stress	Bulk Stress	Mid LVDT Strain	Probe Strain	Full LVDT Strain	Mid LVDT Modulus	Probe Modulous	Full LVDT Moduous
	kPa	kN	kPa	kPa				MPa	MPa	MPa
1	103.42	0.36703	45.2838	355.544	0.000129	0.000136	0.000140	350.32	334.01	322.51
2	103.42	0.53531	66.0456	376.306	0.000194	0.000204	0.000211	340.15	324.42	313.44
3	103.42	0.81585	100.6573	410.917	0.000306	0.000321	0.000333	329.22	314.01	301.93
4	68.95	0.25926	31.9863	238.836	0.000095	0.000099	0.000110	337.86	324.67	290.46
5	68.95	0.36999	45.6486	252.499	0.000146	0.000152	0.000168	313.73	300.93	272.32
6	68.95	0.53624	66.1600	273.010	0.000227	0.000240	0.000257	291.15	275.44	257.29
7	68.95	0.81723	100.8272	307.677	0.000364	0.000381	0.000408	276.83	264.70	246.89
8	34.47	0.14850	18.3215	121.731	0.000058	0.000061	0.000078	317.97	302.08	235.67
9	34.47	0.25819	31.8545	135.264	0.000116	0.000119	0.000148	275.59	267.32	215.67
10	34.47	0.37262	45.9735	149.383	0.000182	0.000189	0.000228	253.16	243.70	201.34
11	34.47	0.53466	65.9648	169.375	0.000285	0.000296	0.000348	231.65	222.71	189.36
12	20.69	0.14797	18.2558	80.326	0.000069	0.000072	0.000110	263.59	254.97	166.24
13	20.69	0.25928	31.9892	94.059	0.000142	0.000149	0.000208	225.38	215.25	153.58
14	20.69	0.37301	46.0216	108.092	0.000222	0.000231	0.000309	207.20	199.00	148.82

Table 5.6 Resilient Modulus Test Results for A-2-4 Soil (Sample B)

Sample : No. 2
Date: Feb.10, 2000
Opt. Moisture Cont 10.60%
Opt. Density : 122.1 pcf

Soil Identification: A-2-4 SR70
Test Procedure: **T292-91I**
Lab. Moisture Cont. : 10.70%
Lab. Density : 131 pcf

Test No.	Confining Presure	Axial Load	Dev. Stress	Bulk Stress	Mid LVDT Strain	Probe Strain	Full LVDT Strain	Mid LVDT Modulus	Probe Modulus	Full LVDT Modulus
	kPa	kN	kPa	kPa				MPa	MPa	MPa
1	103.42	0.3719	45.8787	356.1387	0.000129	0.000140	0.000145	354.65	327.63	316.28
2	103.42	0.5321	65.6448	375.9048	0.000198	0.000210	0.000218	331.36	312.88	300.45
3	103.42	0.8157	100.6381	410.8981	0.000311	0.000318	0.000338	323.95	316.76	298.08
4	68.95	0.2564	31.6390	238.4890	0.000099	0.000107	0.000121	319.26	294.51	261.33
5	68.95	0.3688	45.5055	252.3555	0.000155	0.000162	0.000180	294.52	280.59	253.26
6	68.95	0.5369	66.2384	273.0884	0.000239	0.000251	0.000269	276.64	263.48	246.17
7	68.95	0.8227	101.5006	308.3506	0.000367	0.000385	0.000403	276.64	263.50	251.71
8	34.47	0.1482	18.2891	121.6991	0.000062	0.000065	0.000090	292.89	279.85	203.89
9	34.47	0.2602	32.1037	135.5137	0.000130	0.000138	0.000166	246.95	232.95	192.97
10	34.47	0.3713	45.8115	149.2215	0.000202	0.000209	0.000249	226.52	219.35	184.05
11	34.47	0.5304	65.4339	168.8439	0.000312	0.000323	0.000371	209.73	202.58	176.54
12	20.69	0.1479	18.2496	80.3196	0.000084	0.000087	0.000131	216.25	210.11	139.41
13	20.69	0.2550	31.4586	93.5286	0.000174	0.000179	0.000242	180.44	176.10	130.18
14	20.69	0.3726	45.9757	108.0457	0.000265	0.000272	0.000349	173.33	169.29	131.58

Table 5.7 Resilient Modulus Test Results for A-2-4 Soil (Sample C)

Sample : No. 3
Date: Mar.14, 2000
Opt. Moisture Cont : 10.60%
Opt. Density : 112.1 pcf

Soil Identification: A-2-4 SR70
Test Procedure: **T292-91I**
Lab. Moisture Cont. : 10.58%
Lab. Density : 111.6 pcf

Test No.	Confining Presure	Axial Load	Dev. Stress	Bulk Stress	Mid LVDT Strain	Probe Strain	Full LVDT Strain	Mid LVDT Modulus	Probe Modulus	Full LVDT Modulus
	kPa	kN	kPa	kPa				MPa	MPa	MPa
1	103.42	0.3728	45.9785	356.2385	0.000118	0.000124	0.000143	388.93	370.76	321.61
2	103.42	0.5364	66.1682	376.4282	0.000181	0.000194	0.000216	365.95	341.36	306.68
3	103.42	0.8208	101.2396	411.4996	0.000285	0.000304	0.000336	355.50	332.54	301.28
4	68.95	0.2579	31.8068	238.6568	0.000091	0.000096	0.000115	347.90	329.68	277.74
5	68.95	0.3674	45.3204	252.1704	0.000139	0.000148	0.000173	325.80	307.04	261.86
6	68.95	0.5313	65.5314	272.3814	0.000213	0.000227	0.000261	308.10	288.68	250.76
7	68.95	0.8223	101.4229	308.2729	0.000329	0.000355	0.000403	307.96	285.87	251.74
8	34.47	0.1483	18.2924	121.7024	0.000056	0.000060	0.000084	323.83	302.83	217.49
9	34.47	0.2568	31.6756	135.0856	0.000114	0.000114	0.000159	276.93	276.91	199.08
10	34.47	0.3662	45.1662	148.5762	0.000172	0.000185	0.000235	262.93	243.84	191.84
11	34.47	0.5415	66.7856	170.1956	0.000262	0.000284	0.000347	254.57	235.11	192.48
12	20.69	0.1482	18.2762	80.3462	0.000069	0.000074	0.000133	264.17	247.76	137.38
13	20.69	0.2603	32.1029	94.1729	0.000138	0.000145	0.000238	232.63	221.48	135.00
14	20.69	0.3740	46.1259	108.1959	0.000210	0.000229	0.000339	219.40	201.71	136.00

Table 5.8 Resilient Modulus Test Results for Limerock (Sample A)

Sample : No. 1
Date: Mar.30, 2000
Opt. Moisture Cont 7.45%
Opt. Density : 130 pcf

Soil Identification: Limerock, Lee Co. #1B
Test Procedure: **T292-91I**
Lab. Moisture Cont. : 7.38%
Lab. Density : 127 pcf

Test No.	Confining Presure	Axial Load	Dev. Stress	Bulk Stress	Mid LVDT Strain	Probe Strain	Full LVDT Strain	Mid LVDT Modulus	Probe Modulus	Full LVDT Modulus
	kPa	kN	kPa	kPa				MPa	MPa	MPa
1	103.42	0.3731	46.0171	356.2771	0.000041	0.000046	0.000062	1123.34	1003.33	741.90
2	103.42	0.5403	66.6433	376.9033	0.000071	0.000078	0.000099	938.92	850.13	673.02
3	103.42	0.8199	101.1289	411.3889	0.000130	0.000140	0.000170	776.14	719.80	594.35
4	68.95	0.2597	32.0292	238.8792	0.000027	0.000033	0.000046	1177.08	983.91	692.97
5	68.95	0.3703	45.6797	252.5297	0.000048	0.000054	0.000073	945.34	849.65	625.70
6	68.95	0.5394	66.5294	273.3794	0.000084	0.000090	0.000117	794.15	742.21	570.07
7	68.95	0.8172	100.7963	307.6463	0.000150	0.000159	0.000197	671.40	632.67	511.90
8	34.47	0.1474	18.1852	121.5952	0.000014	0.000017	0.000032	1285.50	1061.86	564.80
9	34.47	0.2575	31.7560	135.1660	0.000035	0.000040	0.000061	901.97	799.63	516.84
10	34.47	0.3677	45.3574	148.7674	0.000061	0.000066	0.000096	741.89	684.77	472.89
11	34.47	0.5412	66.7581	170.1681	0.000104	0.000111	0.000150	644.98	599.99	443.66
12	20.69	0.1474	18.1787	80.2487	0.000017	0.000020	0.000042	1099.61	921.20	433.70
13	20.69	0.2597	32.0381	94.1081	0.000041	0.000045	0.000080	780.71	712.30	402.87
14	20.69	0.3733	46.0484	108.1184	0.000071	0.000077	0.000120	651.93	600.03	382.67

Table 5.9 Resilient Modulus Test Results for Limerock (Sample B)

Sample : No. 2
Date: Mar.6, 2000
Opt. Moisture Cont 7.40%
Opt. Density : 130.6 pcf

Soil Identification: Limerock Lee Co.#1B
Test Procedure: **T292-91I**
Lab. Moisture Cont. : 7.30%
Lab. Density : 125.0pcf

Test No.	Confining Presure	Axial Load	Dev. Stress	Bulk Stress	Mid LVDT Strain	Probe Strain	Full LVDT Strain	Mid LVDT Modulus	Probe Modulus	Full LVDT Modulus
	kPa	kN	kPa	kPa				MPa	MPa	MPa
1	103.42	0.3669	45.2521	355.5121	0.000044	0.000042	0.000072	1038.01	970.47	631.29
2	103.42	0.5338	65.8386	376.0986	0.000077	0.000083	0.000113	857.43	793.76	581.47
3	103.42	0.8177	100.8652	411.1252	0.000141	0.000150	0.000190	716.10	673.34	529.71
4	68.95	0.2605	32.1348	238.9848	0.000031	0.000036	0.000068	1041.60	890.26	469.24
5	68.95	0.3660	45.1411	251.9911	0.000055	0.000060	0.000102	816.19	746.38	440.95
6	68.95	0.5391	66.4916	273.3416	0.000094	0.000101	0.000153	708.97	659.27	434.27
7	68.95	0.8195	101.0873	307.9373	0.000166	0.000172	0.000243	609.69	587.75	415.58
8	34.47	0.1489	18.3704	121.7804	0.000015	0.000016	0.000062	1248.67	1121.01	298.25
9	34.47	0.2574	31.7439	135.1539	0.000039	0.000040	0.000115	813.52	785.70	275.35
10	34.47	0.3725	45.9445	149.3545	0.000070	0.000076	0.000168	657.31	608.43	274.24
11	34.47	0.5410	66.7354	170.1454	0.000120	0.000126	0.000244	557.55	528.60	274.05
12	20.69	0.1492	18.4015	80.4715	0.000018	0.000022	0.000099	1006.66	837.47	186.59
13	20.69	0.2602	32.1005	94.1705	0.000048	0.000051	0.000172	671.50	623.92	186.17
14	20.69	0.3652	45.0456	107.1156	0.000085	0.000089	0.000248	531.46	508.12	181.61

Table 5.10 Resilient Modulus Test Result for Limerock (Failed)

Sample : No. 3
Date: Feb.24, 2000
Opt. Moisture Cont 15.10%
Opt. Density : 111.3

Soil Identification: Limerock Ga.Co.#2B
Test Procedure: **T292-91I**
Lab. Moisture Cont. : 15.20%
Lab. Density : 111.2 pcf

Test No.	Confining Presure	Axial Load	Dev. Stress	Bulk Stress	Mid LVDT Strain	Probe Strain	Full LVDT Strain	Mid LVDT Modulus	Probe Modulus	Full LVDT Modulus
	kPa	kN	kPa	kPa				MPa	MPa	MPa
1	103.42	0.3647	44.9816	355.2416	0.000007	0.000147	0.000193	6648.18	306.17	232.58
2	103.42	0.5410	66.7284	376.9884	0.000017	0.000192	0.000260	3814.37	348.14	256.49
3	103.42	0.8078	99.6406	409.9006	0.000115	0.000318	0.000410	866.58	313.03	243.16
4	68.95	0.2568	31.6802	238.5302	0.000008	0.000134	0.000206	4036.39	235.86	153.64
5	68.95	0.3670	45.2621	252.1121	0.000014	0.000179	0.000274	3279.17	252.27	164.91
6	68.95	0.5383	66.3950	273.2450	0.000074	0.000252	0.000362	894.39	263.14	183.64
7	68.95	0.8015	98.8656	305.7156	0.000190	0.000401	0.000552	519.39	246.50	179.20
8	34.47	0.1454	17.9342	121.3442	0.000006	0.000086	0.000221	2904.01	209.56	81.22
9	34.47	0.2593	31.9868	135.3968	0.000019	0.000139	0.000344	1651.84	229.52	92.87
10	34.47	0.3634	44.8218	148.2318	0.000079	0.000211	0.000442	565.19	212.14	101.46
11	34.47	0.5417	66.8177	170.2277	0.000156	0.000308	0.000566	428.59	216.75	118.01
12	20.69	0.1465	18.0748	80.1448	0.000020	0.000137	0.000346	917.10	131.66	52.23
13	20.69	0.2549	31.4407	93.5107	0.000099	0.000241	0.000515	318.73	130.28	61.03
14	20.69	0.3700	45.6416	107.7116	0.000159	0.000329	0.000643	286.74	138.54	71.01

Table 5.11 Difference of Resilient Modulus Test Results Among the Measurements

Soil Type	A-3			A-2-4			Limerock		
Difference	Middle LVDT vs Probe	Full LVDT vs Probe	Middle LVDT vs Full LVDT	Middle LVDT vs Probe	Full LVDT vs Probe	Middle LVDT vs Full LVDT	Middle LVDT vs Probe	Full LVDT vs Probe	Middle LVDT vs Full LVDT
Sample A	5.8%	13.6%	22.7%	4.4%	14.7%	24.2%	11.5%	31.0%	66.8%
Sample B	9.5%	14.9%	28.7%	4.6%	14.3%	23.6%	8.6%	49.2%	151.0%
Sample C	6.3%	13.8%	23.8%	6.3%	21.4%	38.3%			
Average	7.2%	14.1%	25.0%	5.1%	16.8%	28.7%			

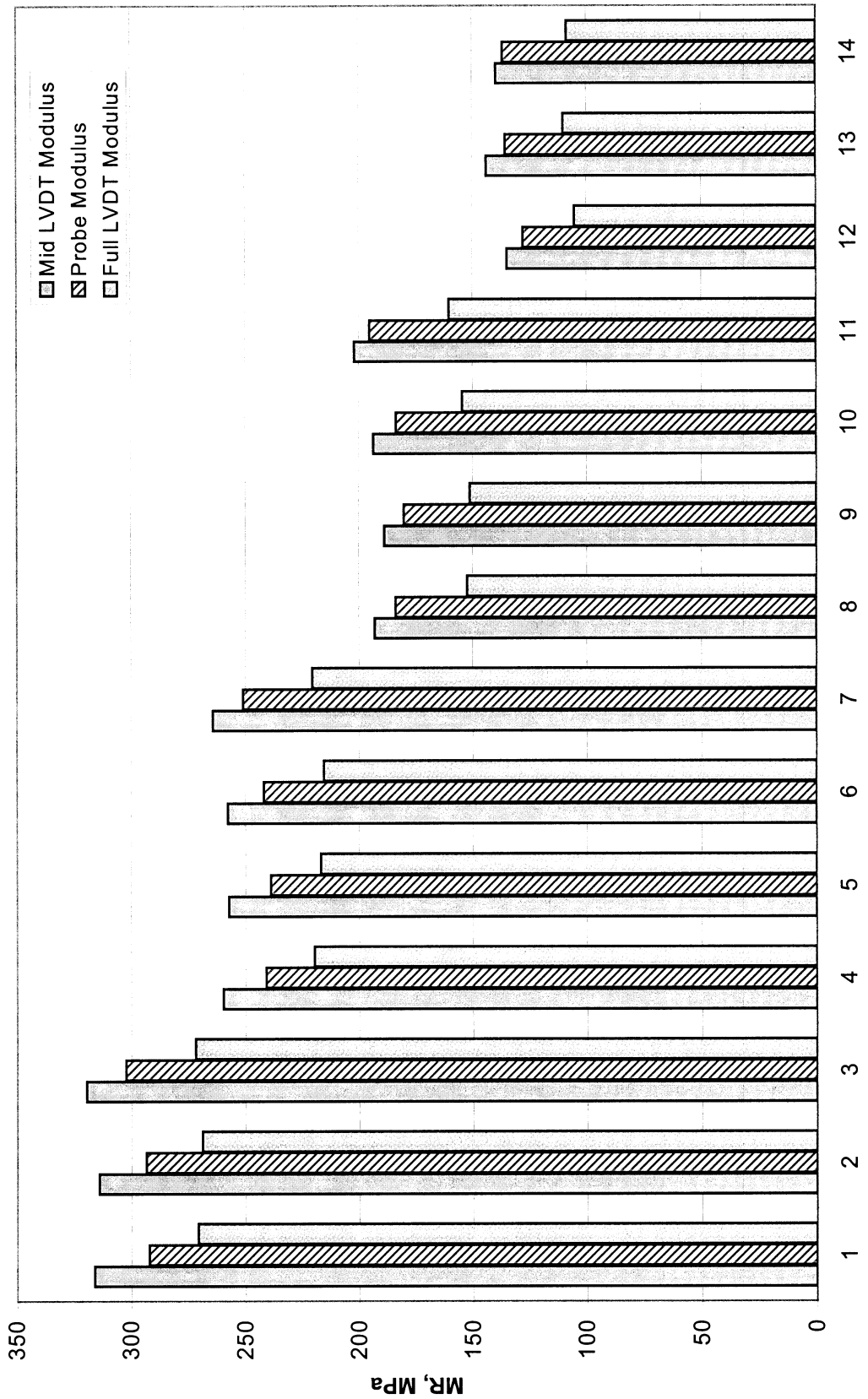

Figure 5.1 Resilient modulus test result for A-3 soil (Sample A)

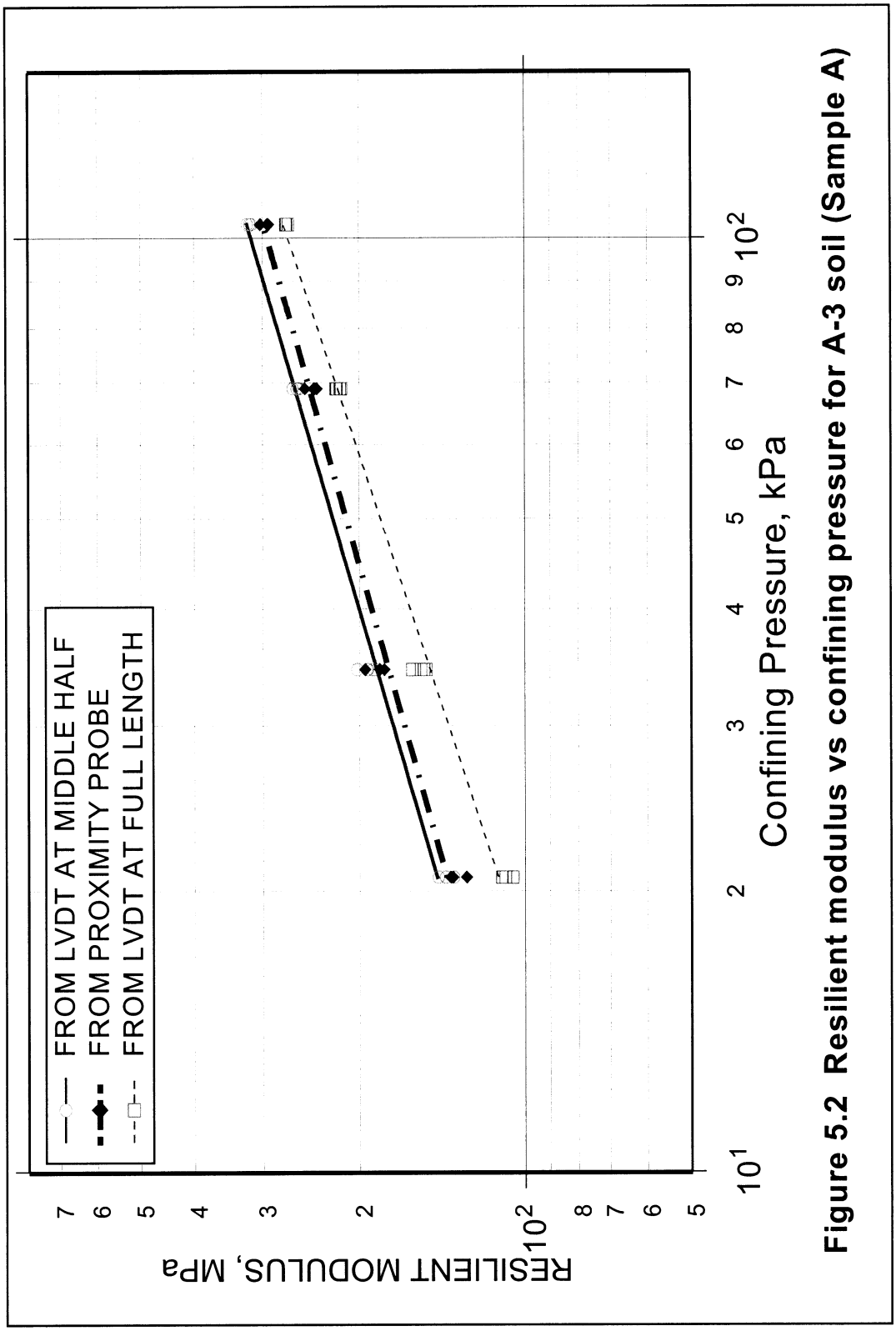

Figure 5.2 Resilient modulus vs confining pressure for A-3 soil (Sample A)

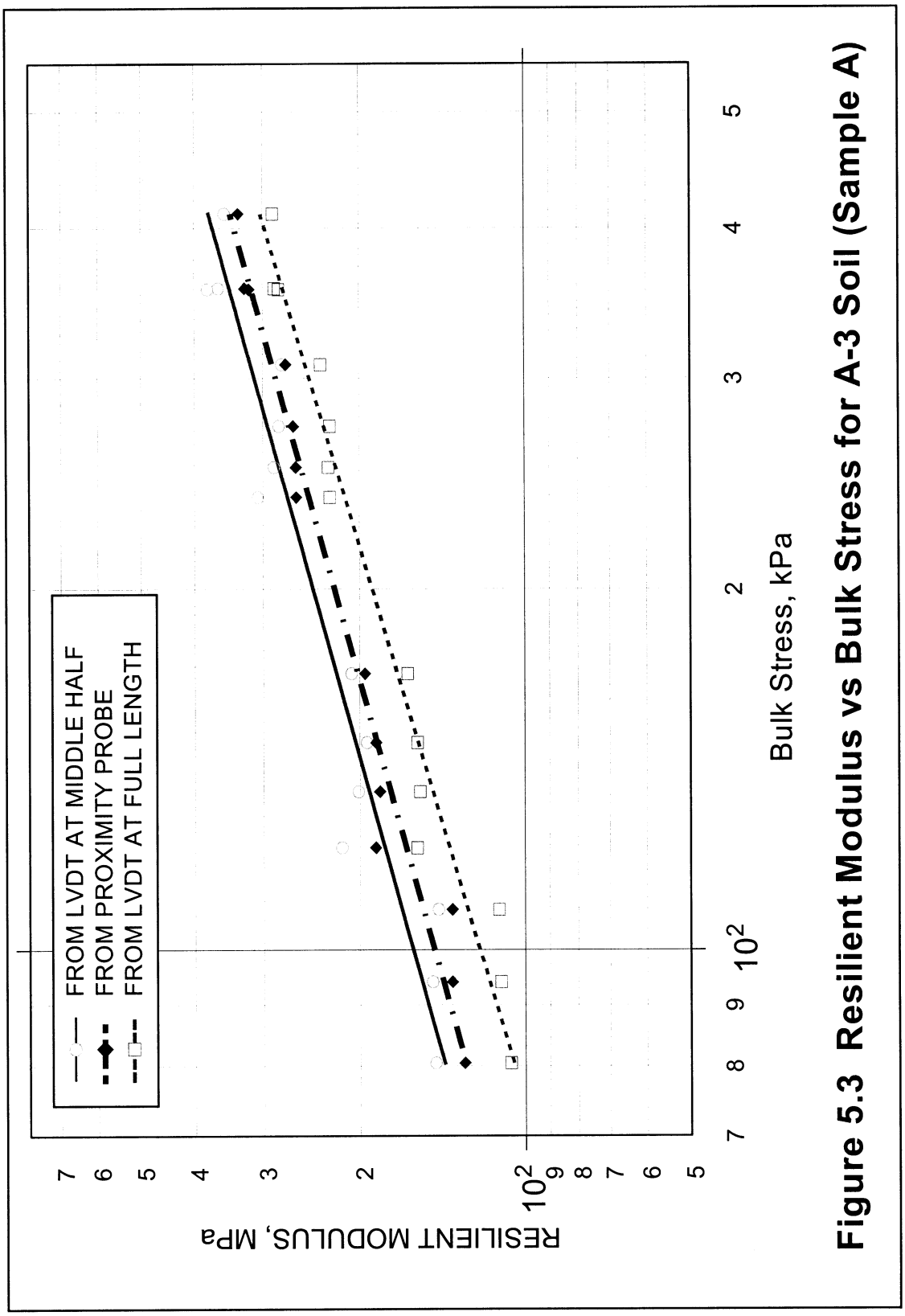

Figure 5.3 Resilient Modulus vs Bulk Stress for A-3 Soil (Sample A)

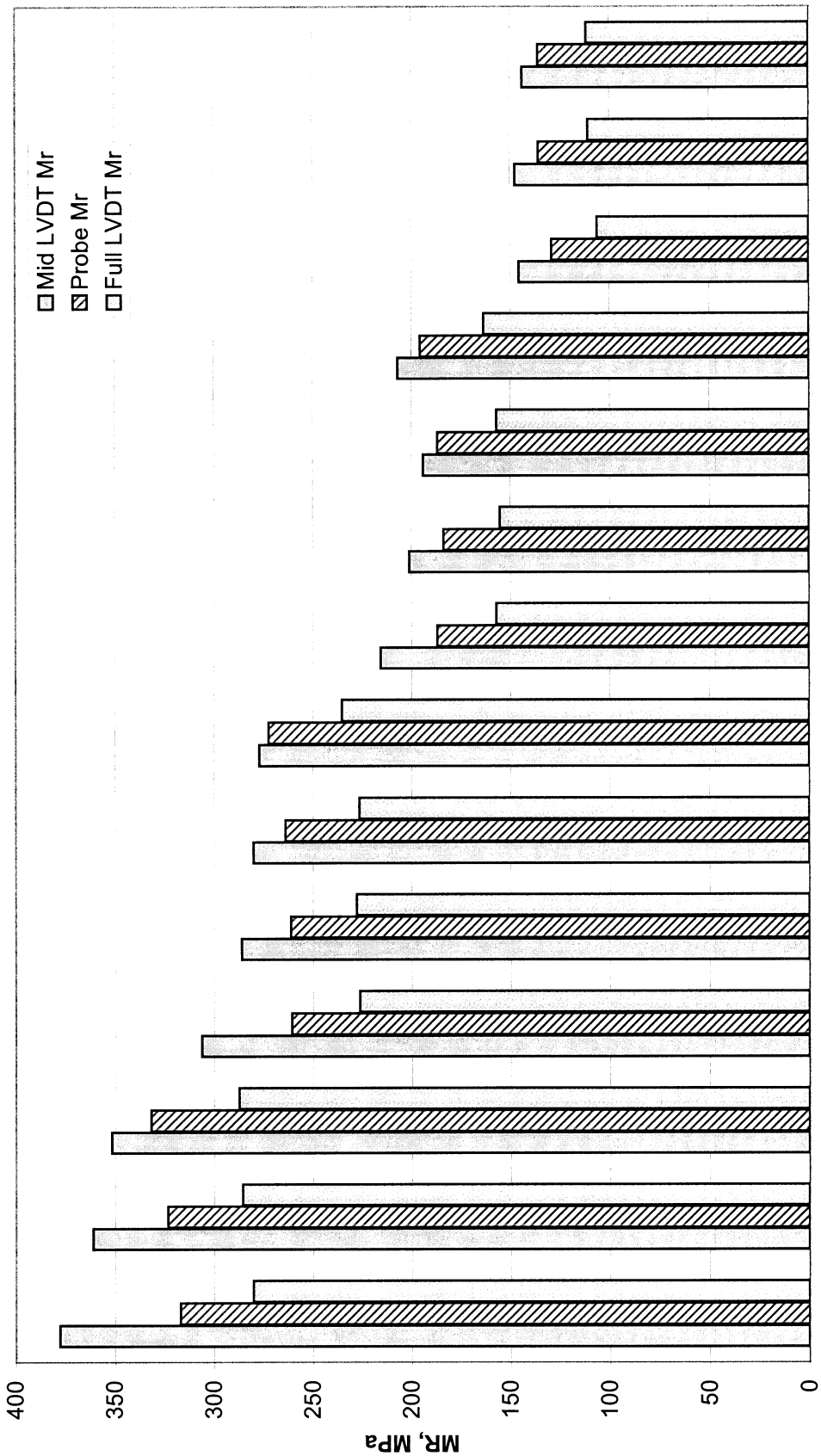

Figure 5.4 Resilient modulus test result for A-3 soil (Sample B)

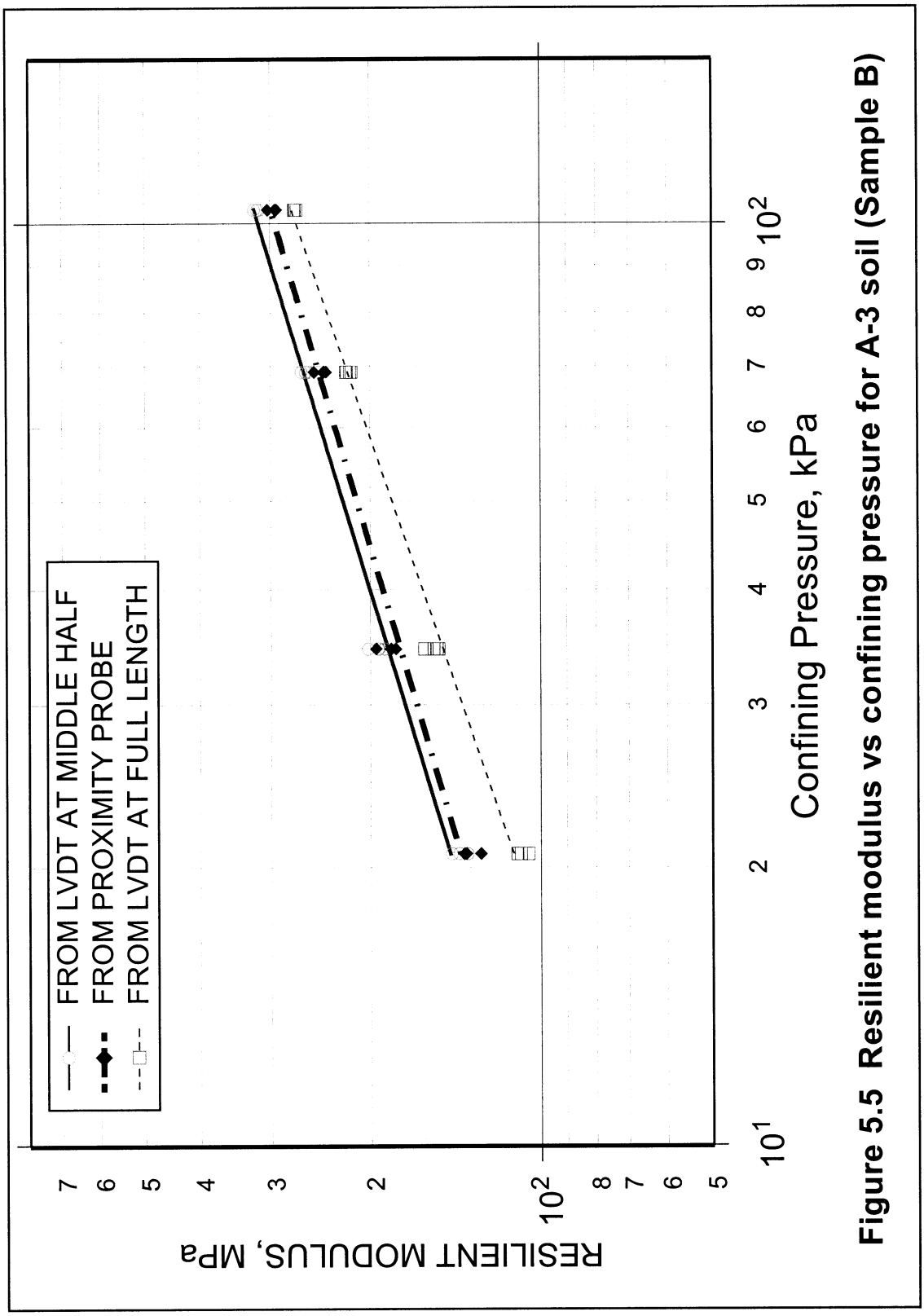

Figure 5.5 Resilient modulus vs confining pressure for A-3 soil (Sample B)

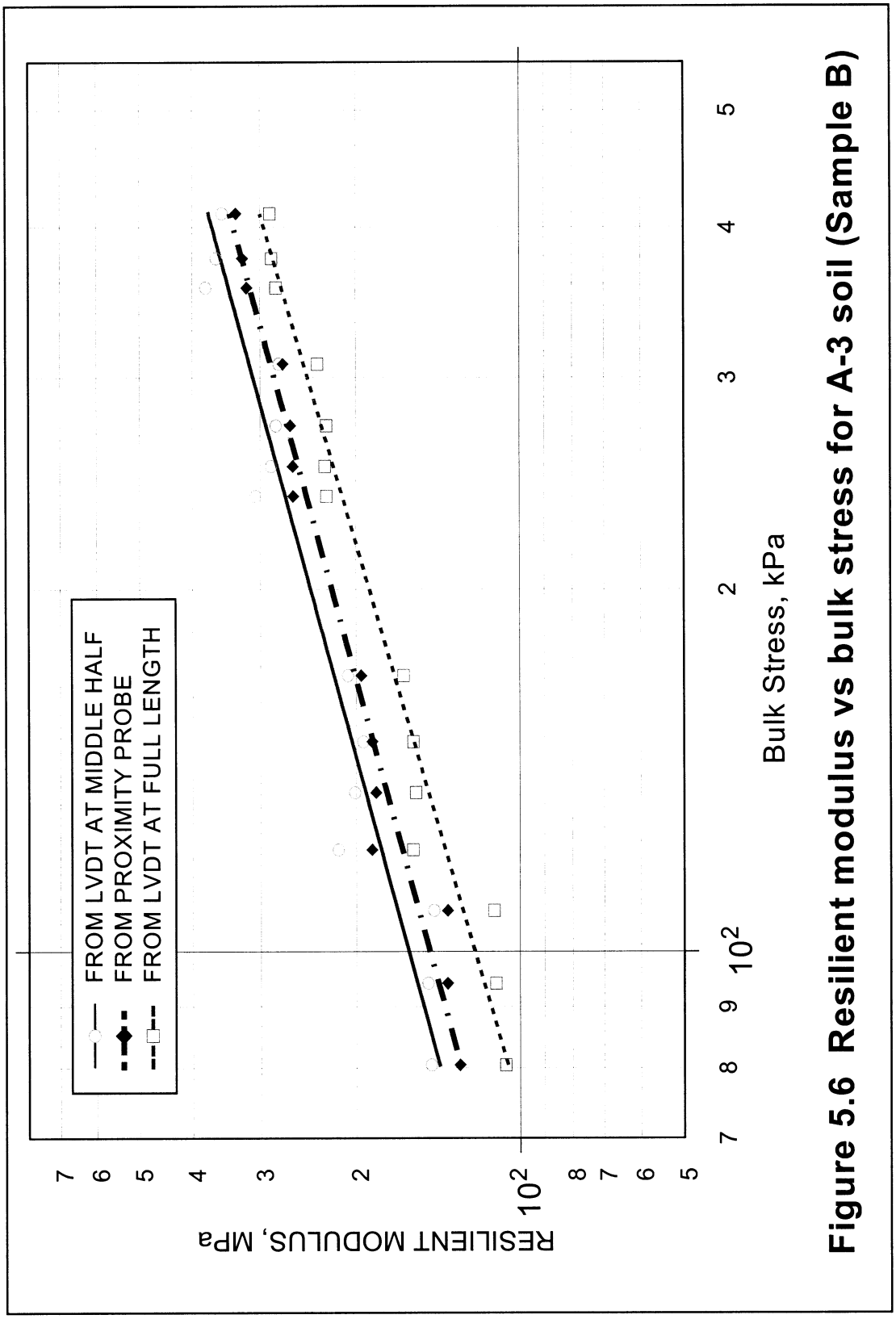

Figure 5.6 Resilient modulus vs bulk stress for A-3 soil (Sample B)

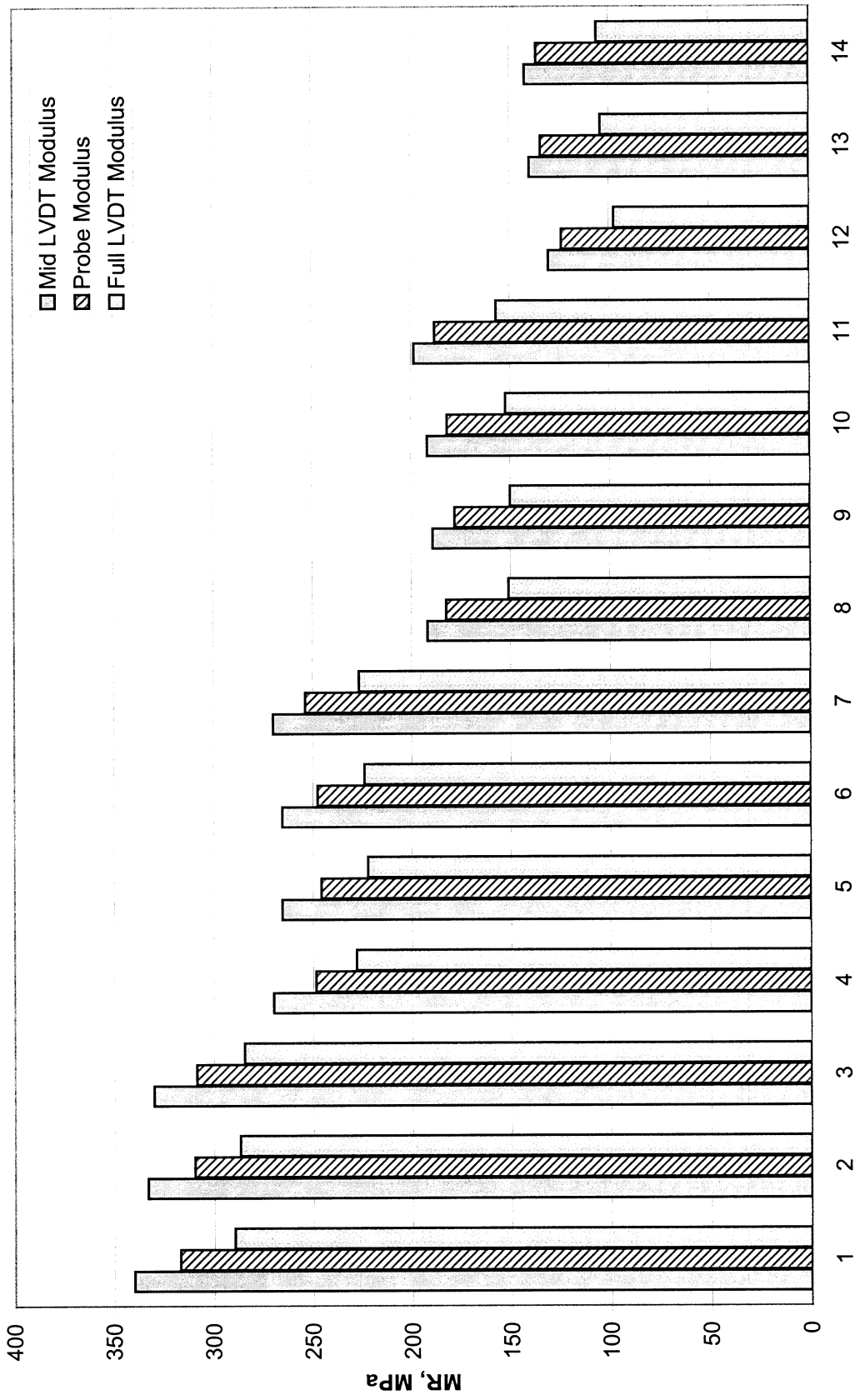

Figure 5.7 Resilient modulus test result for A-3 soil (Sample C)

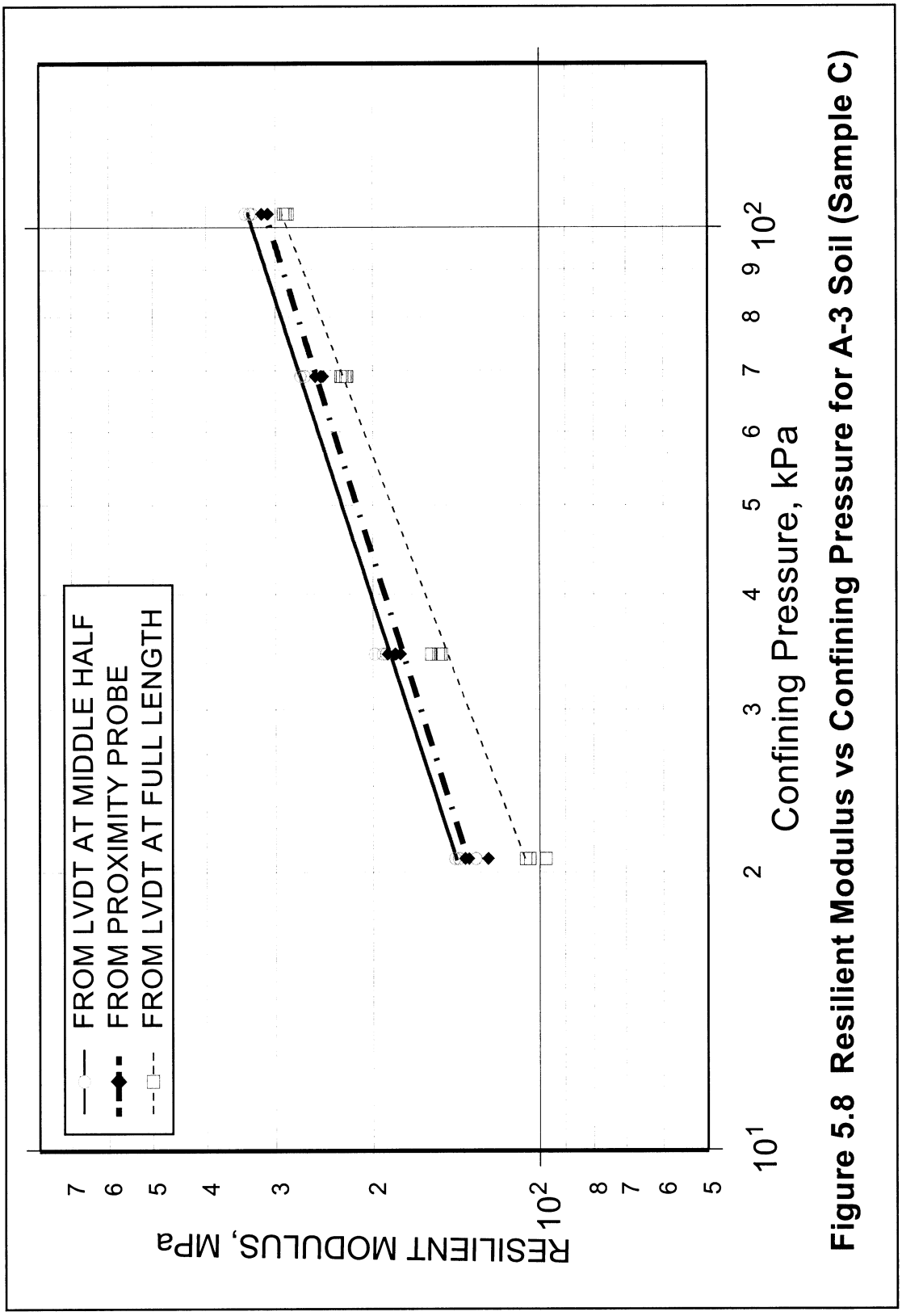

Figure 5.8 Resilient Modulus vs Confining Pressure for A-3 Soil (Sample C)

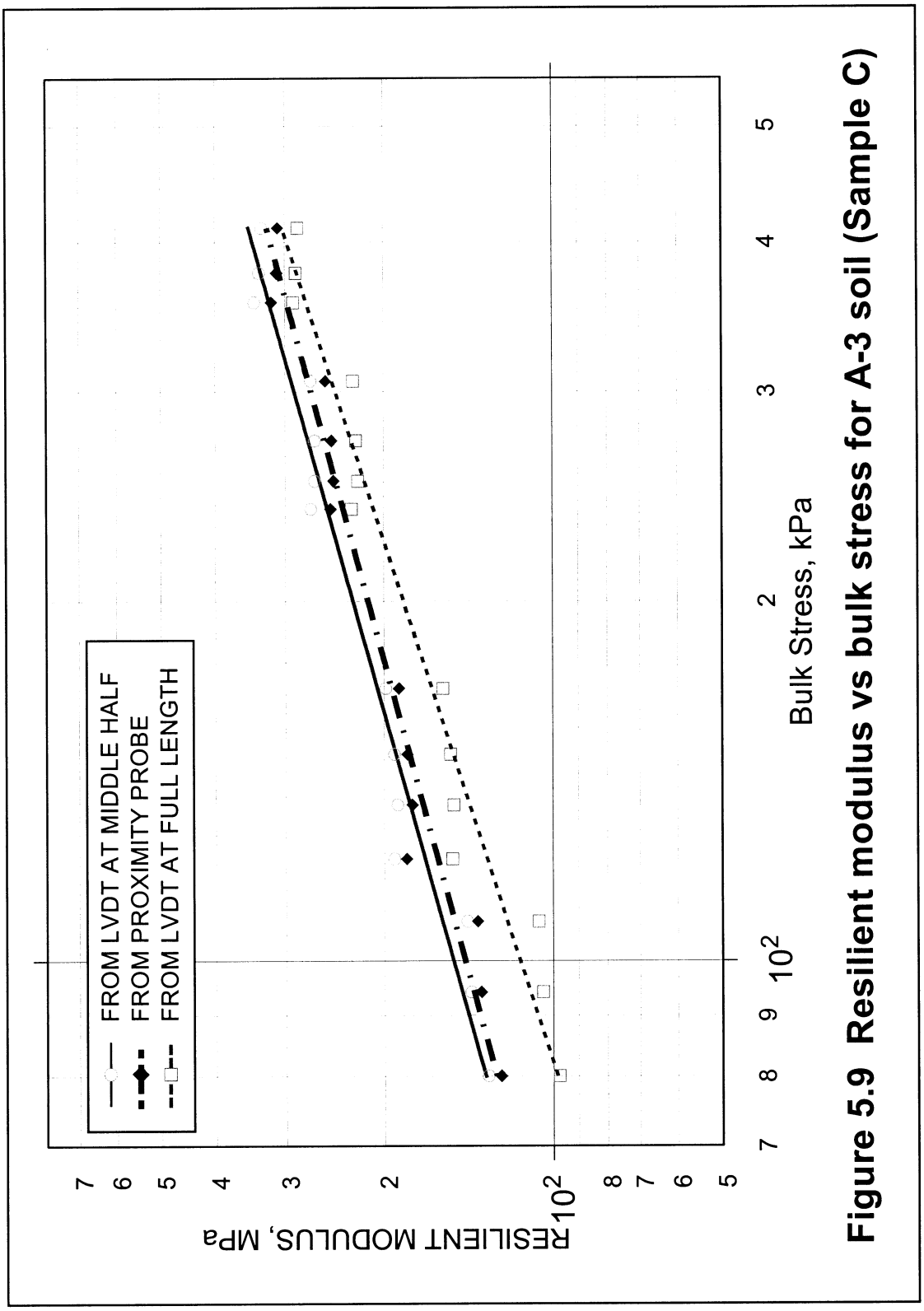

Figure 5.9 Resilient modulus vs bulk stress for A-3 soil (Sample C)

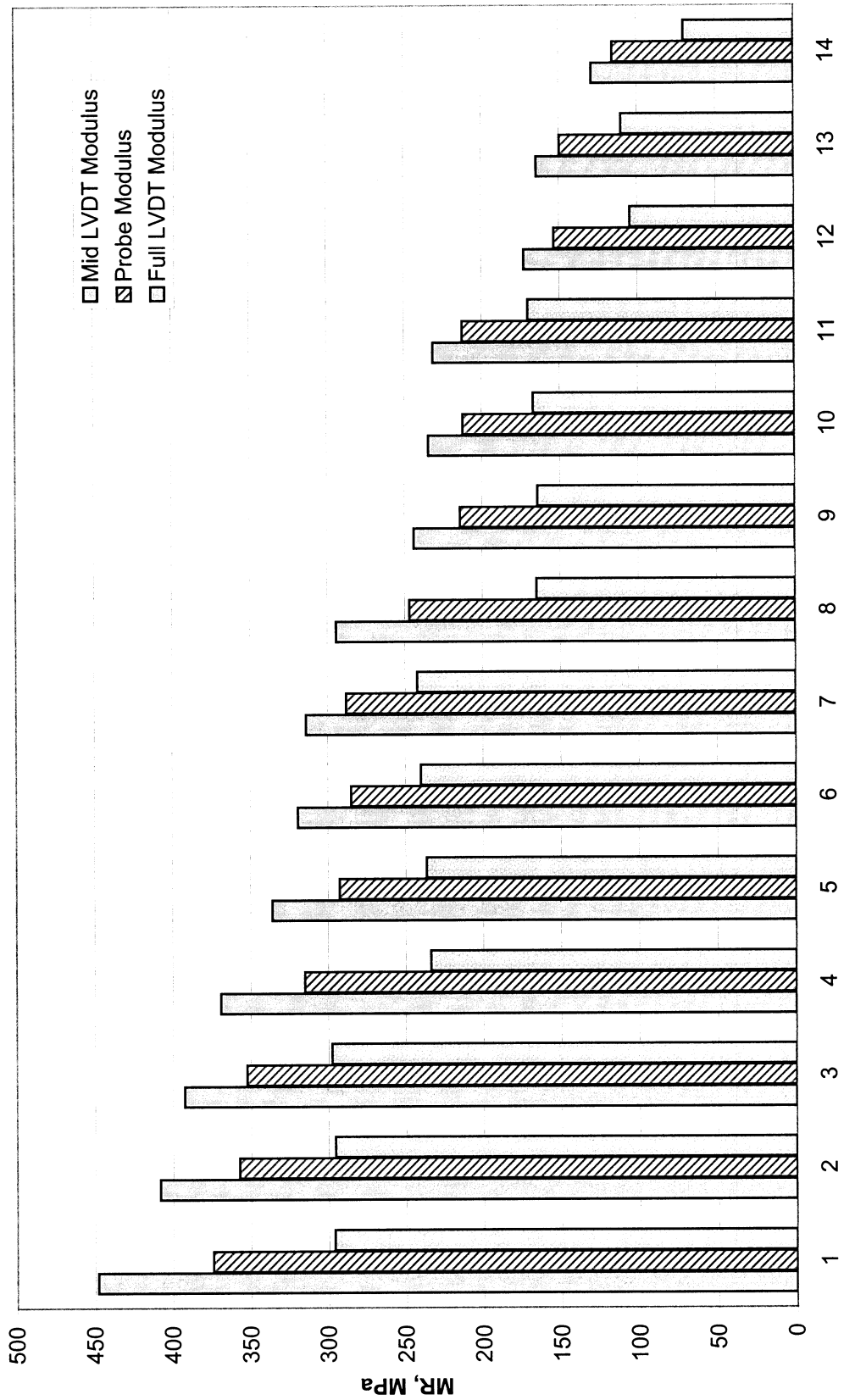

Figure 5.10 Resilient Modulus Test Results for A-3 Soil (Sample D)

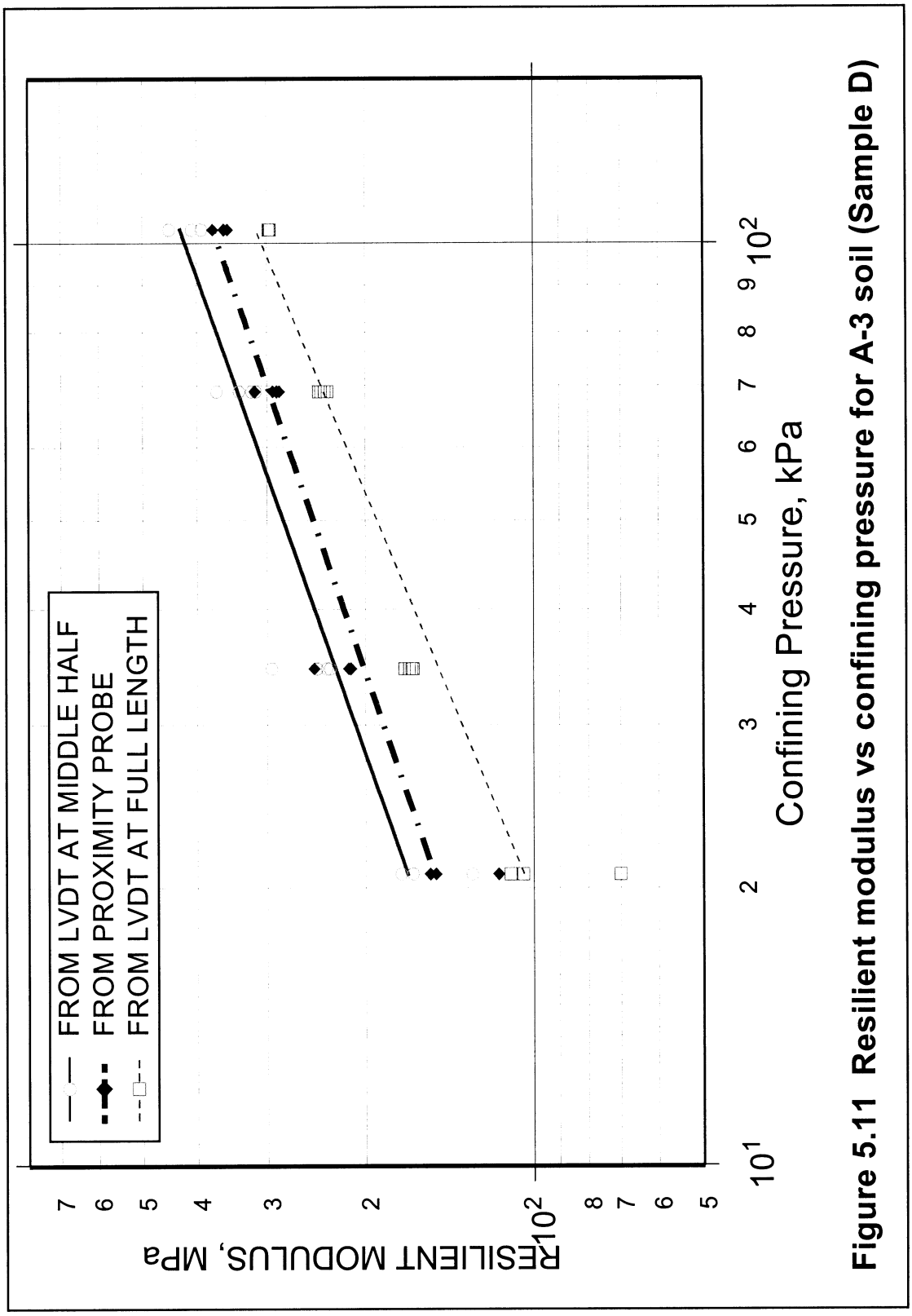

Figure 5.11 Resilient modulus vs confining pressure for A-3 soil (Sample D)

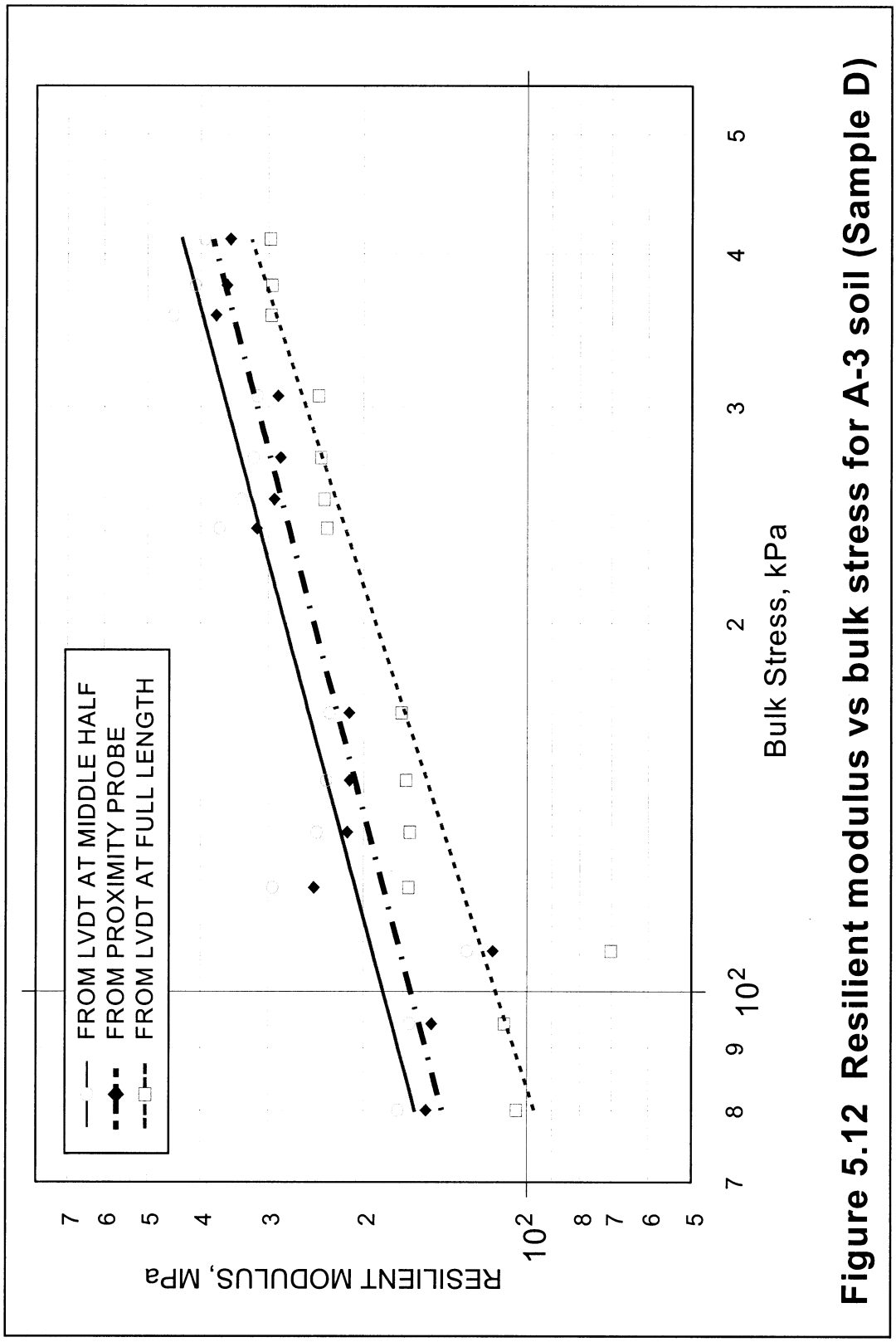

Figure 5.12 Resilient modulus vs bulk stress for A-3 soil (Sample D)

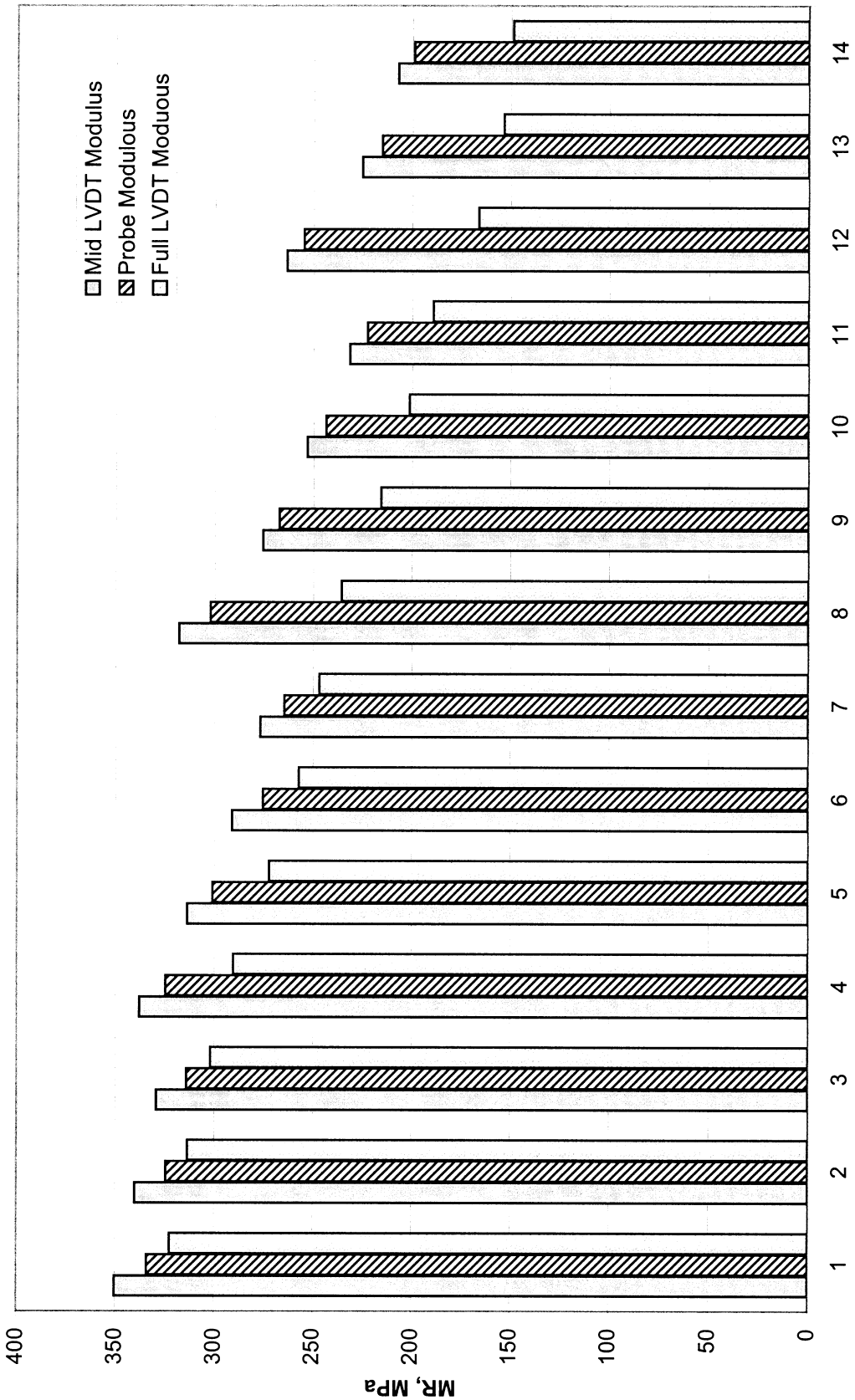

Figure 5.13 Resilient modulus test result for A-2-4 soil (Sample A)

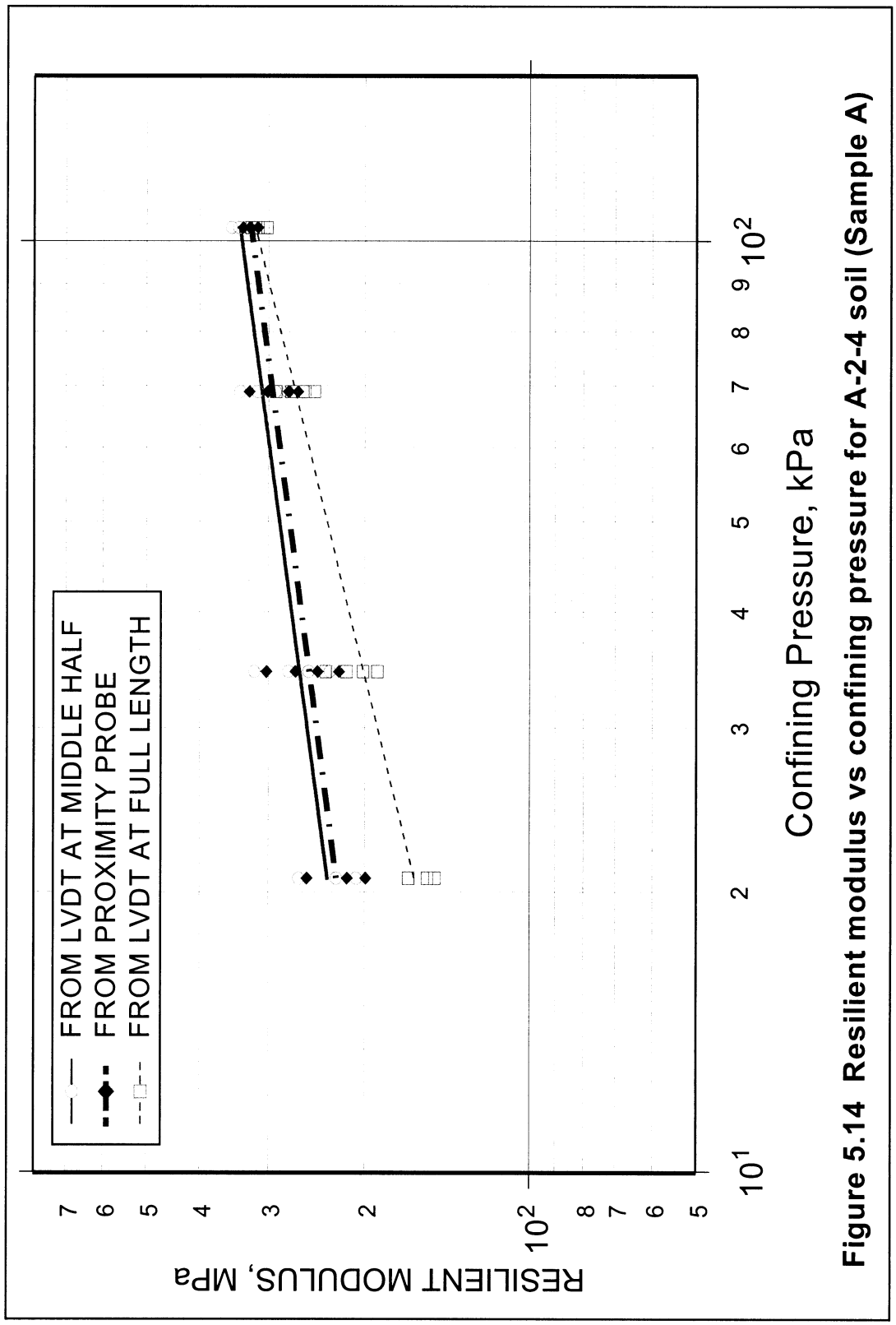

Figure 5.14 Resilient modulus vs confining pressure for A-2-4 soil (Sample A)

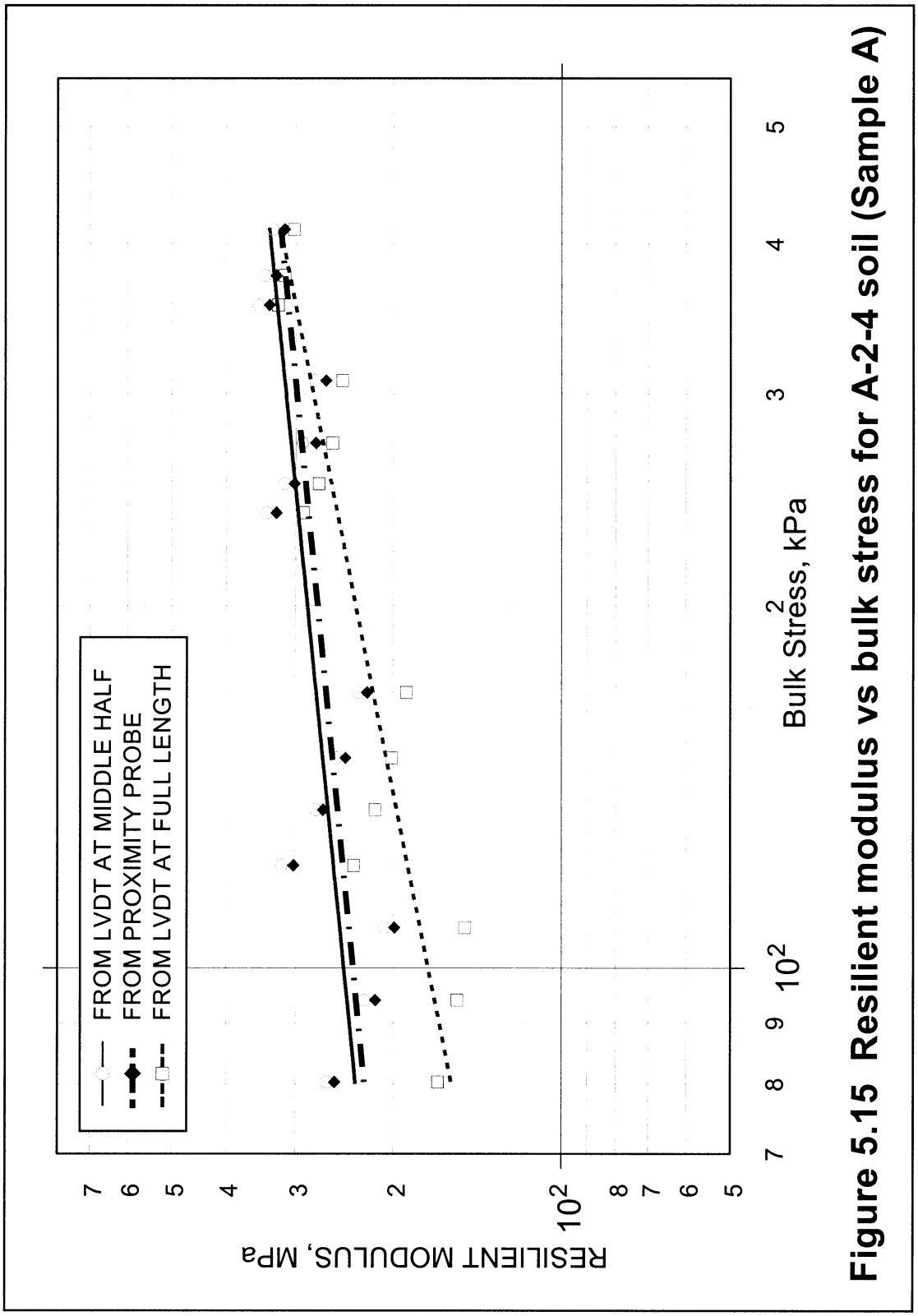

Figure 5.15 Resilient modulus vs bulk stress for A-2-4 soil (Sample A)

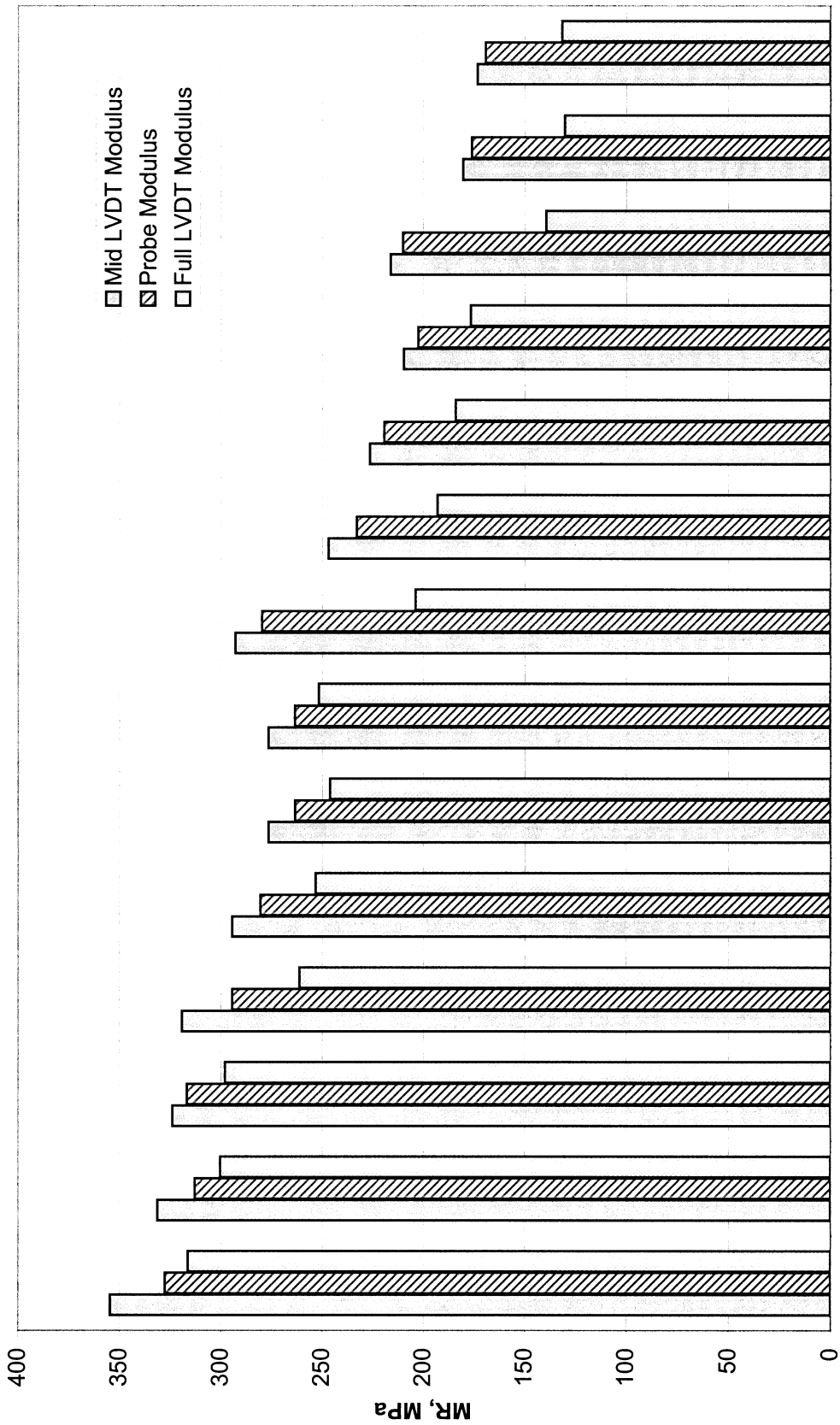

Figure 5.16 Resilient modulus test result for A-2-4 soil (Sample B)

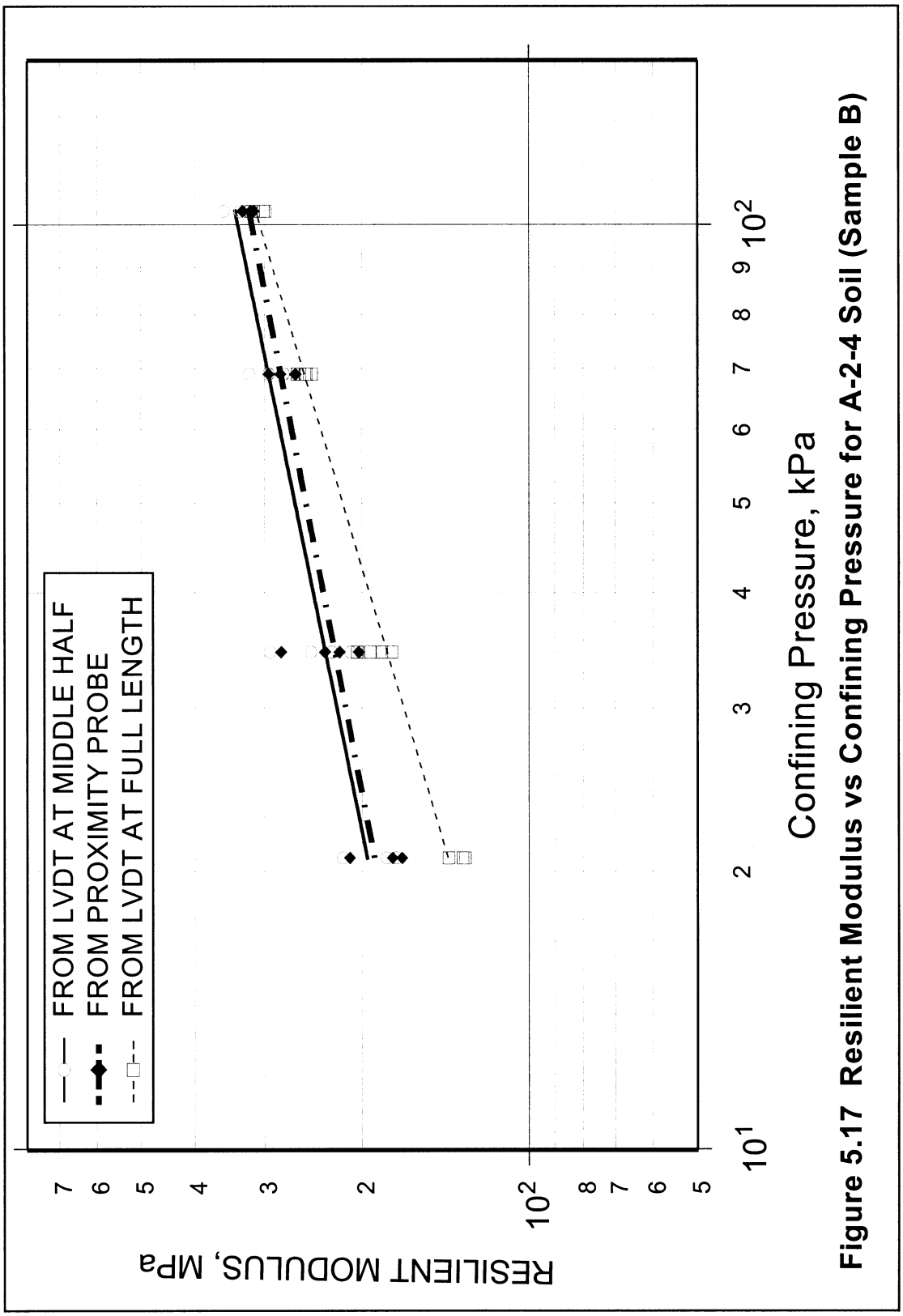

Figure 5.17 Resilient Modulus vs Confining Pressure for A-2-4 Soil (Sample B)

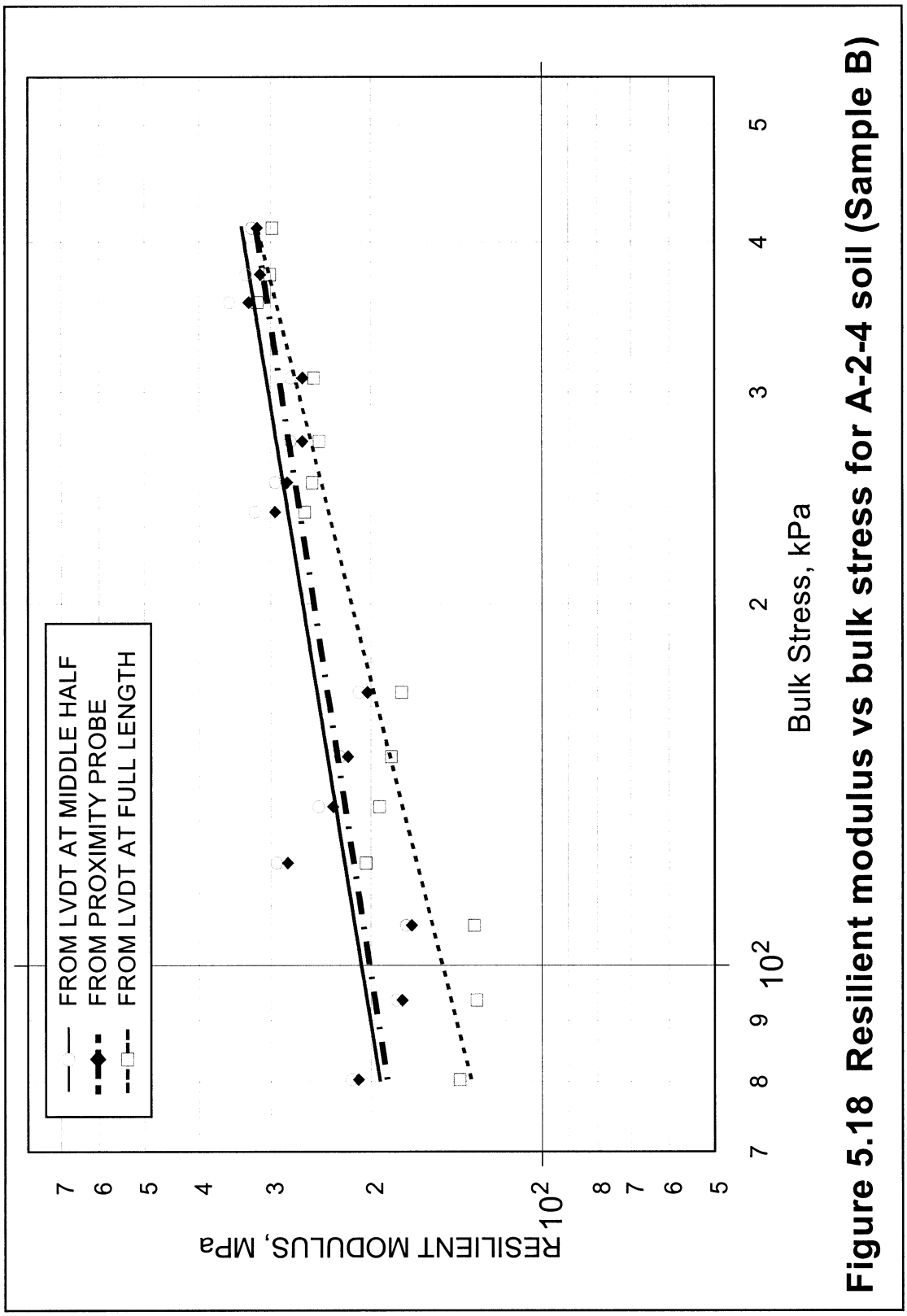

Figure 5.18 Resilient modulus vs bulk stress for A-2-4 soil (Sample B)

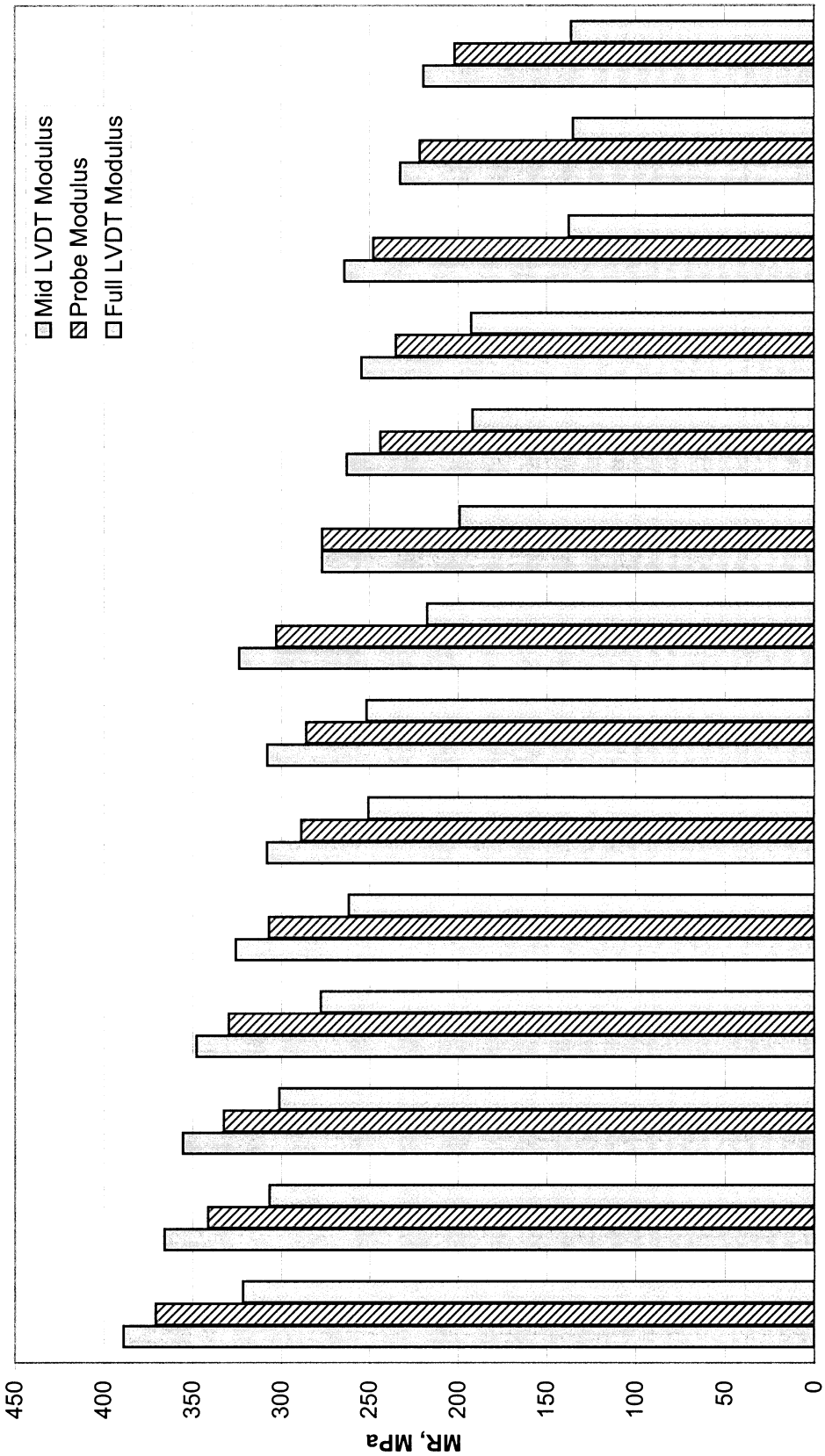

Figure 5.19 Resilient modulus test results for A-2-4 soil (Sample C)

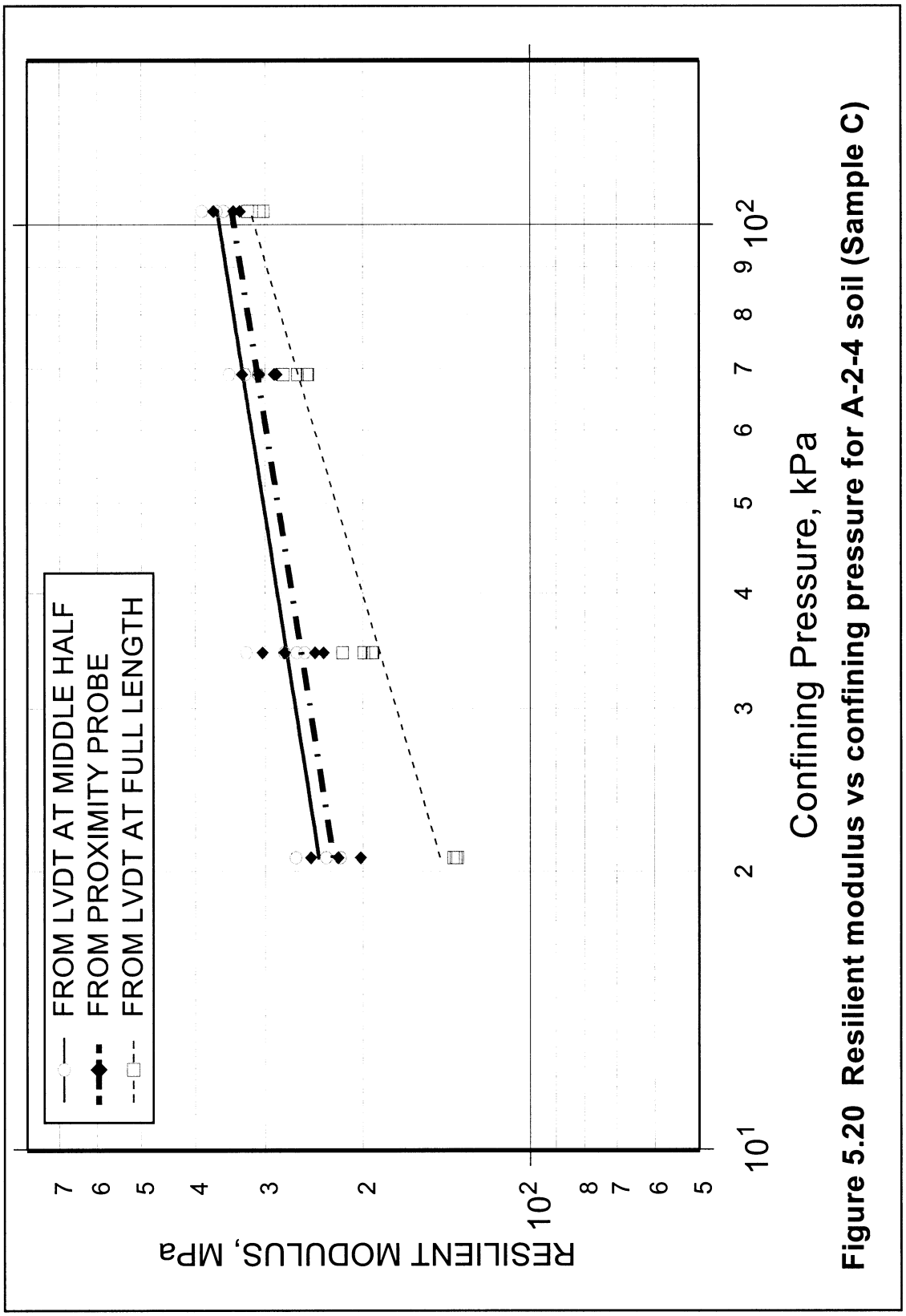

Figure 5.20 Resilient modulus vs confining pressure for A-2-4 soil (Sample C)

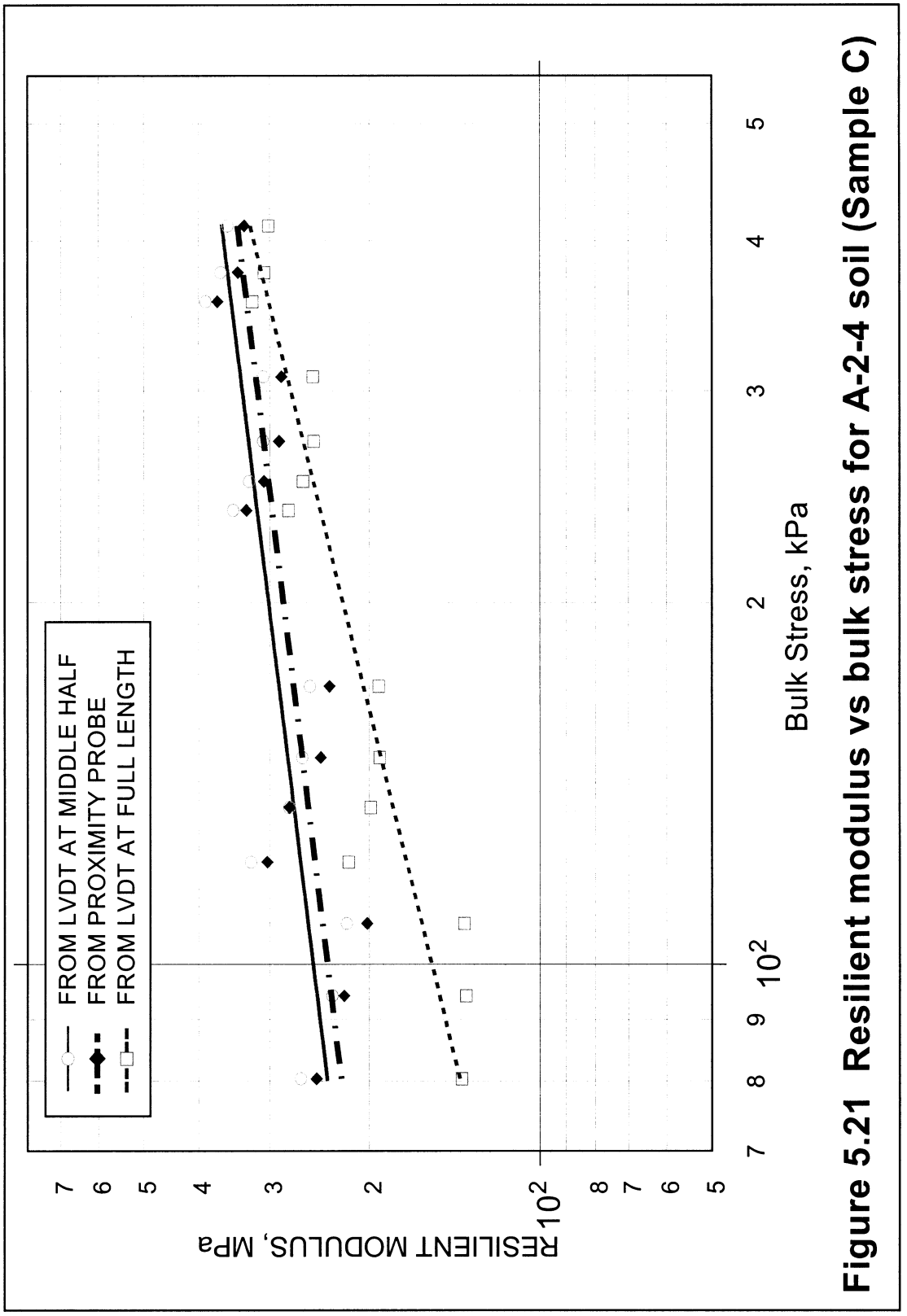

Figure 5.21 Resilient modulus vs bulk stress for A-2-4 soil (Sample C)

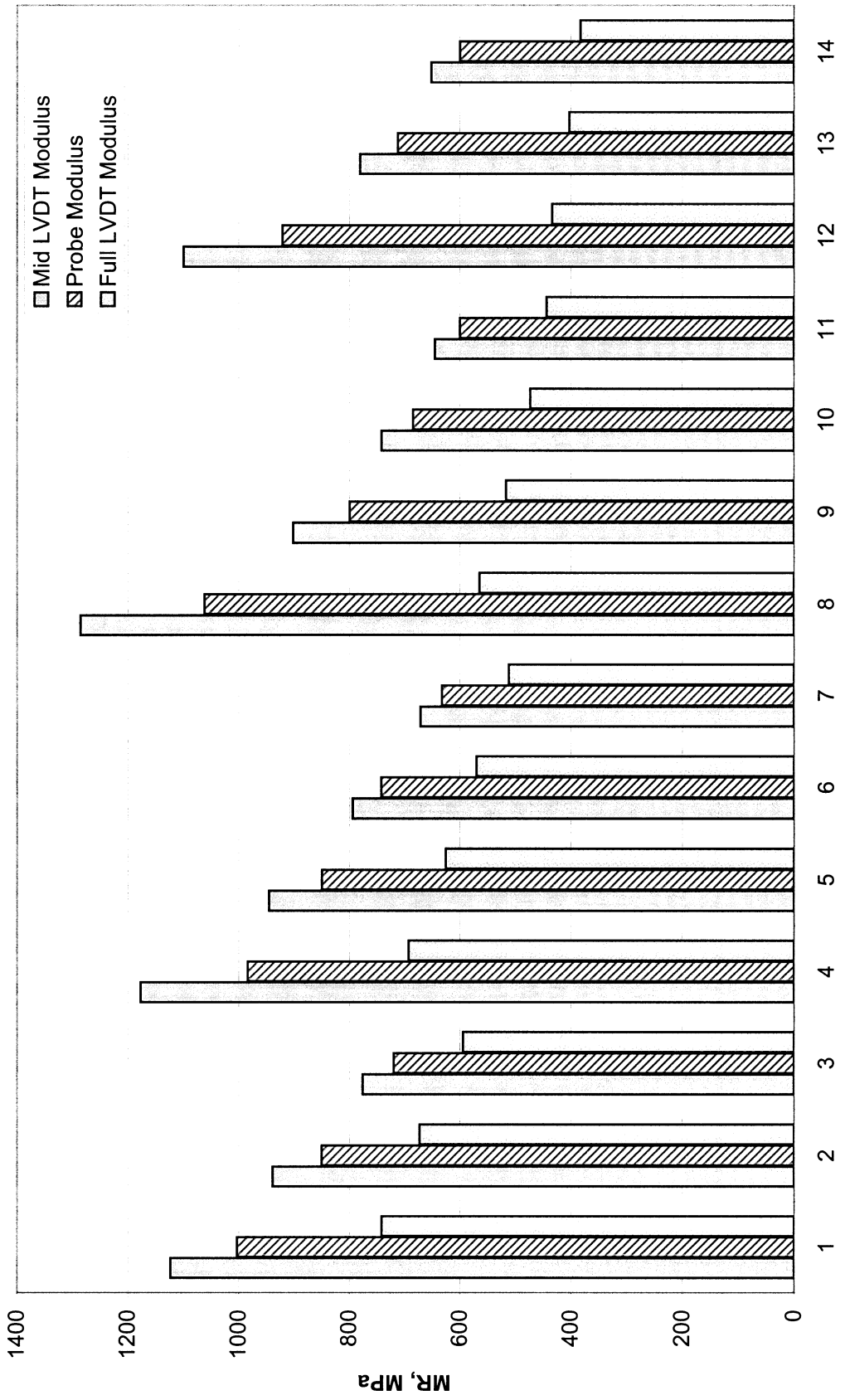

Figure 5.22 Resilient modulus test results for limerock (Sample A)

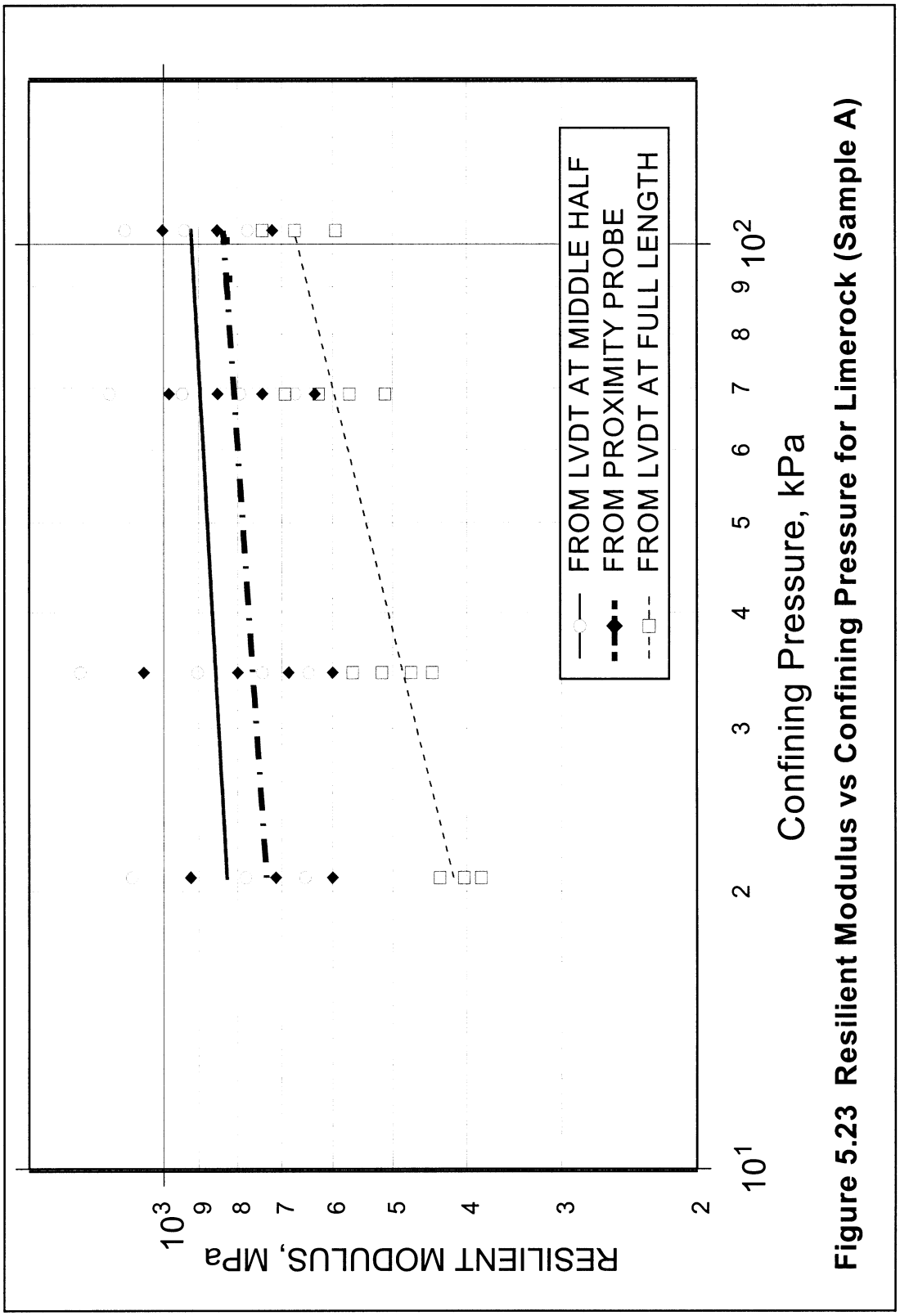

Figure 5.23 Resilient Modulus vs Confining Pressure for Limerock (Sample A)

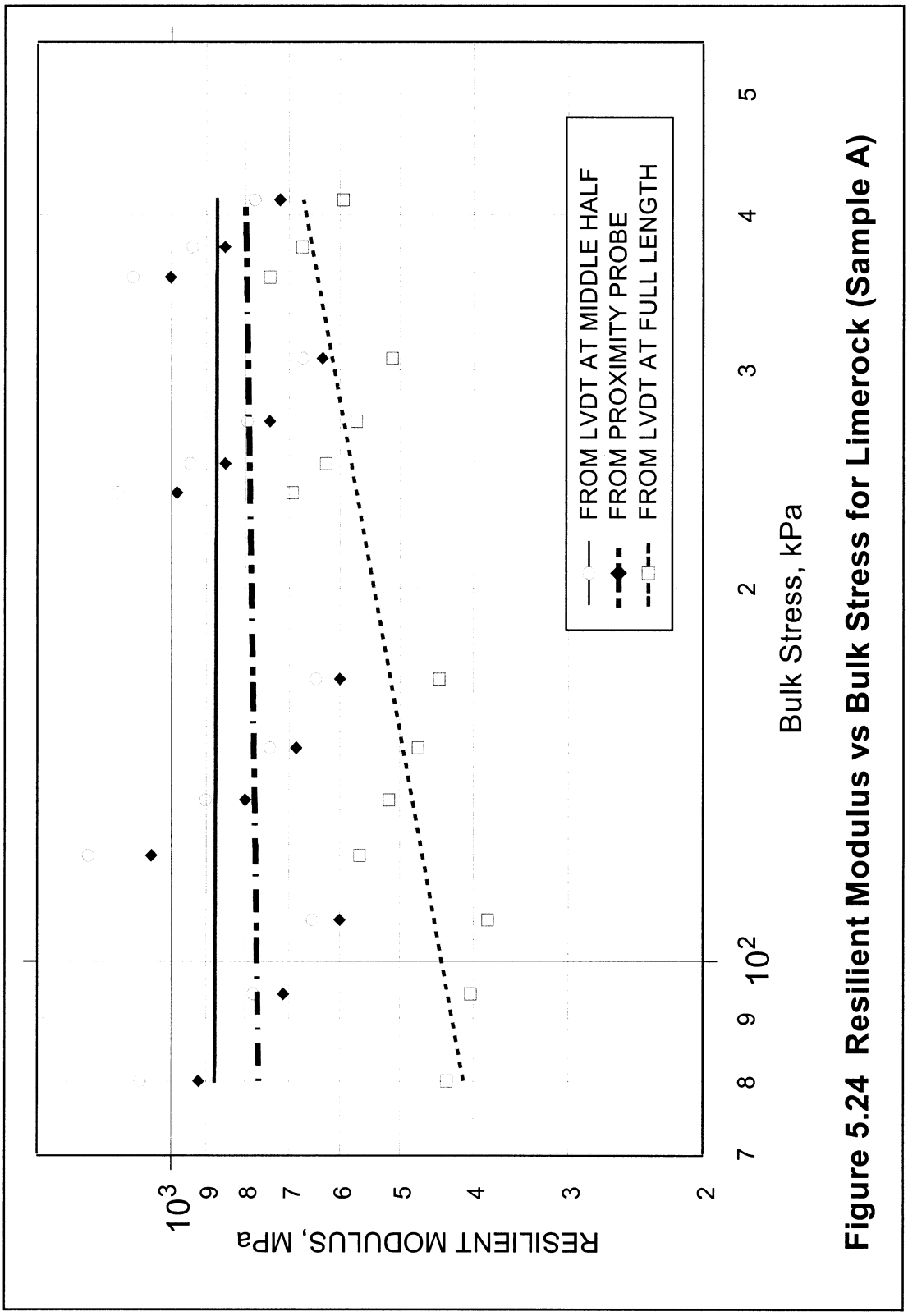

Figure 5.24 Resilient Modulus vs Bulk Stress for Limerock (Sample A)

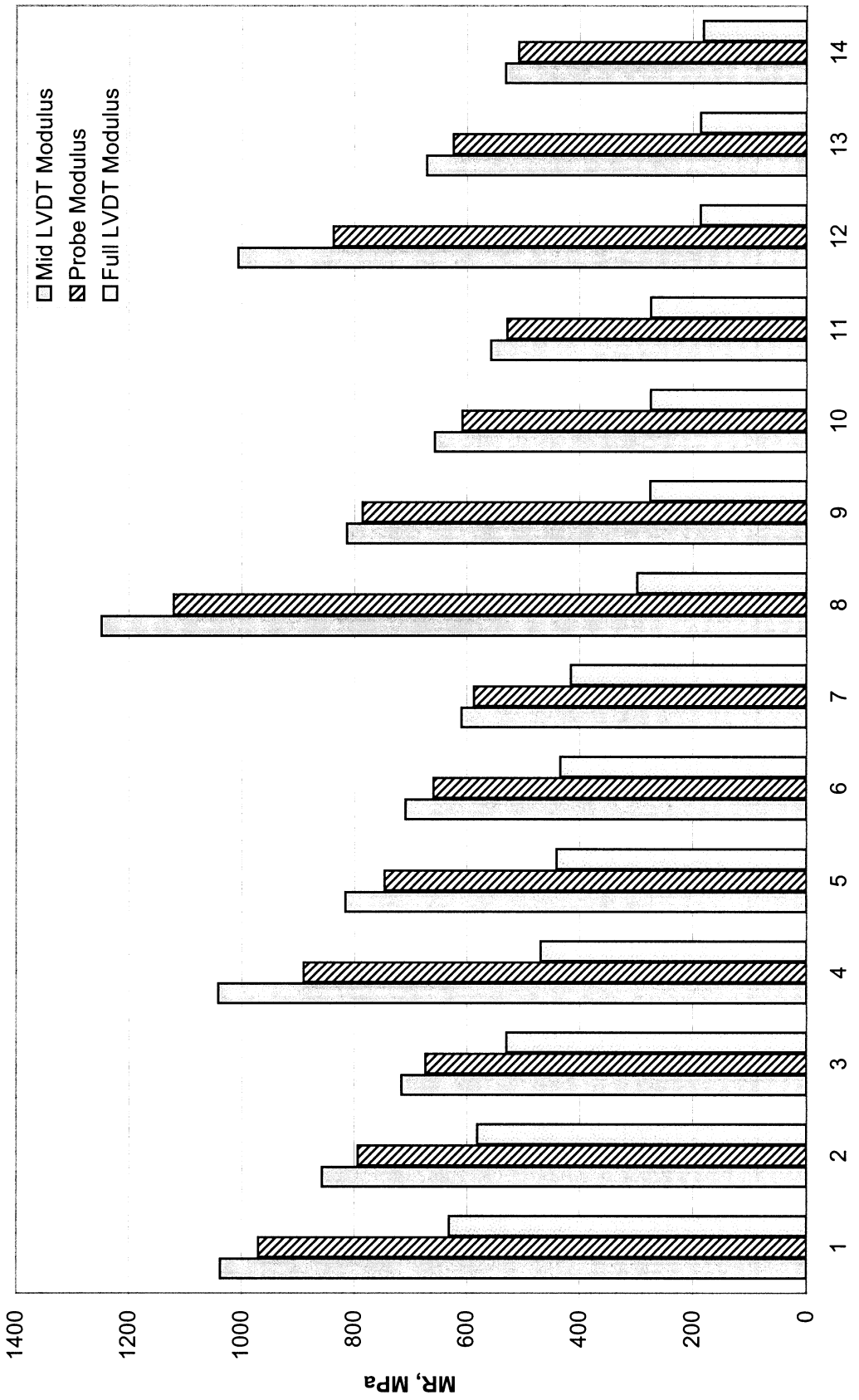

Figure 5.25 Resilient modulus test results for limerock (Sample B)

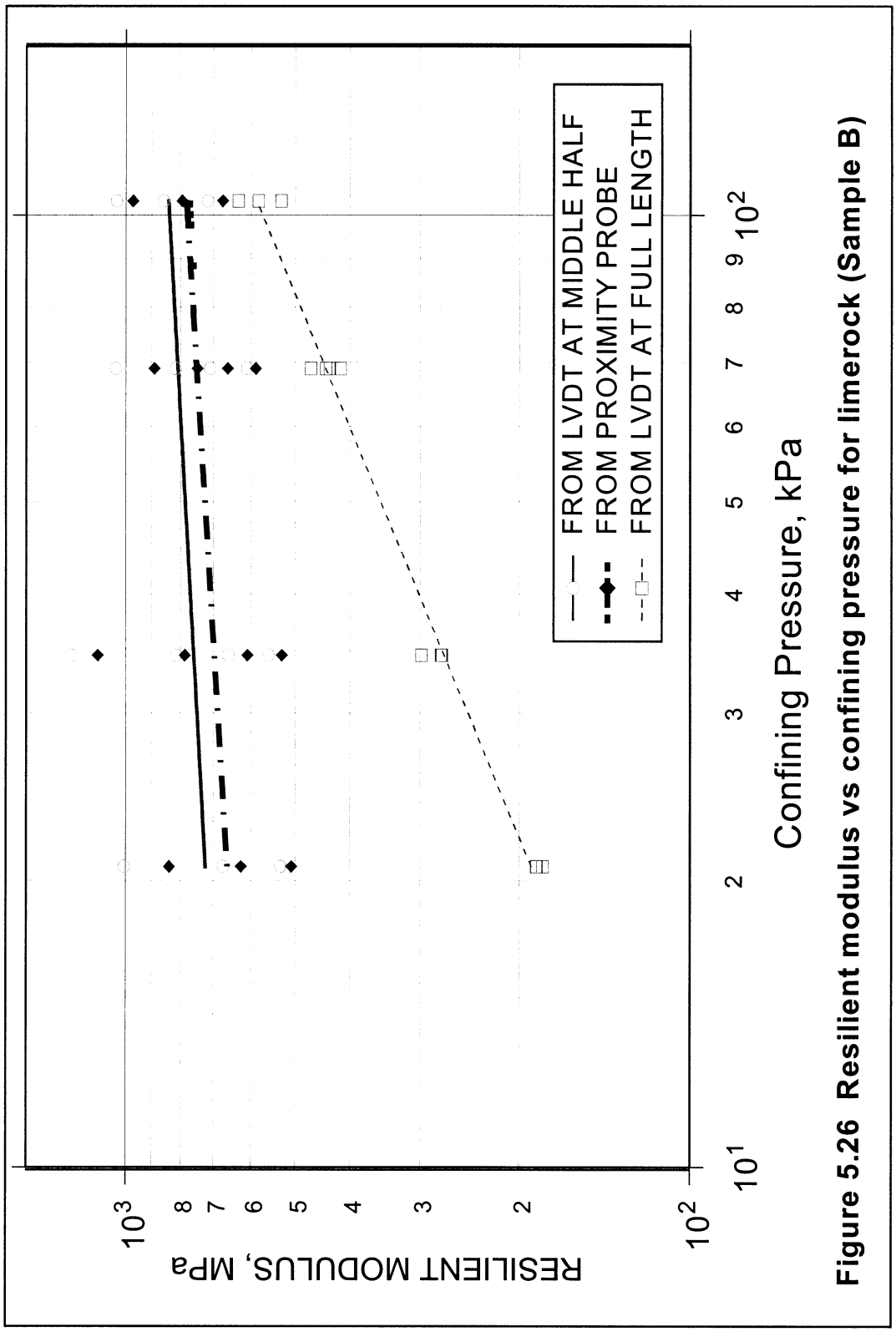

Figure 5.26 Resilient modulus vs confining pressure for limerock (Sample B)

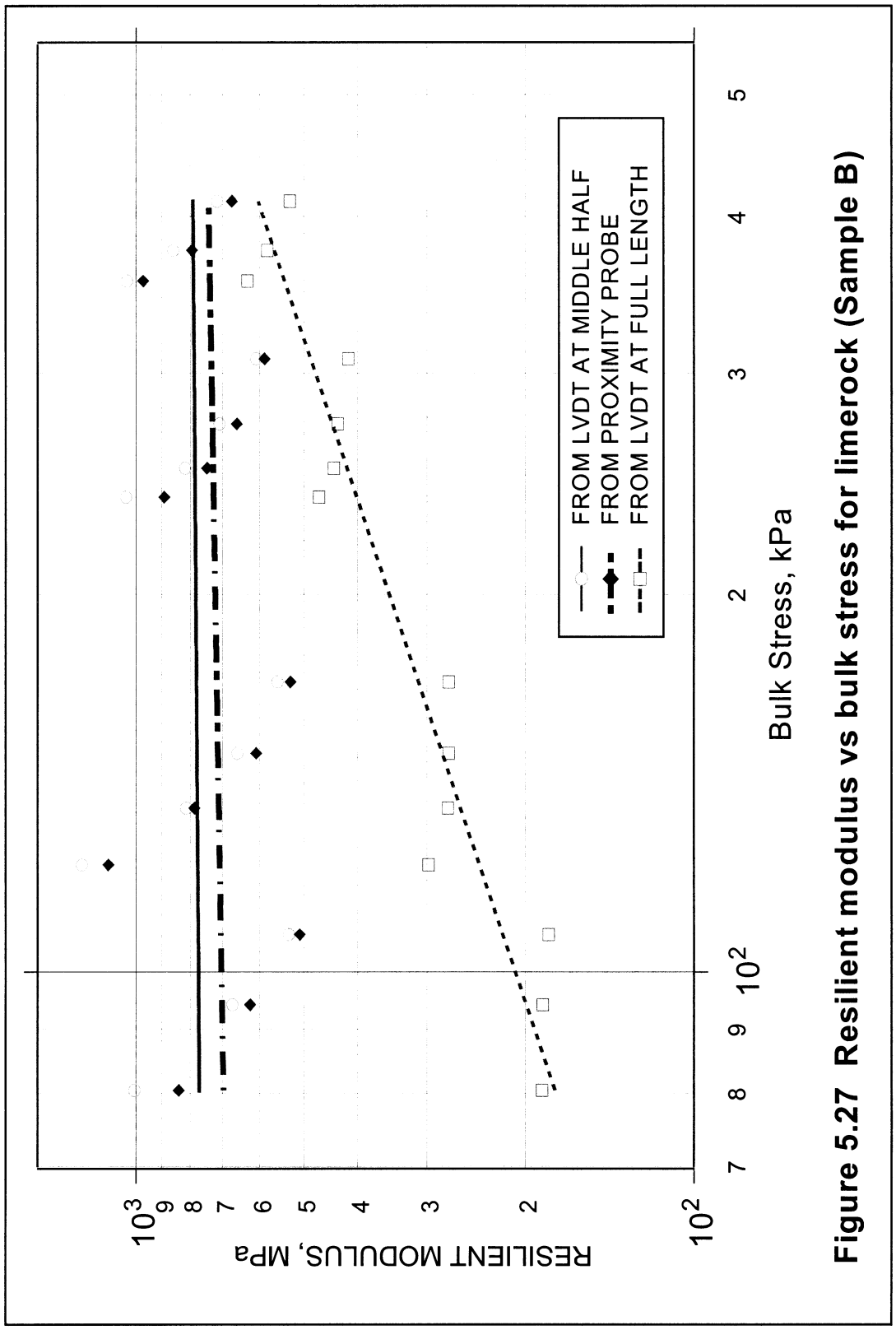

Figure 5.27 Resilient modulus vs bulk stress for limerock (Sample B)

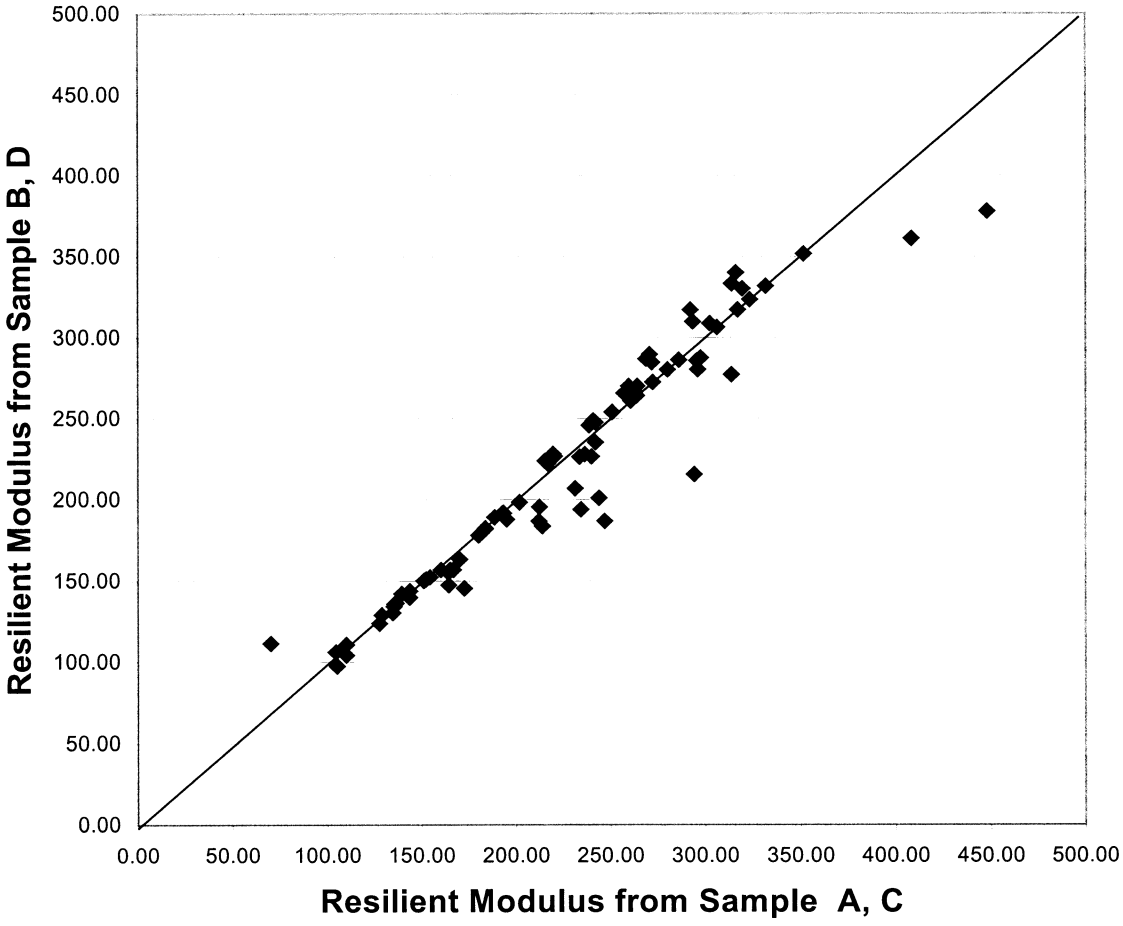

Figure 5.28 Repeatability of resilient modulus tests for A-3 soils

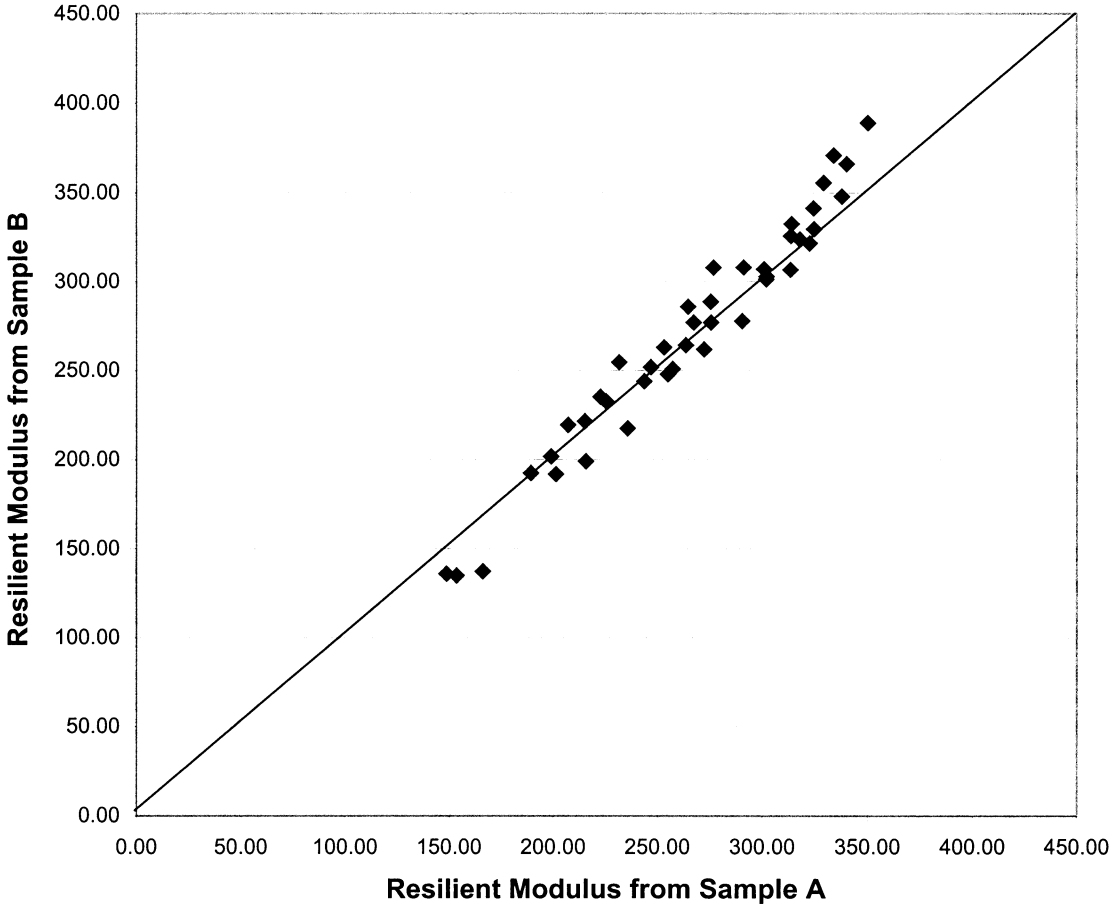

Figure 5.29 Repeatability of resilient modulus tests for A-2-4 soils

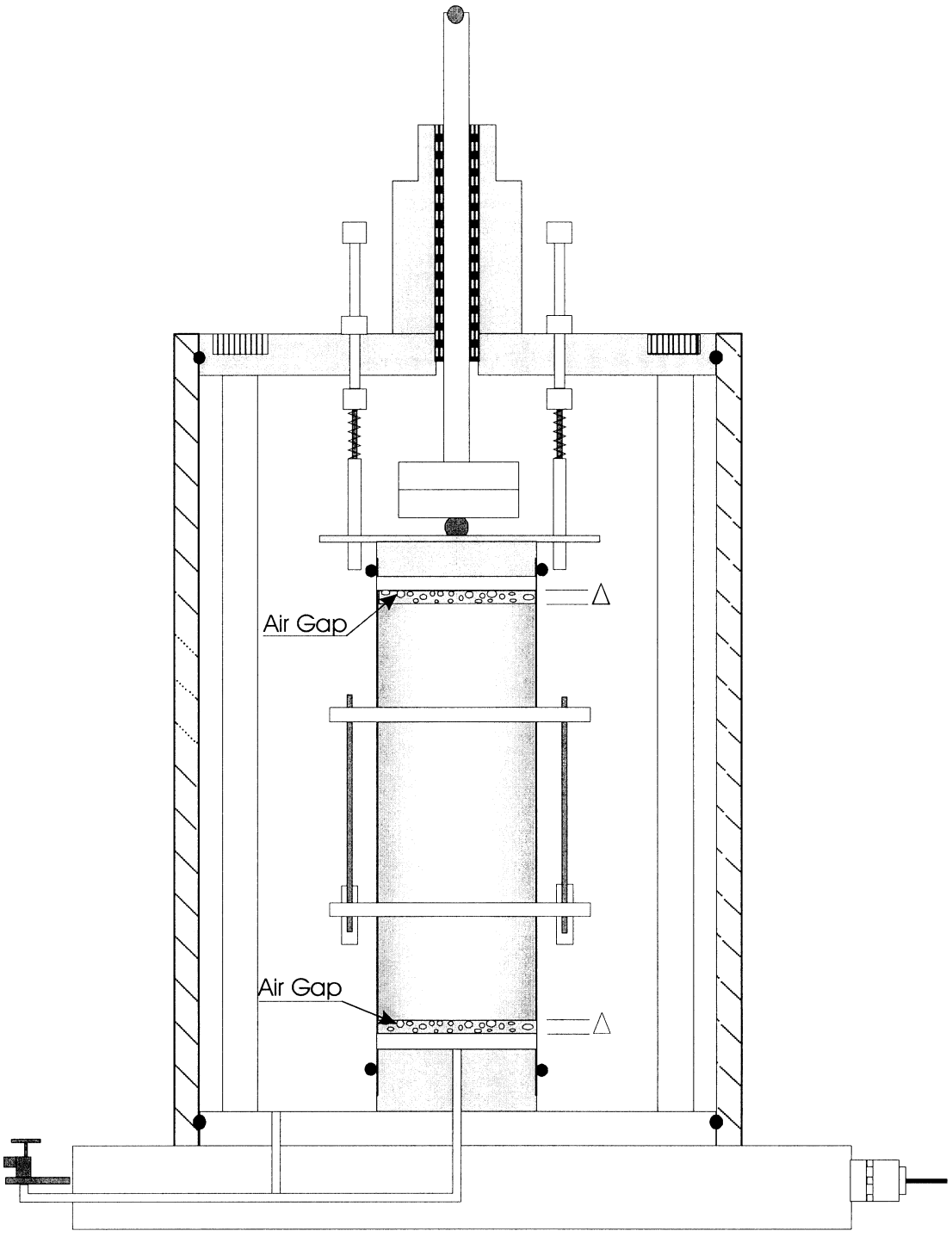

Figure 5.30 End effect of the full-length LVDTs

CHAPTER 6

CONCLUSIONS AND RECOMMENDATIONS

6.1 Conclusions

The conclusions, based on the observations and analyses from this laboratory experimental study, are summarized below.

1. The laboratory resilient modulus testing program was successfully conducted by using specimens of selected granular materials and Florida limerock with both measurements of LVDTs and non-contacting proximity probes simultaneously on a single sample. The resilient modulus test was repeatable and the test results were believed to be representative.

2. The resilient modulus values measured from the middle-positioned LVDTs (gauge length ratio of 0.5) were higher than those from the proximity probe measurement for the limerock and granular materials. The reasons for this difference may

be due to frictions between the LVDT sensors and the noises induced to the proximity probes.

3. The resilient modulus values measured from the full-length-positioned LVDT measurement were lower than that from the proximity probe measurement and the middle-positioned (gauge length ratio of 0.5) LVDT measurement. The main reason for this difference could be due to the end effect.

4. The application of non-contacting proximity probe with a gauge length ratio of one half gave accurate and reliable results in the measurement of axial deformation of resilient modulus tests. Typically, the results from the proximity probe measurement were about 5~10% lower than those from the middle-positioned LVDT measurement but about 15% higher than those from the full-length-positioned LVDT measurement for granular materials.

6.2 Recommendations

The following recommendations are made based on the analysis and observations from this laboratory study:

1. The proximity probes appeared to be a good alternative of the LVDTs. The major advantage of the proximity probes was the lower chance of test failure. However, it needed to mount metallic targets that moved rigidly with the specimen.

2. One of the major concerns in resilient modulus testing is the positioning and mounting of the deformation measurement device. An improved mounting method of the devices on the specimen will possibly increase the reliability of non-contact measurement as well as the LVDT measurements.

3. For granular materials, vibratory or gyratory compaction may be a better choice for preparation of test specimens in the laboratory.

4. Further studies should be made on the improvement of LVDT measurement and the evaluation of other non-contact measurement, such as the electro-optical system.

APPENDIX

Macro for Data Reduction

```
Sub Analysis()
    MsgBox ("Please Put the cursor to the A1 Cell")
    Application.Run "PERSONAL.XLS!findCycles"
    Application.Run "PERSONAL.XLS!deleteCyclesMoreThan49"
    Application.Run "PERSONAL.XLS!deleteFirst15Cycles"
    Application.Run "PERSONAL.XLS!averageOneVarible"
    Application.Run "PERSONAL.XLS!averageAll"
    Application.Run "PERSONAL.XLS!keepAverageDeleteRest"
    Application.Run "PERSONAL.XLS!findMaxAndMin"
    Application.Run "PERSONAL.XLS!caculatePeakVallyDifference"
    Application.Run "PERSONAL.XLS!calculateModulus"
End Sub

Sub findOneCycle()
    ActiveWindow.SmallScroll Down:=102
    ActiveCell.Offset(100, 0).Rows("1:1").EntireRow.Select
    Selection.Insert Shift:=xlDown
    ActiveCell.Offset(1, 0).Rows("1:1").EntireRow.Select
End Sub
```

```
Sub findCycles()
    Dim i As Integer
    ActiveCell.Offset(14, 0).Rows("1:1").EntireRow.Select
    For i = 1 To 50
      Application.Run "PERSONAL.XLS!findOneCycle"
    Next i
End Sub

Sub deleteCyclesMoreThan49()
    ActiveWindow.ScrollRow = 1
    ActiveCell.Offset(-5050, 0).Rows("1:1").EntireRow.Select
    ActiveWindow.ScrollRow = 4970
    ActiveWindow.SmallScroll Down:=-31
    ActiveCell.Offset(4949, 0).Rows("1:1").EntireRow.Select
    ActiveWindow.ScrollRow = 5873
    ActiveWindow.ScrollRow = 6164
    ActiveWindow.ScrollRow = 6275
    ActiveWindow.SmallScroll Down:=54
    ActiveCell.Rows("1:1382").EntireRow.Select
    Selection.Delete Shift:=xlUp
    ActiveWindow.ScrollRow = 1
    ActiveCell.Offset(-4949, 0).Rows("1:1").EntireRow.Select
End Sub

Sub deleteFirst15Cycles()
    ActiveWindow.ScrollRow = 1436
    ActiveWindow.SmallScroll Down:=-17
```

```
    ActiveCell.Rows("1:1414").EntireRow.Select
    Selection.Delete Shift:=xlUp
    ActiveCell.Rows("1:1").EntireRow.Select
End Sub
Sub averageOneVarible()
    ActiveWindow.ScrollRow = 5060
    ActiveWindow.ScrollRow = 4006
    ActiveWindow.ScrollRow = 3012
    ActiveWindow.ScrollRow = 3384
    ActiveWindow.ScrollRow = 3956
    ActiveWindow.SmallScroll Down:=-174
    ActiveWindow.LargeScroll Down:=-9
    ActiveWindow.SmallScroll Down:=7
    ActiveCell.Offset(3536, 1).Range("A1").Select
    ActiveCell.FormulaR1C1 = _
        "=(R[-102]C+R[-203]C+R[-304]C+R[-405]C+R[-506]C+R[-
    607]C+R[-708]C+R[-809]C+R[-910]C+R[-1011]C+R[-1112]C+R[-
    1213]C+R[-1314]C+R[-1415]C+R[-1516]C+R[-1617]C+R[-1718]C+R[-
    1819]C+R[-1920]C+R[-2021]C+R[-2122]C+R[-2223]C+R[-2324]C+R[-
    2425]C+R[-2526]C+R[-2627]C+R[-2728]C+R[-2829]C+R[-2930]C+R[-
    3031]C+R[-3132]C+R[-3233]C+R[-3334]C+R[-3435]C+R[-3536]C)/35"
    ActiveCell.Offset(1, 0).Range("A1").Select
End Sub

Sub averageAll()
ActiveCell.Offset(-1, 0).Range("A1").Select
    Selection.AutoFill Destination:=ActiveCell.Range("A1:I1"),
```

```
    ActiveCell.Range("A1:I1").Select
    Selection.Copy
    ActiveCell.Offset(1, 0).Range("A1").Select
    ActiveWindow.SmallScroll Down:=107
    ActiveCell.Range("A1:I99").Select
    ActiveSheet.Paste
End Sub

Sub keepAverageDeleteRest()
    ActiveCell.Offset(-1, 0).Range("A1").Select
    ActiveCell.Select
    ActiveWindow.SmallScroll Down:=101
    ActiveCell.Range("A1:I100").Select
    Selection.Copy
    ActiveCell.Select
    Selection.PasteSpecial   Paste:=xlValues,   Operation:=xlNone,
SkipBlanks:= _
        False, Transpose:=False
    ActiveCell.Offset(-1, 0).Rows("1:1").EntireRow.Select
    ActiveWindow.ScrollRow = 11
    ActiveCell.Offset(-3534, 0).Rows("1:3535").EntireRow.Select
    ActiveCell.Activate
    Application.CutCopyMode = False
    Selection.Delete Shift:=xlUp
End Sub

Sub findMaxAndMin()
```

```
    ActiveCell.Offset(-1, 0).Rows("1:1").EntireRow.Select
    Selection.Delete Shift:=xlUp
    ActiveWindow.SmallScroll Down:=98
    ActiveCell.Offset(102, 1).Range("A1").Select
    ActiveCell.FormulaR1C1 = "=MAX(R[-102]C:R[-3]C)"
    Selection.AutoFill Destination:=ActiveCell.Range("A1:I1")
    ActiveCell.Range("A1:I1").Select
    ActiveCell.Offset(1, 0).Range("A1").Select
    ActiveCell.FormulaR1C1 = "=MIN(R[-103]C:R[-4]C)"
    Selection.AutoFill Destination:=ActiveCell.Range("A1:I1")
    ActiveCell.Range("A1:I1").Select
    ActiveCell.Offset(0, 8).Range("A1").Select
End Sub

Sub calculateModulus()
    ActiveCell.Offset(0, -10).Range("A1:K1").Select
    Selection.Copy
    ActiveCell.Offset(2, -1).Range("A1").Select
    Selection.PasteSpecial  Paste:=xlValues,  Operation:=xlNone,
SkipBlanks:= False, Transpose:=False
    ActiveCell.Offset(-2, 0).Rows("1:1").EntireRow.Select
    ActiveWindow.ScrollRow = 1
    ActiveCell.Offset(-118, 0).Rows("1:119").EntireRow.Select
    ActiveCell.Activate
    Application.CutCopyMode = False
    Selection.Delete Shift:=xlUp
    ActiveCell.Offset(0, 1).Columns("A:C").EntireColumn.Select
```

```
    Selection.Delete Shift:=xlToLeft
    ActiveCell.Offset(0, 4).Columns("A:A").EntireColumn.Select
    Selection.Delete Shift:=xlToLeft
    ActiveCell.Offset(2, -5).Range("A1").Select
    ActiveCell.FormulaR1C1 = "Axial Load"
    ActiveCell.Offset(1, 0).Range("A1").Select
    ActiveCell.FormulaR1C1 = "=R[-2]C/0.224809"
    ActiveCell.Offset(-1, 1).Range("A1").Select
    ActiveCell.FormulaR1C1 = "Dev. Stress"
    ActiveCell.Offset(1, 0).Range("A1").Select
'    ActiveCell.FormulaR1C1 = "=RC[-1]/3.1415926/4"
'    convert to SI
    ActiveCell.FormulaR1C1= "=RC[-1]/3.1415926/4.0/0.0254/0.0254"
    ActiveCell.Offset(-1, 1).Range("A1").Select
    ActiveCell.FormulaR1C1 = "Mid LVDT Strain"
    ActiveCell.Offset(1, 0).Range("A1").Select
    ActiveCell.FormulaR1C1 = "=(R[-2]C[-1]+R[-2]C)/2/4"
    ActiveCell.Offset(-1, 1).Range("A1").Select
    ActiveCell.FormulaR1C1 = "Full LVDT Strain"
    ActiveCell.Offset(1, 0).Range("A1").Select
    ActiveCell.FormulaR1C1 = "=(R[-2]C+R[-2]C[1])/2/8"
    ActiveCell.Offset(-1, 1).Range("A1").Select
    ActiveCell.FormulaR1C1 = "Probe Strain"
    ActiveCell.Offset(1, 0).Range("A1").Select
    ActiveCell.FormulaR1C1 = "=(R[-2]C[1]+R[-2]C[2])/2/4"
    ActiveCell.Offset(-1, 1).Range("A1").Select
    ActiveCell.FormulaR1C1 = "Mid LVDT Modulus"
```

```
    ActiveCell.Offset(1, 0).Range("A1").Select
    ActiveCell.FormulaR1C1 = "=RC[-4]/RC[-3]/1000"
    ActiveCell.Offset(-1, 1).Range("A1").Select
    ActiveCell.FormulaR1C1 = "Full LVDT Modulus"
    ActiveCell.Offset(1, 0).Range("A1").Select
    ActiveCell.FormulaR1C1 = "=RC[-5]/RC[-3]/1000"
    ActiveCell.Offset(-1, 1).Range("A1").Select
    ActiveCell.FormulaR1C1 = "Probe Modulus"
    ActiveCell.Offset(1, 0).Range("A1").Select
    ActiveCell.FormulaR1C1 = "=RC[-6]/RC[-3]/1000"
    ActiveCell.Offset(-3, -7).Range("A1").Select
    ActiveCell.FormulaR1C1 = "Axial Load"
    ActiveCell.Offset(0, 1).Range("A1").Select
    ActiveCell.FormulaR1C1 = "Mid LVDT1"
    ActiveCell.Offset(0, 1).Range("A1").Select
    ActiveCell.FormulaR1C1 = "Mid LVDT2"
    ActiveCell.Offset(0, 1).Range("A1").Select
    ActiveCell.FormulaR1C1 = "Full LVDT1"
    ActiveCell.Offset(0, 1).Range("A1").Select
    ActiveCell.FormulaR1C1 = "Full LVDT2"
    ActiveCell.Offset(0, 1).Range("A1").Select
    ActiveCell.FormulaR1C1 = "p1-p2"
    ActiveCell.Offset(0, 1).Range("A1").Select
    ActiveCell.FormulaR1C1 = "p3-p4"
    ActiveCell.Offset(3, 1).Range("A1").Select
End Sub
```

BIBLIOGRAPHY

Ayushman, G., L. Shao, and H. B.Roy, Radial Strain Measurements In Resonant Column And Torsional Shear Tests, Transportation Research Record, National Research Council, Washington D.C., Vol. 1548, 1996

Boyce, J.R., and Brown,.S.F., Measurement of Elastic Strain in Granular Material, Geotechnique, Vol. XXVI, No. 4, pp. 637-640, 1976

Burland, J.B., and Symes, M., A Simple Axial Displacement Gauge for Use in the Triaxial Apparatus, Geotechnique, Vol. 32, No. 1, Pp. 62-65, 1982

Chisolm, E.E., and F.C. Townsend, Behavior Characteristics of Gravelly Sand and Crushed Limestone for Pavement Design, Army Waterways Experiment Station, FAA-RD-75-177, 1976

Claros, G., and S. Drabkin, Modifications to Resilient Modulus Testing Procedure and Use of Synthetic Samples for Equipment Calibration, Transportation Research Board, National Research Council, Washington D.C., Vol. 1278, 1990

Dupas, J.M, A. Pecker, P. Bozetto, and J.J. Fry, A 300-mm diameter triphial Al with a Double measuring Device, ASTM STP 977, Philadelphia, PA pp. 132-142, 1988

Filho, C.L. De M., Measurement of Axial Strains In Triaxial Tests on London Clay, Geotechnical Testing Journal, Vol.8, No.1, March, pp.3-13, 1985

Garksdale, R.D. Editor, Test Procedures for Characterizing Dynamic Stress-Strains Properties of Pavement Materials, Transportation Research Board, Special Report No. 162, 1975

Gookin, W. B., M.F. Riemer, R.W. Boulanger, and J. D. Bray, Development of cyclic triaxial apparatus with broad frequency and strain ranges, Transportation Research Record, National Research Council, Washington D.C., Vol. 1548, 1996

Linton, P.F., M.C. McVay, and D. Bloomquist., Measurement of Deformations in the Standard Trixial Environment with a comparision of local versus global measurement on a fine, fully drained sand, ASTM, Special Technical Pulication, No. 977, pp. 202-215, 1988

Maher, M.H., W. J. Papp, Jr., and N. Gucunski, Measurement of Soil Resilient Properties Using Noncontacting Proximity Sensors, Transportation Research Record, National Research Council, Washington D.C., Vol. 1548, 1996

Nazarian, S., R. Pezo, S. Melarkode, and M. Picornell, Testing Methodology For Resilient Modulus Of Base Materials, Transportation Research Record, National Research Council, Washington D.C., Vol. 1547, 1996

Pezo, R., M. Picornell, and S. Nazarian, Evaluation of Strain Variation Within A Triaxial Specimen Due to End Effects, Transportation Research Record, National Research Council, Washington D.C., 1997

Pezo, R., M. Picornell, and S. Nazarian, Evaluation Of Strain Variation Within A Triaxial Specimen Due To End Effects, Transportation Research Board, National Research Council, Washington D.C., 1998.

Ping, W.V., L. Ge, and H. Godwin, Evaluation of Pavement Layer Moduli Using Field Plate Bearing Load Test, Transportation Research Record, National Research Council, Washington D.C., No. 1501, 1995.

Ping, W.V., J. Liu, and Z. Yang, Effect of Specimen Size on Resilient Characteristics of Pavement Soils, Research Report No. FL/DOT/RMC/0636(6)-4538, 1999

Ping, W.V., Z. Yang, and P. M. Hoang, A Comparison Study of Laboratory Testing Procedures for Resilient Modulus of Subgrade Soils, Transportation Research Record, National Research Council, Washington D.C., 1998.

Sweere, G.T.H., Unbound Granular Base for Roads, Ph. D. Thesis, Technical University of Delft, 1990.